Light Self-Trapping in Polymeric Media based on Polymethylmethacrylate with Distributed Phenanthrenequinone Molecules

DISSERTATION

zur Erlangung des akademischen Grades
Doctor rerum naturalium (Dr. rer. nat.)

vorgelegt dem Rat der

Physikalisch-Astronomischen Fakultät

der Friedrich-Schiller-Universität Jena

von

Diplom-Physikerin Elen Tolstik

geboren am 25. November 1984 in Minsk (Weißrussland)

Gutachter:

1. Prof. Dr. Richard Kowarschik

2. Prof. Dr. Herbert Stafast

3. Prof. Dr. John T. Sheridan

Tag der Disputation: 13.01.2011

Contents

Chapter 1   Introduction

Among the optical effects that are intensively investigated in recent decades is the phenomenon of self-action of light beams in nonlinear optical media, which is characterized by a refractive index depending on the intensity of the light wave (e.g. self-trapping and self-focusing of optical beams, self-phase modulation of optical pulses etc.). The interaction of the light with a nonlinear material allows to realize the direct optical conversion of images and to control the space-time light structure. The formations of localized spatial structures, so-called optical solitons, which are solutions of the nonlinear differential equations describing such phenomena, are the focus of scientific and practical interest [1-6]. The reason for these intensive studies of solitons is the possibility of their use in modern communication systems, like high-speed systems of fiber-optical information transfer, including self-trapping structure formation due to nonlinear optical effects, creation of waveguiding optical elements with tunable characteristics etc.

Owing to diffraction, a collimated beam of light with a diameter d usually spreads with an angle of λ/d. However, already almost 50 years ago it was found that this spreading could be avoided in a nonlinear optical medium, which possesses an intensity-dependent index of refraction that increases with light intensity [7-9]. As a result, the beam forms a dielectric waveguide for itself with solitons as self-trapping solutions. These optical spatial solitons correspond to self-directed beams, which are limited in the across-track direction orthogonal to the direction of propagation [1]. Thereby the natural diffraction divergence of the propagating beam is compensated by the refraction of light when the refractive index is higher in the central part of the beam than at its periphery. The effect of the suppression of the diffraction by the local variation of the refractive index occurs therefore as a result of the exceptional properties of nonlinear media (i.e. the nonlinear increase of the refractive index in a region with higher intensity), leading to the spatial self-focusing of the beam. There is a dynamic balancing between diffraction of the beam and self-focusing due to the nonlinearity of the medium. Since the light wave is captured in an area with higher refractive index, such an area represents a waveguide or self-written channel, thus forming a

spatial soliton structure. If several of such light channels are formed in parallel, an interaction between them can happen [6]. In other words, solitons propagate and interact with each another while displaying properties that are associated with real particles (quasi-particles).

The evidence for a similar nonlinear behaviour of wave/particle systems has finally been discovered not only in optics, but in almost all areas of physics, chemistry, biology, medicine, climate and weather research and even in economics. There is also a broadening of temporal pulses propagating in media that possess a frequency- or wavelength-dependent chromatic dispersion or a group-velocity dispersion. These are called "temporal solitons" [10]. Other examples in nature for solitons are e.g. gigantic sea waves, called "Tsunami", the Amazonas tidal wave, called "Pororoca", the atmospheric soliton in Australia, called "Morning Glory Cloud", the conduction of pulsed nerve-cell stimulations or the soliton model for nucleons in theoretical nuclear physics, so-called "Skyrmions".

The practical realization of self-trapping depends to a large extent on the choice of a suitable photosensitive material [11]. Such requirements, like deep modulation of the refractive index (higher than 10^{-4}) and the occurrence of the nonlinear properties of the medium by the interaction with laser irradiation, can be realized in photorefractive crystals during the dynamic recording of waveguides [4,12-15]. Photorefractive waveguides and diffractive structures are widely used to control laser beams, to spatially correct the profiles of light beams and to form specified space-time structures of laser radiation for optical information processing and holographic interferometry. However on the other hand, the high cost of photorefractive crystals, their significant sensitivity to environmental factors (like external irradiation, variation of humidity and temperature etc.), the necessity to use high control voltages (several kilovolts) and the complete destruction of the photoinduced soliton structure in the absence of light excitation limit appreciably the application of photorefractive crystals for optical communication and data transfer [16,17]. The splicing of damaged waveguides, the confinement of light beams to guarantee conditions for a steady-state information transfer and the fabrication of a variety of different optical splitters and switching systems for optical signals require the formation of waveguide channels that conserve their properties for a long time without a supporting radiation source. These tasks, as well as

constantly emerging new problems in fiber-optical technologies determine the need for further research and the development of new photosensitive materials for the generation of optical waveguide structures.

Among new photosensitive optical media for recording of stationary self-trapping structures, it is particularly important to develop polymeric materials that possess high transparency in the visible spectrum and stability of the recorded information over a wide temperature range [18-21]. Extensive usage of the photopolymeric media in various fields of science and technology are associated with the possibility to save information about the amplitude and phase of the object wave during hologram recording with high density data transfer [22-25]. Polymeric compositions are characterized by a wide range of spectral sensitivity, a high resolution, a recording capability with a sufficiently large modulation of the refractive index and the possibility of a subsequent enhancement of photoinduced structures [19,25-28]. Moreover, photopolymeric materials allow the formation of integrated and diffractive optical elements and of reflection and transmission holograms. The possibility to create a channel in polymers without damaging its surface is especially suitable for applications as waveguide-based photonic devices (i.e. interferometers, resonators, optical waveguide couplers, switches, elements of optical memory, and selective optical and electromagnetic commutators) [29-32]. The advantages of polymeric materials are low cost, technological simplicity and the possibility of replication. In addition, the physical and chemical properties of polymers, their optical characteristics and spectral range of absorption can be varied by selecting light-sensitive active components during the synthesis of the material. These attractive properties ensure that polymers represent the most commonly used material of all photorefractive materials and are associated with the invention of new kinds of recording polymeric media.

Thereby, the main aim of the investigation of the nonlinear optical effect is to form spatially localized laser-beam distributions in the photopolymer and to generate self-trapping structures. In order to achieve the mentioned goals, the following tasks have to be solved:

▪ examination of the distribution of a light field in a nonlinear medium, causing self-trapping of the beam as a result of the balance between diffraction and nonlinear focusing;

▪   investigation of the photorefractive formation of light-induced diffractive structures in polymeric materials;

▪   application of the holographic relaxation technique in order to study the optical properties of polymeric materials (refractive index, modulation depth, dynamics of the photoinduced response) and selecting the optimal composition of materials suitable for self-channeling;

▪   implementation of the numerical simulation of self-trapping in photopolymeric materials possessing the properties of nonlinear focusing and thermal defocusing of light beams;

▪   experimental confirmation of the formation of waveguide channeling in a photosensitive polymeric material as a result of laser beam self-action.

The study of already well known light-sensitive polymers and the development of new polymeric compositions with optimal requirements for light self-trapping and generation of stationary waveguides are essential. Different firms, such as DuPont, Polaroid or Bell, as well as numerous research institutes are engaged in developing new, commercially used photosensitive media [19-21]. The most commonly used materials for information storage and technical holography are high-resolution silver-halide photographic emulsions [33], dichromated gelatines [34,35], photochromic and porous glasses [36,37], photoresists, liquid crystals [38], and various polymeric compositions [21,22]. This also includes polymeric media based on polymethylmethacrylate (PMMA) with the distributed photosensitive molecules anthracene [25,39], xanthone [26] or phenanthrenequinone (PQ) [23,40-44] (the last two possess an additional diffusion-amplification mechanism).

In the majority of cases the method of the preparation of polymeric layers is based on the photochemical reaction of polymerization (of radicals, cationic or anionic polymerization) and accompanied by diffusion processes [22]. An inaccurate choice of the photopolymerized compositions, an extremely high or low viscosity of polymers, a temperature variations when used can lead to a thermodynamic non-equilibrium of the polymeric layers and result in changes of the mechanical, optical and diffusion properties ("material aging") [45-49]. Relaxation normally progresses very slowly and has an unfavourable influence on the recorded photoinduced structure continuing for many years. Besides, the

preparation of heterogeneous layers together with the effect of humidity, which is present in most polymers due to absorption of moisture from air, cause strong light-scattering and produces background noise [22,50,51]. These negative factors, corroborating with shrinkage and surface relief formation [52-54], can change or destroy the recorded diffractive structure, and consequently the stored information cannot be retrieved completely.

The task of developing photosensitive polymeric media is to get the required optical properties with a minimum of adverse effects. The company "DuPont" and the "Polaroid Corporation" fabricate the most popular commercially available photo-polymerized media providing high diffraction efficiency (up to 90 %) of the recorded holograms and are widely used in applied holography [19,24,53,55]. On the other hand, most of this materials require the extra wet chemical post-processing making their manufacturing complicated and results in a significant material shrinkage (about 3-4 % during recording [53]) and in a scattering noise [22].

The process of the preparation of layers in such material as dichromated gelatin requires special equipment and limits the lifetime of the samples to a few hours only [19,34,35]. The recording medium with anthracene needs the oxygen saturation before exposure and the removal of free oxygen after that leads to high time expenditure (8-15 days), material deformation and decreasing of diffraction efficiency [25,39]. Moreover, the mobility of the anthracene molecules results in a gradual degradation of the holograms reducing the life-time of high-qualitative holograms to about 8-10 hours. All mentioned unfavourable characteristics of photomaterials exclude them from being a feasible medium for self-trapping.

During the course of the present Thesis, investigations of composite polymeric materials based on PMMA as host matrix with addition of light-sensitive molecules of the photosensitive PQ-dopant were performed. Based on previous studies, the material was selected according to its optical quality and ability to record most efficiently and stable holograms with the effect of diffusion amplification, using radiation in the visible of an average power of a few mW [40-44]. Recording by polymeric materials based on PQ-PMMA has been known since the beginning of the 90th [28,41,46,47,56]. PMMA-material was initially sensitive to UV light, but its sensitivity has been extended to the region of the visible spectrum by injection of photo-sensitizer materials. The generation of the diffractive structure in the PQ-

PMMA occurs as a result of the modulation of optical parameters in the course of the photochemical hydrogen reduction by the redox cycling agent PQ with the formation of a semiquinone radical [42,57]. Its subsequent addition to a polymer macromolecule forms a stable photoproduct. Two holograms, phase-shifted approximately by π, are created and partially cancelled by each other. One of these holograms is due to the migration of PQ-molecules in the volume of the polymer, while the other represents the photoproduct. This mechanism provides the recording of the diffractive structure in real time by using a laser source which irradiates in the absorption band of PQ (480-540 nm).

An increase of temperature during the post-exposure time activates the mobility of free PQ-molecules leading to a destruction of the grating generated by them in the polymer [42,46,56-58]. At the same time, the grating, which produced the distribution of the photoproduct in the layer, is stable. An increase of the modulation of the total refractive index occurs together with the formation of a highly efficient hologram. Thereby, the PQ-PMMA polymer provides the useful possibility to exploit the diffusion mechanism for an amplification of the photoinduced periodical structure. It results to the high values of the refractive-index modulation ($10^{-4} - 10^{-3}$).

Another advantage is that PQ-PMMA material does not require an extra chemical processing. An additional optical fixation of the hologram makes the polymeric layer insensible to ambient radiation and also increases for years the stability of the generated spatial structure of the refractive index. By this technique, many applications of the PQ-PMMA material for self-trapping realization and for the creation of stationary stable waveguides are possible. The high radiation resistance of the polymer and the ability to restore to some extent areas that are damaged due to the thermal action allow to apply radiation of high peak power and to transfer information between pulsed beams in fiber-optical networks.

As a result of the negligible diffusion of the photoproducts, the lifetime of a suitably formed space structure of the refractive index is large, but its properties depend strongly on the method of preparation of the photopolymeric medium. The method developed by us of layer formation of glassy PMMA and PQ components, which are capable to form strong chemical bonds with polymeric chains, consists of mixing the initial ingredients, subsequent pouring of the solution on glass substrates and drying [42,57,58]. The selection of the appropriate solvent,

choosing the optimum proportion of polymer and dye and the suitable synthesis and drying conditions provided the opportunity to create for the first time polymeric layers of good optical quality with a high PQ-concentration and a thickness of hundreds of micrometers. The initial rigidity of such media practically excludes the local change or shrinkage of the volume (several orders of magnitude less than the polymers mentioned above) and the wavefront distortion causing a possible information loss. A distinctive feature of the new preparation method is the ability to increase the concentration of light-sensitive PQ-molecules up to a few mole percent, which significantly increases the depth of the refractive-index modulation [42]. By this technique also favourable conditions are created for the recording of both, transmission and reflection holograms with diffraction efficiencies approaching 100 % (after diffusion amplification and light fixation). The obtained diffractive structures possess the necessary criterions for self-guided light-channel formation in the medium.

In addition, polymers comprising PMMA as the base give a possibility to generate light self-interaction in it without photolithographic techniques [59]. The modulation of the nonlinear refractive index and a suitable matching of the necessary correlation between the light intensity and the diameter of the incident beam permit to form a direct self-trapping in the polymer. Especially interesting from the viewpoint of physics is the fact that self-trapping has never been investigated previously in the PQ-PMMA medium.

Therefore, the light-sensitive PQ-PMMA polymeric compositions with the described optimal combination of physical-mechanical, technological and holographic parameters are attractive candidates to be used in the photoinduced structure formation and self-trapping generation. There are several stages of investigation involved, which are described in separate chapters of the presented Thesis.

The second chapter deals with the basic mechanisms and the common approach for describing the self-trapping process of light in a nonlinear medium. As an approximation a cylindrical light beam with a rectangular profile of intensity has been assumed. The solution of the wave equation provides the conditions of self-focusing of a Gaussian beam.

The third chapter describes the formation mechanism of stable diffractive structures in a polymeric medium with diffusion amplification. An overview of the

various existing PQ-PMMA photopolymeric media used for recording of volume diffractive structures is given, by which the choice of the optimal PQ-PMMA composition is justified.

The fourth chapter focuses on the holographic method of investigating PQ-containing polymeric media. The chemical synthesis, the preparation of the PQ-PMMA layers and some of their copolymeric modifications showed various optical and chemical properties of the material. Examination of the photoinduced recording of structures, of the diffusion amplification and of the fixation processes have been performed with the aim of selecting an optimal PQ-PMMA composition and its subsequent application for self-trapping.

The physical effect of self-channeling in PQ-PMMA media, predicted theoretically and observed experimentally, is discussed in the fifth chapter. The presented mathematical model describes qualitatively the main features of the generated waveguide. It correctly evaluates the spatial scale of the structure, identifies the influence on the self-trapping generation of various properties of the medium, of the beam geometry and of other nonlinear interaction characteristics. Particular attention is paid to the effect of thermal beam expansion, which in conjunction with the photorefractive nonlinearity of the medium results in the possibility to control optically the geometrical parameters of the generated channel.

The last part contains a description of the practical usage of the developed photopolymeric elements. It is shown that stable holographic structures in PQ-PMMA compositions are suitable as displays for the presentation of images, as interference filters and as other diffractive optical elements. The generated channels of stationary waveguides can be applied in telecommunication systems for a high-density transfer of information data, for the development of polymeric fiber-optic splitters as well as for the splicing of waveguides and their reconstitution after waveguide damages.

Chapter 2   Self-Trapping in Nonlinear Media

2.1. Formation of soliton-like structures in nonlinear materials

Light manipulated by light itself is a matter of investigation for the optical-processing technologies in nonlinear media during the past decades [1-4]. The formation of a straight channel by laser illumination due to self-trapping, self-writing or generation of optical solitons has a wide application in optical data processing and technologies, like optical waveguide generation, information transmission, spectroscopy, microscopy, optical sensing, optical switching etc. [2,6,11,60-63]. The self-interaction of light in nonlinear media defines the intensity of the propagating wave by the dependence on the complex refractive index. It occurs due to the photoinduced generation of two refractive boundary surfaces by an optical beam with finite spatial cross-section, which propagates self-focused and without divergence in a medium.

The suppression of the diffraction divergence of the laser beam in the medium by the mechanism of self-focusing nonlinearity is a widely used and well investigated effect of a self-trapped optical beam (so-called "spatial optical soliton") [3]. It is based on a strong nonlinear interaction between the wave and the medium through which the beam is propagating [11]. Solitons occur in nature in all physical systems of particle waves, propagating in nonlinear media without dispersion in time or space [2]. They are observed in hydrodynamics, nonlinear optics, plasma- and astrophysics, biology [3,6,62,63] and in different kinds of material, like glass, polymers and semiconductors [31,64-66]. The spatial boundary structure corresponds to the light beam with stable properties and a well defined cross-section. It does not change its profile by travelling through nonlinear media. The local modulation of the refractive index (n) due to the compensation of the "lens effect" and the natural divergence lead to a change of the wave front of the beam and generate an irregularity of the refractive index in the illuminated area.

The dependence of the refractive index of the media on the intensity exists in many physical processes (electro-optical orientation or induced Kerr effect,

photorefractive effect, electrostriction, resonance and thermal nonlinearity etc.) [8,67-69]. In the case of the Kerr effect the change of the refractive index appears as a consequence of the change of the spatial orientation of the molecules and their alignment along the lines of the electromagnetic field. The modulation of the refractive index can also be attributed to the nonlinearity of the electric polarization. A change of the density of the medium as well as the related modulation of the refractive index can happen due to the energy dissipation when the medium is heated by a powerful light wave.

The investigation of solitons started in 1962, when the possibility of self-guiding of a planar optical beam in a medium was first suggested [7]. Bright and dark solitons, optical vortices, quadratic and photorefractive solitons, the self-trapping effect , incoherent, temporal and discrete spatial solitons – all these terms denote different types of photorefractive, self-trapping mechanisms [15,70-72].

The invention of spatial solitons in photorefractive media was a very important event for optical physics. As they cross the material, these wave packets are causing a strong modulation of the refractive index of the medium of about $10^{-4} - 10^{-3}$. For the generation of the photorefractive self-trapping only a quite small optical power (μW) is required. Because of the scattering of light on the heterogeneities of the medium, the photorefractive material provides the possibility to directly observe the solitons during beam propagation [3].

Solitons can be useful for various applications like e.g. beam control and can also be used for the formation of light channels by CW laser irradiation [2]. Photorefractive crystals (SBN, BTO, BSO et al.), in which the formation of solitons is caused by the electro-optical modification of the refractive index due to light propagation, are the most widely used optical devices in this rather new field of research [3,9,11-15,73]. In addition to photorefractive crystals, some polymeric materials are being used recently for self-trapping purposes, because they can easily and cheaply be manufactured and allow to vary the spectral region by different sensitive additions (dye-molecules).

In order to take a closer look at the main principles of self-trapping of light beams in nonlinear media, one has to examine the effect of light modification in more detail. Light can influence the irradiated area of the material and, as a consequence, can change its propagation by different mechanisms (self-focusing, self-defocusing, self-modulation, formation of solitons etc.). The wave diffraction in

nonlinear media is differs from diffraction effects in linear materials. Propagating optical beams in any uniform medium can cause broadening of the beam due to natural diffraction [2,3,6]. A nonlinear effect is responsible for the changes of the refractive index or of the absorption factor of the media. These changes of the index of refraction depend on the light intensity. The diffraction compensates the refraction effect because of a higher value of the refractive index within the illuminated area than outside of it. Thus, the light beam generates its own waveguide, capturing the light in the area with a higher refractive index.

It is possible to find some characteristics of the wave propagation processes by a phenomenological description of the refractive index and without a detailed examination of the physical mechanism of nonlinearity. In the case of continuous cross-section beams a nonlinear addition (Δn) to the real part of the refractive index arises and modifies n of the media according to the following equation [3]:

$$n = n_0 + \Delta n(I),$$
                                         2.1

where n_0 is the initial refractive index in linear approximation, Δn is a complex function, which is determined by the particular mechanism of the nonlinear response in the medium and which depends on the light intensity I. In the simplest case the nonlinear part of the refractive index can be described as a power series of the electro-optical field strength:

$$\Delta n = n_2 |A|^2 + n_4 |A|^4 ...,$$
                                         2.2

where $A = a \cdot \exp[i\varphi]$ is the complex amplitude of the light wave that connected with the beam intensity by $I = \dfrac{c n_0}{8\pi} |A|^2$, φ is the phase of the wave, n_2 and n_4 are expansion coefficients that are determined by the nonlinear properties of the medium.

For investigation of the features of the nonlinear effect it is sufficient to examine the lowest term of the expansion of Eq. 2.2. However with high light intensities the nonlinear refractive index starts to deviate from the dependence $n_2 |A|^2$ and higher terms are playing a more important role. The competing influence of nonlinearities is increasingly activated. Such deviations were observed experimentally for

nonlinear materials like semiconductor waveguides, glasses doped by semiconductors and some polymers [3].

The sign of the coefficient n_2 in Eq. 2.2 is determined by the physical mechanism of the nonlinear response. For a Kerr nonlinearity one has usually $n_2 > 0$, whereas for a thermal nonlinearity $n_2 < 0$. In the case of resonant nonlinearities the sign of the light-induced refractive-index changes is depend on the arrangement of the laser radiation frequency relative to the absorption and luminescence pattern. For equal profiles of absorption and emission (which characterize metal vapors, for instance) it is $n_2 > 0$ in the short-wave region and $n_2 < 0$ in the long-wave region. If one examines complex molecular media (dye solutions), the Stokes shift of the absorption and luminescence patterns will be activated with $n_2 > 0$ in the absorption band and with $n_2 < 0$ in the luminescence band.
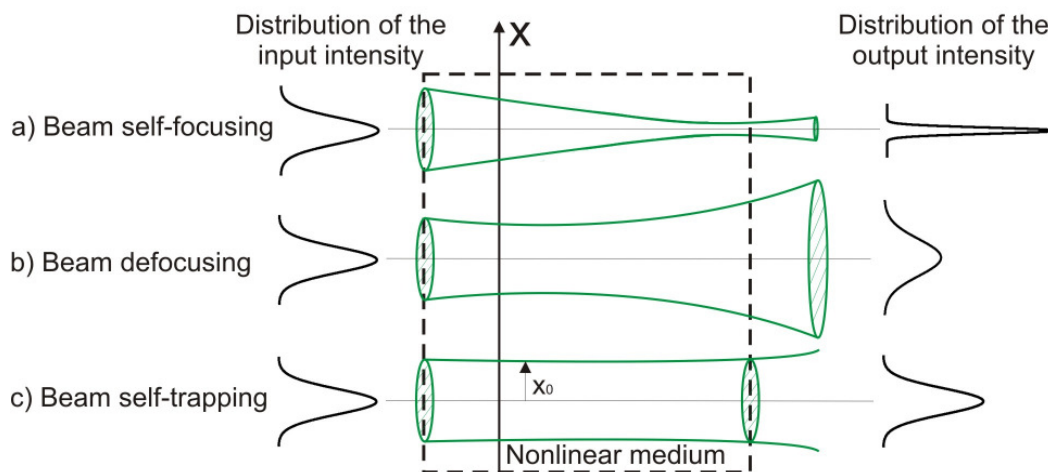
Fig. 2.1. Propagation of a laser beam in a medium [a] with a focusing nonlinearity and [b] with a defocusing nonlinearity of the refractive index; [c] exhibits the effect of self-trapping, when the mechanism of nonlinear self-focusing is compensated by the divergence caused by diffraction.

According to this rather simple description of the index of refraction, the character of the evolution of the light beam depends on the sign of the nonlinearity. In a medium with $n_2 > 0$ the refractive index increases due to increasing light intensity [Fig. 2.1 [a]]. If the intensity has its maximum at the beam axis and its minimum at its borders one observes anisotropy of the refractive index in the medium. The refractive index reaches a maximum with maximum intensity (i.e. in the center of the beam) and a minimum at the boundary areas. The

nonlinear refraction leads to a concentration of energy. The peripheral parts of the beam start to deviate and to shift to the side with bigger refractive index (in our case to the direction of the beam axis). The modulation of the wave front along the beam axis results in its self-focusing. Accordingly, in media with such nonlinearities, an initially parallel beam will be focused. In this case, the medium can play the role of a "collecting lens". This effect has a positive feed back character; the weakly increasing intensity in a certain area of the light beam leads to a concentration of the beam in this area and consequently to an even stronger rising of intensity.

In the case of $n_2 < 0$ the refractive index of the medium decrease with higher intensity (the maximum intensity decreases at the output of the medium). The nonlinear medium plays the role of a "negative lens". The wave front of the beam becomes divergent and the initially parallel beam will attain a diffraction expansion in the medium, corresponding to a defocusing effect [Fig. 2.1 [b]].

Narrowing of the beam is connected with diffraction. The diffraction divergence is inversely proportional to the radius of the light beam at the entrance to the nonlinear medium (x_0). In consequence of a decreasing x_0 the divergence will increase and compensate the nonlinear compression, accordingly. Thus, self-trapping of the optical beam occurs by achieving a good balance between diffraction and nonlinearity of the medium and induces a self-lensing or self-focusing effect, correspondingly. The beam is propagating in the medium with a plane wavefront and without diffraction and any change of its dimensions [Fig. 2.1 [c]]. There is a strong dependence of the beam power on the refractive index, causing correlations between diffraction and self-focusing. Change of intensity or of beam shape results in a distortion of self-focusing and the failure of the material.

In the case of self-trapping we are considering now a cylindrical beam with rectangular amplitude distribution and radius x_0 [8]. According to Eq. 2.2 the refractive index is equal to n_0 outside of the beam cross-section and to $n = n_0 + n_2 |A|^2$ inside [Fig. 2.2]. The light propagates till to the interface between the optically denser medium and the less dense part. The effect of the total

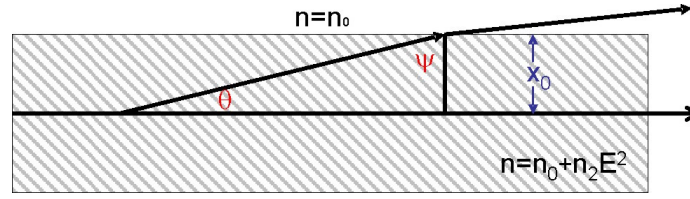internal reflection of the beam at the interface line occurs for rather large angels ψ of the beam [Fig. 2.2].

Fig. 2.2. Propagation of the beam in the nonlinear medium.

The critical angle θ_0, corresponding to the slope angle against the axis of the beam, is equal to:

$$\theta_0 = \arccos[\frac{n_0}{n_0 + n_2|A|^2}] . \qquad 2.3$$

Considering the case of $n_2|A|^2 \ll n_0$, one obtains from Eq. 2.3:

$$\theta_0^2 = \frac{2n_2|A|^2}{n_0} . \qquad 2.4$$

Light waves with $\theta > \theta_0$ exit the cylindrical cross-section of the beam, whereas beams with $\theta < \theta_0$ are propagating in the direction of the beam axis and inside the beam envelope. For light beams with plane phase fronts at the entrance of the nonlinear medium, the angle θ is determined by diffraction. For a light beam with radius x_0 the angle of the diffraction divergence can be determined as [8]:

$$\theta_d = \frac{0.61 \cdot \lambda_0}{2x_0 n_0} , \qquad 2.5$$

where λ_0 is the wavelength in vacuum.

The behaviour of the beam can be described as contributions from the nonlinear parts of refraction and diffraction, which are defined by the angles θ_0 and θ_d, respectively. For a critical angle $\theta_0 < \theta_d$ the beam is spread by divergence. But in this case, the beam is not so strongly broadened as in the linear case. For $\theta_0 = \theta_d$ we get the condition of self-trapping with complete compensation of refraction and diffraction. This equality is valid for the special condition of a beam with maximum intensity and for a nonlinear medium. Thus, the

threshold condition for the formation of self-focusing and the generation of a waveguide channel can be written as:

$$\theta_0 = \sqrt{\frac{2n_2|A_{th}|^2}{n_0}} = \theta_d = \frac{0.61 \cdot \lambda_0}{2x_0 n_0},$$

2.6

where A_{th} is the threshold amplitude of the light field corresponding to the case of compensation of the light divergence by light refraction due to photoinduced change of the refractive index. Considering the equations $P = I_0 \pi x_0^2$, where I_0 is the light intensity in the middle of the beam, and $I = \frac{cn_0}{8\pi}|A|^2$, which describe the dependence of the power of the light beam on beam intensity and electrical field strength, one obtains from Eq. 2.6 the following equation for the threshold power of the self-trapping channel:

$$P_{th} \approx \frac{c \cdot \lambda_0^2}{172 \cdot n_2}.$$

2.7

In the case $P > P_{th}$ one finds that the light beams are deviating from the axis by the self-focussing effect.

Provided that the beam characteristics remain constant in the cross-section area, the self-trapping effect can be defined by a so-called "self-focusing length" (L_{s-f}) of the optical beam [74]. As a consequence of the formation of self-trapping in a nonlinear medium caused by the mutual compensation of self-focusing and divergence, the laser beam is usually focused within the medium. Starting at this focal point, the light beam propagates, forming a straight channel in the medium. The divergence of the beam appears again just after it is leaving the nonlinear medium. The effect of self-channeling will be confirmed when the length of the channel formed by self-trapping is found to be several times longer than the self-focusing length. The self-focusing length can be determined approximately as the distance to the point, where the light beam with a plane phase front is focussed in the nonlinear medium [8,74]:

$$L_{s-f} = \frac{x_0}{\theta_0} = x_0 \sqrt{\frac{n_0}{2n_2|A|^2}}.$$

2.8

The presented expression for the self-focusing length is valid under the condition that the amplitude of the electric field strength A is much bigger than the threshold magnitude A_{th} [Eq. 2.6]. By inserting the expression of the power $P = I_0 \pi x_0^2$ of the light beam into Eq. 2.8 one obtains the following equation:

$$L_{s-f} = \frac{x_0^2 \cdot n_0}{4} \sqrt{\frac{c}{P \cdot n_2}} \, , \qquad\qquad 2.9$$

which is valid for $P \gg P_{th}$. A general definition of the self-focusing length can be derived as:

$$L_{s-f} = \frac{x_0^2 \cdot n_0}{4} \sqrt{\frac{c}{n_2}} \frac{1}{\sqrt{P} - \sqrt{P_{th}}} \, . \qquad\qquad 2.10$$

When $P = P_{th}$, the length of self-trapping approaches infinity [$L_{s-f} \to \infty$], which corresponds to the self-channeling effect.

2.2. Evolution of the Gaussian laser beam under the condition of nonlinearity

The self-trapping effect can be observed by the change of its amplitude and polarization and by the shape of the angular distribution of the radiation or the frequency spectrum of the light beam. Thus, the laser beam can be represented as a coherent electromagnetic radiation and described using Maxwell equations [12]. For beams with small angular divergence and weak change of the refractive index of the medium the vectorial wave equation can be reduced to the scalar one. The evolution of the wave in a nonlinear medium and for the stationary case with the slowly varying envelope approximation can be described by the so-called short-wave equation of the light field [8,12,75]:

$$\Delta_\perp A - 2ik \frac{\partial A}{\partial z} = -\frac{2k^2 \Delta n}{n_0} A \, , \qquad\qquad 2.11$$

where $\Delta_\perp$ is the transversal Laplace operator, z is the direction of the beam propagation, $k = \frac{2\pi n_0}{\lambda_0}$ is a wave number and Δn is the nonlinear change of the

refractive index. The dimension of the coordinates in the Laplacian in Eq. 2.11 determines the dimensions of the self-trapping channel. For spatial optical solitons there are one-dimensional and a two-dimensional cases.

Equation 2.11 can be transformed into equations for the wave amplitude and phase using $A = a \cdot exp[i\phi]$:

$$\frac{\partial\phi}{\partial z} - \frac{1}{2k}\left(\frac{\partial\phi}{\partial x}\right)^2 - \frac{1}{2k}\left(\frac{\partial\phi}{\partial y}\right)^2 + \frac{k}{2}\left(\frac{\partial^2 a/\partial x^2 + \partial^2 a/\partial y^2}{k^2 a} + \frac{2\Delta n}{n_0}\right) = 0 \qquad 2.12$$

and

$$-k\frac{\partial a^2}{\partial z} + \frac{\partial}{\partial x}\left(a^2\frac{\partial\phi}{\partial x}\right) + \frac{\partial}{\partial y}\left(a^2\frac{\partial\phi}{\partial y}\right) = 0. \qquad 2.13$$

Whereas Eq. 2.12 determines the trajectory of the light beam, Eq. 2.13 defines the change of the spatial distribution of the light-field intensity $[I = \frac{cn_0}{8\pi}a^2]$. The expression $\frac{\partial^2 a/\partial x^2 + \partial^2 a/\partial y^2}{k^2 a}$ in Eq. 2.12 describes the action of diffraction. With the following approximation for a Gaussian beam $a = a_0 \cdot exp[-\frac{x^2 + y^2}{2x_0^2}]$, the referred quotient of Eq. 2.12 can be transformed for the central part of the beam ($x, y \ll x_0$) to:

$$\frac{\partial^2 a/\partial x^2 + \partial^2 a/\partial y^2}{k^2 a} = -\frac{\lambda^2}{2\pi^2 x_0^2}. \qquad 2.14$$

The light beam divergence can be decreased by a change of the nonlinear refractive index in the case of $\Delta n > 0$. It is possible to derive from Eq. 2.12 and Eq. 2.14 the threshold condition for the self-focusing of the Gaussian beam:

$$\frac{2\Delta n_{th}}{n_0} = -\frac{\lambda^2}{2\pi^2 x_0^2}. \qquad 2.15$$

From Eq. 2.12 one can conclude that in the case of a plane wave front $[\frac{\partial\phi}{\partial x} = \frac{\partial\phi}{\partial y} = 0]$ at some point z_0 the expression $\frac{\partial\phi}{\partial z}$ becomes equal to zero.

Accordingly, the wave front remains plane for all $z \geq z_0$, and the light wave propagates without divergence.

In the approximation of a cubic nonlinearity one has $\Delta n = n_2|A|^2$. Considering a Gaussian beam power [$P = \dfrac{cn_0x_0^2}{8}|A|^2$] Eq. 2.15 can be rewritten for the threshold power as:

$$P_{th} = \frac{c\lambda_0^2}{32\pi^2 n_2}.$$
<div align="right">2.16</div>

The difference between the expression for a Gaussian light beam [Eq. 2.16] and the corresponding equation for a cylindrical light beam with a rectangular intensity profile is in the numerical factor. Thereby, to estimate the self-focusing length for a Gaussian beam it is possible to use Eq. 2.10, p.16. In experiments the threshold power and self-focusing length may vary from those given above. This is connected with the formation of waveguide modes in the generated light channel, with a saturation effect of the nonlinear refractive-index change, or with a self-focusing instability. Though, the examined mechanisms of light self-focusing allow the choice of a nonlinear medium and the conditions of laser interaction with it, possessing the formation of waveguide channels.

2.3. Self-trapping generation in polymeric materials

The above mentioned method allows to describe theoretically the formation of the spatial self-trapping structures in nonlinear media based on the mechanism of the photoinduced modulation of the refractive index. With the aim of the self-trapping formation we examined a PQ-PMMA polymeric material with nonlinear properties in which the photoinduced modulation of the refractive index is generated in a range of about $10^{-4} - 10^{-3}$ [42,57]. In such polymers, that have the capability to compensate mutually diffraction and nonlinear effects, the light beam could form a straight channel with a length which is several times longer than the self-trapping length [59,76,77].

Basically the physics of self-writing and self-trapping in polymers is very similar to the physics of propagating spatial solitons which is based on the interaction of

light with media [29-32,64-66,75,78-83]. The channels are generated by a good correlation between the linear diffraction of light and the effect of nonlinear self-focusing. The first formation of a self-written channel was accomplished by S. Frisken in 1993 in UV-cured epoxy (a tapered waveguide) [78]. After this discovery broad-range research has been performed with other photorefractive media. Self-channeling and self-focusing in photopolymers has been proven to be a self-registration process forming planar waveguides in the photopolymerisable resin, in liquid polymer diakrilat, in undoped glasses et al. [64-66,75,79-83].

Polymeric waveguides were realized mostly by using photolithography followed by developing and etching processes [31,32,82,84,85]. In some polymers the mechanism of self-trapping and self-focusing is based on the photopolymerization process which leads to a change of the permanent refractive index [64,79,83]. Self-trapping and self-focusing happens also by some molecular orientation processes and by a suitable distribution of electron clouds [65,81,86]. Planar waveguides can be produced by doping optically active organic molecules contained in the polymeric medium [32,82]. The formation of light channels in polymeric layers was mainly made due to the focusing of light onto the lateral side of the material and by shifting the light beam over the surface of the sample [59]. Waveguiding structures were also realized using femtosecond-laser micromachining [82] and a mask to perform three-dimensional direct-writing lithography [84,85,87].

Our experimental and theoretical investigations are differ fundamentally from mentioned techniques. They are based on direct self-trapping of the beam focused within the polymeric sample. By selection of suitable experimental conditions and a good correlation between diffraction and self-focusing, the light itself can generate a channel in the medium by nonlinear effects.

Chapter 3   Investigation of Polymeric Compositions with Holographic Methods

Investigations of the light-propagation processes in photorefractive materials can be executed by performing light diffraction on periodical structures. One of the most widely used method is the fixation of a high-frequency interference pattern in the light-sensitive media by photochemical and photophysical processes, i.e. by recording a holographic grating and observation of its evolution in time [39,47]. The recording of holograms is accomplished by the interference of two coherent laser beams illuminating with the spectral band width of the photomaterial [88]. This radiation process results in the change of the material density and, consequently, in the modulation of the refractive index. The characteristics of the generated periodical structure can be investigated by several methods (holographic grating relaxation technique [89], holographic relaxation spectroscopy [90], transient grating technique for short-living gratings [91], four-wave interaction in the nonlinear media [92], forced Rayleigh scattering [44,93] etc.). The obtained diffractive element forms a distribution of concentration gradients due to diffusion processes and defines all optical properties of the recording material. Recording and relaxation of the hologram is detected by the intensity variations of light diffracted from the photoinduced periodical structure.

3.1. Photorefraction mechanism for the formation of photoinduced structures

Phototransformation in most photopolymeric materials involves the diffusion of one or more of the components leading to a density change with a following formation of the modulation Δn of the refractive index [19]. If the value of Δn reaches $\sim 10^{-4}$ and more, one can say that the polymeric material possesses photorefractive properties [94]. For analysing the photorefraction mechanism one can use the Lorentz-Lorenz formula [95,96], (also known as the Clausius–Mossotti relation):

$$\frac{n^2 - 1}{n^2 + 2} = \sum_i R_i C_i . \qquad\qquad 3.1$$

It describes the average refractive index of the medium n of the particles as a function of the concentrations C_i of the components and of their refractions R_i [molecular, if concentration is a quantity of particles in a unit of volume, or molar, if it is in molar in a unit of volume].

Thus, an activation of the photorefraction process occurs due to the change of refraction or concentration of the material. The refraction R_i is the change in direction of a wave due to a change in its speed. It occurs when light waves travel from a medium with a given refractive index to a medium with another at an angle. At the boundary between the media, the wave's phase velocity is altered, usually causing a change in direction. Its wavelength increases or decreases but its frequency remains constant. Accordingly, the refraction describes the contribution of particles to the refractive index and strongly depends on the molar polarizability. Thereby, the more the polarizability of the photoproduct molecules differs from the polarizability of the phototransformed molecules, the stronger are the changes of the photoreaction or of the refractive index, respectively.

Another possibility to vary n is to modify the concentration of components by changing the material density ρ. The contribution of such a change of the density to the modulation of n can be written according to [94] in the following form:

$$\Delta n(W) = \frac{(n^2 + 2)(n^2 + 1)}{6 \cdot n} \frac{\Delta\rho(W)}{\rho} + \frac{(n^2 + 2)^2}{6 \cdot n} C(W)\Delta R , \qquad 3.2$$

where $\Delta\rho(W)$ is the density change created by the light exposure W, $C(W)$ is the concentration of the formed photoproduct, ΔR is the change in photorefraction of the sensitive component, i.e. the refraction variation of the active particles as a result of the photoreaction. A considerable influence of the photoinduced density change on Δn is known for phase grating recording materials containing dichromate gelatin and photopolymerized compositions.

The investigation of the diffusion of the components in the recording medium shows that in some cases the photoinduced diffusion can amplify and stabilize the phase holograms during the period of post-exposure [23,25,28,57]. The recording process in the polymeric system during the diffractive-structure formation consists

schematically of two components. The first component (A) diffuses into the polymer, whereas the second one (photoproduct B) constitutes a part of a macromolecule and cannot diffuse [42,56,97]. The diffusion "washes away" the concentration distribution only of one of the substances. The distribution of another one is stable and antiphased to it. Since the contributions to the hologram corresponding to these distributions are also antiphased and, hence, compensate each other, diffusion degradation of one of them should lead to an amplification of the resulting hologram.

Let us now consider a system in which a photoreaction proceeds:

$$A \xrightarrow{\ hv\ } B.$$
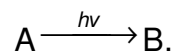
According to the formation of two antiphased gratings in the recording layer (by mobile substance A and immobile substance B) the modulation of the refractive index of the holographic grating will be described by the following expression (using Lorentz-Lorenz formula [Eq. 3.1]):

$$\Delta n = \frac{(n^2 + 2)^2}{6 \cdot n} [R_B \Delta C_B - R_A \Delta C_A], \qquad 3.3$$

where R_B and R_A, ΔC_B and ΔC_A are the molar refractions and absolute values of the concentration modulations of the photoproduct B and of the mobile molecules A, correspondingly.

As a result of diffusion amplification the distribution of the substance A becomes homogenous in the layer and its contribution to the modulation of the refractive index degrades. The solution of the diffusion equation with an initially sinusoidal distribution of the concentration gives a modulation of the refractive index in the following form:

$$\Delta n = \frac{(n^2 + 2)^2}{6 \cdot n} [R_B \Delta C_B - R_A \Delta C_A(t_e) \exp[-\gamma(t - t_e)]], \qquad 3.4$$

where $\Delta C_A(t_e)$ is the change of the concentration of the substance A induced by the light field, t is the amplification time of the hologram, t_e is the light exposure time. The rate constant of the amplification process (γ) is defined as follows:

$$\gamma = D(\frac{2\pi}{\Lambda})^2 \, ,$$ 3.5

with the spatial hologram period of the illuminated area Λ and the diffusion coefficient D. The phase portrait after the amplification process of the hologram is formed by the distribution of the molecules attached to substance A:

$$\Delta n = \frac{(n^2 + 2)^2}{6 \cdot n} \cdot \Delta C_B \cdot R_B = \frac{(n^2 + 2)^2}{6 \cdot n} \cdot \Delta C_A(t_e) \cdot R_B \, ,$$ 3.6

and is defined by the product of the concentration modulation of the photoproduct with its molar refraction. Owing to the diffusion of unreacted molecules A, $\Delta C_A(t) \to 0$, $\Delta n(t)$ increases. The amplification factor M of the phase pattern regarding to the refractive-index modulation is determined as:

$$M = \frac{\Delta n(\infty)}{\Delta n(t_e)} = \frac{R_B}{R_B - R_A} \, .$$ 3.7

It corresponds to a complete linking of the photoproduct molecules to the macromolecules: $\Delta C_B = \Delta C_A(t_e)$.

The scheme explaining the process of hologram generation and diffusion amplification by the transformation of the initial substance A into the photoproduct B is illustrated in Fig. 3.1. Before illumination of the polymer, the mobile molecules of the diffusing substance A are homogenously distributed among the polymeric matrix. The interference field of the intensity (I) is represented by a sinusoidal distribution [Fig. 3.1 [a]]. During the recording process the photosensitive molecules A (or dye) attached to the polymeric matrix are forming the immobile substance B (or photoproduct). Meanwhile, the distributions of the concentrations of substances A and B become antiphased and provide an antiphased contributions to the spatial modulation of the refractive index, thereby partially weakening the resulting grating [Fig. 3.1 [b]]. If the contribution to the refractive-index modulation of the immobile substance B (Δn_B) becomes considerably bigger than the contribution of the diffusing substance A ($-\Delta n_A$), the summation of both indices ($\Delta n = \Delta n_B - \Delta n_A$) is representing the refractive-index modulation Δn of the final distribution, which is in phase with the light field.
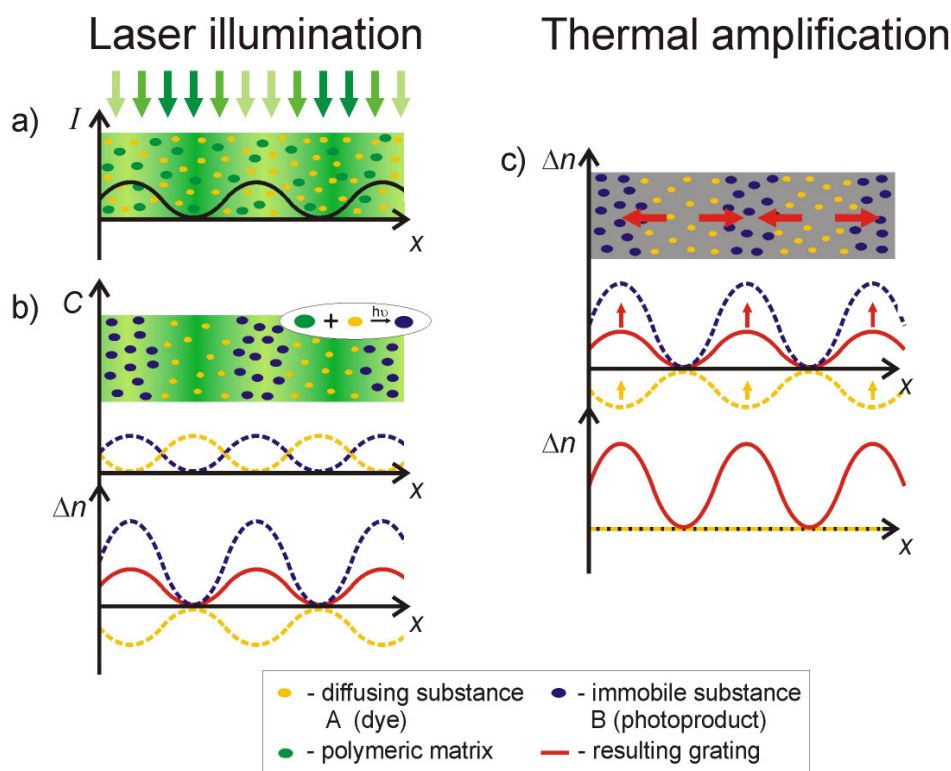
Fig. 3.1. Formation of the spatial distribution during recording and amplification of the holographic grating: [a] distributions of the intensity (I) in the recorded interference pattern; [b] distributions of concentration (C) and refractive-index modulation (Δn) of substances A (diffusing) and B (immobile) and resulting grating after exposure; [c] distributions of Δn after diffusion amplification.

At room temperature the polymeric matrix contains some free volume, which can be considered as an empty space when the densest packing has not been reached [27]. Thermal motion begins when the system is warming up causing amplification of the grating. The solid body expands and forms an additional free volume, allowing even relatively large molecules to diffuse [97]. Thus, during the post-exposure period of time a thermal amplification mechanism can play a positive role and enhances the grating formation due to the diffusion process [Fig. 3.1 [c]]. The photoproduct B stays immobile during heating and stable towards the degradation caused by diffusion. The second structure generated by substance A degrades with a second-degree dependence of the reaction velocity on the spatial frequency and with a linear dependence on the diffusion coefficient [Eq. 3.5, p.23].

After heating, the distribution of the diffusing substance A becomes homogeneous ($\Delta n_A = 0$), while the modulation of the summarized refractive index Δn increases and becomes equal to that of substance B ($\Delta n = \Delta n_B$). The recorded and amplified hologram achieves its maximum efficiency.

3.2. Implementation of the mechanisms of diffusion and amplification into PQ-containing media

The described principle of the hologram formation was realized by the PQ-photoreduction process in a medium composed of a PMMA polymeric matrix [23,98]. The special ability of the PQ as a photosensitive addition to join the polymer under irradiation results in the transformation of the dye-molecules into 9-10-substituted derivatives of phenanthrene (phenanthrene chromophore, HPQR). The diffusion of the dye through the polymeric matrix causes a density change with the subsequent modulation of the refractive index [19,56,57]. The recording of the periodical interference pattern with the following diffusion amplification of one or more components can be described on the molecular level [28,44,46,57]. At first, light absorption leads to a conversion of the PQ-molecules to the excited singlet state of quinine ($^1PQ^*$) and afterwards to the triplet state ($^3PQ^*$):

$$^1PQ + hv \rightarrow {}^1PQ^* \rightarrow {}^3PQ^*.$$
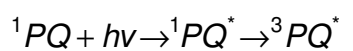
In the absence of oxygen, the triplet state of PQ starts to react with the surrounding molecules (these are macromolecules in the case of polymer glass) detaching a hydrogen atom from the methyl group. This leads to the formation of a couple of radicals: macroradical ($R^\bullet$) and semiquinone radical ($HPQ^\bullet$). Further radicals (even those that belong to different pairs) recombine. At the same time the formation of the chemical bonds occurs between the phenantrene group and the polymer, i.e. the stable photoproduct ($HPQR$) is formed [Fig. 3.2].
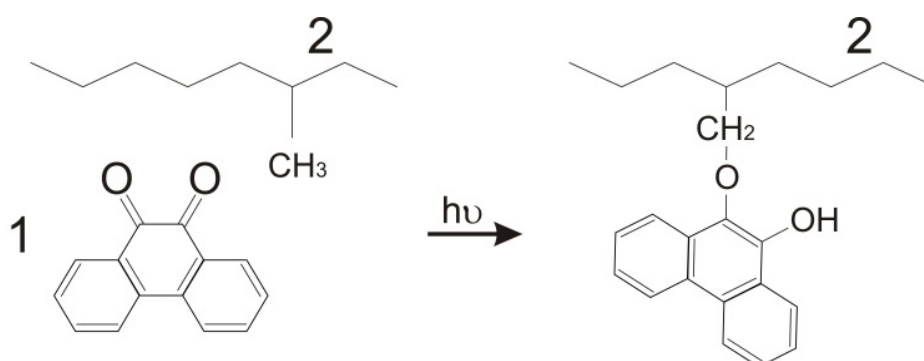

Fig. 3.2. Attaching of the PQ-molecule [1] by the photoreaction to the macromolecule [2] in the polymeric matrix under illumination.

With the HPQR formation an increase of the modulation of the refractive index and a rather weak grating can be already detected:

$$^3PQ^* + RH \rightarrow HPQ^\bullet + R^\bullet \rightarrow HPQR$$

The diffusion of the semiquinone radical plays the role of the "latent image regression" causing the high-frequency gratings to grow more slowly than the low-frequency ones [44,47,56,97]. When phenanthrenequinone molecules are joined to macromolecules, two antiphased partially compensated gratings (generated photoproduct and free PQ-molecules) with sharply different diffusion lifetimes appear [Fig. 3.1 [b], p.24]. Due to their large sizes the macromolecules are practically immovable in comparison with the PQ-molecules, therefore, the grating of the photoproduct is stable. A thermal enhancement of the resulting hologram is observed by the process of diffusion degradation of the antiphased grating (an unreacted PQ "dissolves" over time due to diffusion) [Fig. 3.1 [c], p.24]. At the end of this process a homogeneous spatial distribution of the initial PQ-molecules is achieved. This does not contribute to the modulation of the refractive index of the hologram. Thus, the last step the grating formation is a "metastable" state, the photoinduced structure of which is based on the spatial distribution of phenanthrene chromophores. The period of the amplification process takes place over time periods of minutes to years, depending on the mean velocity at which the components diffuse, respectively.
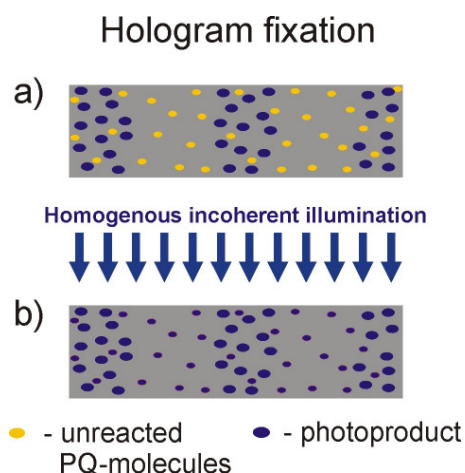

Fig. 3.3. Fixation of the periodical structure in a PQ-PMMA material by incoherent illumination: [a] amplified diffractive structure in the polymer before fixation; [b] fixed polymeric layer.

The photostability of the holograms can be achieved by incoherent irradiation with light in the range of the PQ absorption band. The residual unreacted PQ-molecules, uniformly distributed in the sample volume, are transformed into insensitive photoproducts [Fig. 3.3]. Meanwhile, changes in the chemical composition and consequently in the average refractive index occur, but the spatial modulation of the other parameters stays stable. The medium becomes transparent to outer radiation and the amplified hologram is fixed.

To sum the existing concepts of the diffusion and the chemical properties of the system containing PQ-PMMA it is possible to separate out the several steps of the hologram "life" [42,46,56,97]. At first, light absorption generates radicals due to the conversion of PQ-molecules from the singlet-exited quinine to its triplet state with subsequent hydrogen abstraction from macromolecules. Quinine molecules transform to semiquinone radicals, and a relatively weak grating can be detected. The second step consists of attaching the semiquinone radical to the macromolecule, forming a stable photoreaction product with subsequent change of its refraction. As mentioned already, the high-frequency gratings are amplified more slowly than the low-frequency ones as a consequence of the slower diffusion of the semiquinone radicals. At the next step, the process of thermal diffusion enhancement starts and plays a significant role. The migration of unreacted PQ-molecules results in the degradation of their periodical structure, while the antiphased hologram of the photoproduct is stable. The resulting hologram is then amplified. Higher spatial frequencies of the gratings and higher temperature of the post-exposure process lead to a faster achievement of constant efficiency.

In some cases, when the maximum modulation of the refractive index is reached, one observes a minor degradation process of the hologram (usually not more than a few percents of the n-modulation). One possible cause is binding of the PQ-molecules not to the polymer chain, but to the low-molecular substances in a composition comprising a residual monomer or a solvent (with a concentration of about 5 %). Because of the increased volume, the product of such a chemical additive slowly diffuses, reducing slightly the strength of the grating.

Thus, in spite of a small difference between the optical parameters of the PQ-molecule and of its photoproduct, it is possible to observe a relatively weak grating already during the recording process. Diffusion relaxation of one of two periodical structures results in a phase modulation of the amplification by an order of

magnitude and therefore increases the diffraction efficiency of the formed structure up to the saturation.

3.3. PQ-PMMA polymeric compositions

Stable variation of the refractive index in photopolymers occurs due to the redistribution of the components by diffusion during the illumination time and the post-exposure period. The hardness of the material, determined by the particular method of the polymer synthesis, has an influence on the characteristics of the PQ-diffusion and on the parameters of the formed hologram [48]. A softer PQ-PMMA structure leads to a decrease of the amplification time. Accordingly, the maximum modulation of the refractive index is achieved faster, but the produced holograms possess lower stability, and a degradation process under high temperatures is activated. Any deviation from the process of the optimum synthesis of the rigid PMMA-structure results in a very slow diffusion of the PQ-molecules. Thus, diffusion characteristics are depending strongly on the type of PQ-PMMA layers, the concentration of the residual monomer and dye, the chemical preparation and the treatment of the samples. To find a good balance between all parameters and to choose the best preparation method is the task required next.

There are worldwide several research groups in the field of investigating PQ-PMMA polymers [Belarusian State University (Minsk, Belarus) [42,57,58], Harbin Institute of Technology (Harbin, China) [99-102], National Chiao Tung University (HsinChu, Taiwan) [23,103-108], University of Arizona (Tucson, USA) [43,109-115] and Vavilov State Optical Institute (St. Petersburg, Russia) [25,27,28,37,44, 46-48,56,93,97,98]]. In spite of the apparent resemblance between their researches, each laboratory has its special techniques concerning the manufacturing process of the polymeric materials as well as the selection of optical parameters of the recorded photoinduced structures. The main distinctive characteristic is the method of layer preparation.

The photochemical reaction used in most research centers is based on the free radical bulk polymerization process of a monomer (methylmethacrylate, MMA) with PQ-molecules and a polymerization initiator (usually azo-bis-isobutyrolnitrile, AIBN). The components are composed in different weight ratios, depending on the

particular research institute. The PQ-concentration varies from 0.05 mol.% up to 0.35 mol.%. The basis of the holographic recording is the chain reaction of the radical polymerization providing the photoinduced change of the refractive index and the real-time recording of the particular phase structure [23]. The photoinitiated system absorbs light and generates free radicals. Polymerization of the monomer by free radicals leads to the formation of polymeric chains [20,22,116]. The accompanying diffusion process causes gradients of density and results in the modulation of the refractive index. In some polymeric compositions it is possible to activate additional diffusion, generating thermal enhancement of the grating.

The spectral range of the light illuminating the PQ-containing polymeric media covers the wavelength interval from 350 nm to 600 nm. The effective range of the spectral sensitivity for layers with a thickness of about hundreds microns reduces to 480-540 nm [42,100]. The comparison of the photonic quantum yields in PQ-PMMA for several wavelengths shows that the change of the exciting light from blue to green results in an increase of the quantum yield. This occurs due to the high intermolecular interaction of the light-absorbing centers with the environment and the subsequent increase of the probability for the occurrence of the photochemical reactions [41,109,110,113]. Thereby, the most widely used source of radiation for photoinduced interaction with PQ-PMMA material is the Argon (Ar) laser with a wavelength of 514.5 nm. In some types of PQ-PMMA composites the recording of diffractive structures was observed with laser irradiation at wavelengths of 488 nm and 532 nm [100,115].

The stability of holograms depends on the mobility of the macromolecules, whose increase leads to structure deformation and information loss. The polymers produced in the Institute of St. Petersburg possess minor diffusion during grating recording (the diffusion coefficient of free PQ-molecules is about $10^{-17} \text{cm}^2 / \text{s}$ at 20^oC, and is reaching $10^{-18} \text{cm}^2 / \text{s}$ for macromolecules at the same conditions) [27,44,56]. This reduction of the photoproduct diffusion by an order of magnitude in comparison with the initial PQ-diffusion is due to the increase of the volume of MMA molecules (0.1 nm^3) under photoreaction in the volume of the PQ-molecules (0.15 nm^3-0.18 nm^3) [47]. In the post-exposure period of amplification the diffusion coefficient of the free PQ-molecules increases up to $10^{-15} \text{cm}^2 / \text{s}$ (at 80^oC)

causing diffusion activation, which results in a homogeneous PQ-distribution in the polymeric layer [97]. Thus, faster diffusion of free PQ-molecules leads to a grating amplification during the period of post-exposure. The slower diffusion of macromolecules is responsible for the stable formation of holographic structures.

The change of preparation techniques influences the molecular mobility causing the variation of the process velocity and results in the absence of post-exposure amplification. Samples that are used in Taiwan University possess at room temperature considerably higher diffusion coefficient values ($\approx 10^{-7}\,\mathrm{cm^2/s}$) compared to previous groups [103]. The increase of the diffusion coefficient is caused by several components. The fabrication of polymeric samples is carried out by the prepolymerization technique with subsequent attachment of PQ-radicals either to PMMA or to residual MMA that is available in abundance. Separation of the photochemical reaction during holographic recording from the polymerization of the host monomer molecules during material preparation was made to alleviate shrinkage problems [104]. Such PQ-PMMA materials do not require any post-amplification by annealing; on the contrary the gratings become unstable within few hours by tempering at high temperatures due to an increasing diffusion of both components (PQ-molecules and PQ-MMA groups) [103-105,108]. Moreover, this preparation method allows a small PQ-concentration in the mixture (0.25-0.35 mol.%) causing low values of the diffraction efficiency (one tenth of per cent) that is inefficient for self-trapping generation [23,103,106-108].

Thick PQ-PMMA samples (up to 5 mm) with efficiencies of about several percents after recording and with improved values up to 60 % after tempering amplification were obtained in the Harbin Institute [100-102]. The preparation is based on MMA-PQ polymerization with AIBN as solvent (PQ-concentration is 0.35 mol.%) [101]. Holographic structures recorded with a wavelength of 532 nm showed dark diffusion enhancement of the grating by this PQ-PMMA combination [102]. At Arizona University, using the same preparation method one found a possibility to generate highly efficient photoinduced structures in PQ-PMMA at 488 nm. These structures find a wide application as holographic filters operating at 1550 nm [109-112,114]. Modification of the polymer by the addition of nanoparticles is another way to increase the efficiency of holograms [115]. All these variations generate deep refractive modulation ($\Delta n \approx 10^{-3}$), but scattering

losses increase up to 30 %. Besides, thick samples produced in these research groups possess a significant relief formation and shrinkage (up to several percent of the layer volume) due to compression of the material under light interaction.

The method of radical polymerization used in most research institutes does not let to attain photoinduced structures with 100 % efficiency [42]. One of the reasons is the limited quantity of the photoreduced PQ-molecules that can attach to macromolecules and form photoproducts (usually only ~ 50 % of PQ-molecules take part in the photoreaction). Some portion of the molecules is interacting with a residual monomer forming a low-molecular photoproduct with decreased modulation of the refractive index.

Summing up the obtained data from different research groups it can be noted that the polymerization reaction can be used for preparation of PQ-PMMA samples with large dimensions and moderate refractive-index modulation. But the PQ-concentration is limited in these media causing lower Δn-values. Besides, polymerized PQ-PMMA layers give no complete PQ-photoreaction with the polymeric matrix. Scattering centers as microscopic air bubbles lead to the significant information loss. The dramatic shrinkage distorts the holograms and limits their lifetime [27,104,108]. Thick volume samples cause a high angular and spectral selectivity and could be the reason for the formation of the surface relief. It is seemingly the result of mechanical stress relaxations that lead to macroscopic expansion or compression of the material [19,26,104,105].

One possibility to reduce these undesirable effects and to improve diffraction efficiency of the recorded holographic structures is to use polymeric films with a thickness of hundreds of microns and a high concentration of PQ-molecules, resulting in a significant depth of refractive-index modulation. It entails some complications by using the above presented block polymerization technique with limitated solubility of PQ in MMA (most research groups are using PQ-concentration, which do not contain more than 0.5 mol.% of this addition, resulting in "weak" hologram formation). These difficulties can be solved by preparation of layers with a high dye-concentration and by using a film pouring method with a mixture of PMMA dissolved in an organic solution of PQ-molecules.

Our institute in cooperation with the Minsk University has developed several techniques of layer preparation. The first method based on the photoaddition of PQ-molecules to the purified PMMA, the second one consists in the

polymerization of the monomer. These methods were improved and modified by matching to a good solvent and by optimizing the ratio of components. The main feature of the new methods consists in pouring the liquid viscous PQ-PMMA solution on the glass substrate, followed by a slow drying process. The properties of the polymeric mixture together with specific drying conditions allow to evaporate the solvent completely from the film, saving the high optical quality of the polymeric sample with almost zero disturbing defects. Accordingly, the new method of layer preparation allows to include successfully the PQ-molecules into the polymer with a concentration up to 4 mol.%, which was never obtained before [42,57].

The modifications of the preparation technique and the increase of the PQ-concentration improve the quality of the processes of phase holograms recording, amplification and degradation. The developed PQ-PMMA samples are providing a significantly deeper modulation of the refractive index with a higher n-amplitude and a larger amplification factor during the recording of transmission and reflection holograms with a diffraction efficiency of nearly 100 % [26,42]. The layer preparation by a pouring of the solution provides extra freedom for the variation of material parameters: the films can be produced from polymers with any matched distribution of molecules. A high efficiency of the photoinduced structure in PQ-PMMA materials with long shelf-life due to negligible diffusion of the macromolecules together with nonlinear properties allow to use these polymers for self-trapping purposes.

Several characteristics of the PQ-PMMA medium produced by pouring from the solution were analysed by our research group during recent years [26,42,57,58,117-127]. The main accent was placed on improving the optical quality of the material and on achieving high-efficient and stable diffractive structures. Experimentally it was found that the amplification factor for the transmission grating is usually in the range of 8-9 and the final refractive-index modulation is below $2 \cdot 10^{-3}$ [42]. These values are limited by the initial concentration of PQ-molecules in the polymeric layer. Changing the PQ-concentration from 0.5 mol.% up to 4 mol.% leads to a sixfold increase of Δn [57]. A significant increase of the dye-concentration can cause undesirable formation of low-molecular photoproducts. The presence of PQ-components in large quantities results in a higher probability for the photoreaction between PQ-molecules or for

the PQ interaction with the residual solvent. The investigation of unfavourable effects caused by the PQ-PMMA composition exhibited their negligible contributions for the hologram formation and for the refractive-index modulation. Besides this, dark processes (photoreaction after recording without a radiation source results in amplification or degradation of the grating), scattering noise and considerable effects of shrinkage were not detected in the PQ-PMMA medium during few weeks at room temperature for grating periods of about few microns under slow diffusion processes. It allows high-quality recording and sharp reconstruction of the holograms. Thus, the special PQ-PMMA material produced by our group in cooperation with the Belarusian University possesses good mix of components (e.g. good relationship number of sensitive dye, polymeric matrix and added solvent) and provides the necessary refractive-index modulation in order to produce qualitatively excellent polymeric layers.

A detailed description of the techniques of layer preparation, of the main diffusion characteristics of the produced material will be discussed in the next chapter. Moreover, the influence of the non-sinusoidal profile of the refractive index and of non-local effects as well as of the deformation of surface and volume of the material on the formation of the photoinduced structure will also be examined. Different types of modified PQ-PMMA copolymers prepared by pouring of polymeric solutions in order to generate thin films were analyzed carefully with the aim to select the best composition for stable self-trapping generation.

Chapter 4   Polymeric Media Based on Polymethylmethacrylate with Distributed Phenanthrenequinone Molecules

A simple composition of the polymeric compound material with favourable adhesion properties, an easy mechanism for the formation of holograms and for the corresponding preparation methods using only modest temperatures are the necessary requirements for the production of a medium which is best suited for the generation of self-trapping. The use of unstable photorefractive media with a short storage time can result in defects of the recorded photoinduced structure and can negatively influence on the holograms. Therefore, the production of PQ-PMMA layers with a high concentration of dye-components by pouring of liquid polymeric mixture on glass substrates – as described in chapter 3 – is a major advancement for optical information processing and for holographic interferometry. This ensures to reduce shrinkage and scattering damages of the medium and to enlarge the modulation of the refractive index. By applying a new preparation process, samples with a good combination of physical and holographic characteristics for direct interaction of light and medium were obtained.

In this chapter we present an extensive investigation of the polymeric compositions based on PQ-molecules distributed in the PMMA matrix. Modifications of the necessary copolymer (CP) were performed by two different methods, using either a purified PMMA-polymer or a polymerized MMA-monomer. Surveying and recording of the diffractive structures generated in photorefractive materials allows to select the most stable polymeric composition with best optical and thermal properties for the application of self-trapping.

4.1. Preparation of PQ-PMMA samples and recording of holograms

4.1.1. Formation of polymeric layers with a large PQ-concentration excluding polymerization process

The first method for the preparation of layers that will be discussed in this chapter is a technologically more straight-forward technique based on the addition of a PQ-dopant to the polymeric chain (PMMA) without exploiting the polymerization process. It consists of the formation of films from a liquid solution of PQ-molecules dissolved in a polymer with subsequent drying of the sample under special conditions. The used PMMA was purified from the monomer. By this procedure a reaction between PQ and MMA-links is avoided and a contribution of "negative" gratings to the recording process is excluded [42]. In this way the degree of attaching of the PQ-molecules to the polymeric layer by the impact of light is close to 100 %.

The developed PQ-PMMA chains are long enough for the material to be considered as a polymer (the mean number of monomer units per chain is approximately equal to 300, which is larger than the critical number of about 180 for the simpler PMMA chain) [46,47]. The PQ-PMMA composition consists of a molar mass of $100\,\text{g}/\text{mol}$ for PMMA $[(C_5H_8O_2)_n]$ and of $208\,\text{g}/\text{mol}$ for PQ $[C_{14}H_8O_2]$. The density of the polymer is $1.19\,\text{g}/\text{cm}^3$, and the refractive index of PMMA is equal to 1.49, which is close to the refractive index of glass. With this material, polymeric films can be produced on silicate-glass substrates with negligible influence of the glass on the reconstructed holographic image. The polymer based on purified PMMA with PQ-molecules is called hereafter briefly PQ-PMMA.

For the preparation of layers, the components were weighed in necessary proportions and dissolved in an organic solvent (chloroform). Usually for a polymeric layer thickness of 100 μm a 10 % PMMA solution with an addition of PQ of about 2-4 mol.% of the amount of the polymer was used. The solution was filtrated after mixing in order to decrease the quantity of light-scattering centers. The glass substrates were coated with the liquid solution of the various ingredients to form polymeric films of the necessary dimensions and shape. The mechanical rigidity that is required for holographic application was obtained by subsequent

drying. For a slow removal of the solvent, the samples were placed in a Petri dish for 20 hours at temperatures of $100^{o}C$, which is below the glass transition temperature of the PMMA ($105^{o}C$) [118].

The thickness of the layers was limited by the mechanical properties obtained by the process of film deposition. This is caused by the inability to prepare and to fix uniform polymeric layers with thicknesses up to a few tens of millimetres. Therefore, the average thickness of the PQ-PMMA samples used for the following experiments varied from 100 µm up to 500 µm [Fig. 4.1].
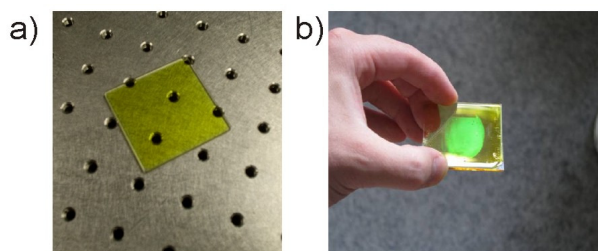

Fig. 4.1. [a] A PQ-PMMA polymeric sample [layer thickness is 100 µm; PQ-concentration is 3 mol.%] and [b] reflection at day light of the diffractive structure formed in a PQ-PMMA layer.

The method of layer preparation by pouring allows to deposit several molar percents of the PQ-molecules into the polymeric matrix. The majority of the samples discussed in the literature were produced by the solution of a block of polymerized MMA-monomer embedded in the moulding box. This process limits the dye-concentration to maximum 0.5 mol.% by the solubility of PQ in the monomer. A good matching of polymeric ingredients and solvent allows to achieve successfully concentration values up to $5 \cdot 10^{-4}$ mol/cm^3, resulting in a higher efficiency of the diffractive structure [57]. Approaching the critical value of 4-5 mol.% of PQ-concentration produces an undesirable heterogeneity of the PQ-distribution in the sample and results in a high probability for activation of the processes of layer crystallization which can destroy the polymer. In the presented experiments we used a PQ-concentration of about 2.5-3 mol.% resulting in high values of the amplitude modulation of the refractive index (up to $\Delta n \approx 10^{-4}$) and in sharp grating recording.

The amount of the spectral sensitivity of a polymeric layer is determined by the sensitive dye added to the polymeric matrix. Typical optical absorptions of the PQ-PMMA samples before exposure and after illumination by green light (514.5 nm) are shown in Fig. 4.2. The absorption factor is determined as the logarithmical ratio of the input (I_{in}) to the transmitted (I_{out}) intensities [$lg(I_{in}/I_{out})$]. The PQ-PMMA samples show a strong absorption below the green wavelength and a

significant absorption coefficient in the wavelength range from 480 nm up to 520-530 nm [42]. The samples are totally transparent for wavelengths longer than 540 nm. Under exposure by Ar-laser radiation the PQ-dopant changes its chemical structure by forming a photoproduct. At the same time, the initially yellowish samples become transparent. Moreover, the absorption band of the PQ-PMMA layer shifts to the blue range. The illuminated samples show absorption only in the UV regime. The change of absorption of the PQs and of the photoproduct is evidence of the difference between their refractive indices in the whole visible spectrum and a proof of hologram formation.
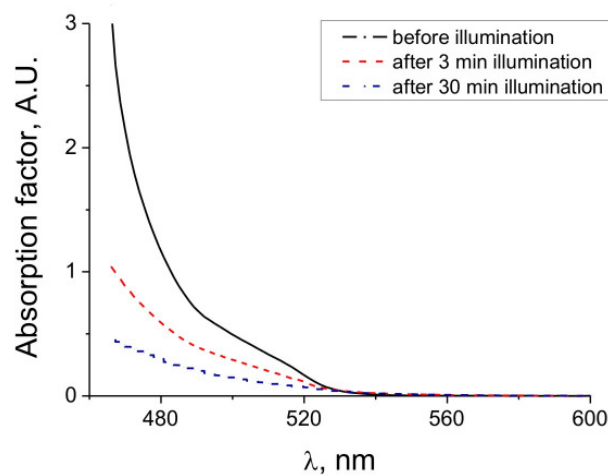

Fig. 4.2. Spectral dependences of the absorption of a PQ-PMMA sample before Ar-laser illumination and after 3 min and 30 min of exposure time, respectively [PQ-concentration is 3 mol.%, input intensity is $60 \, mW / cm^2$ at 514.5 nm].

4.1.2. Recording and reconstruction of diffractive structures

The investigations of the photosensitive material by the holographic relaxation technique enable to observe the temporal evolution of a diffractive structure and to detect even very slow diffusion processes [39,46]. This holographic principle is the most common technique to record coherent interference patterns of the object wave with a reference wave in the photosensitive material with subsequent reconstruction of the hologram due to light diffraction at the recorded interference structure. Moreover, it allows the recording of both, photoinduced reflection and transmission gratings, in the bulk of the material. Volume holograms provide the opportunity to save the information in the whole volume of the medium, thus

representing an optical memory with ultrahigh capacity and low probability for an unwanted damaging of separate parts of the hologram.
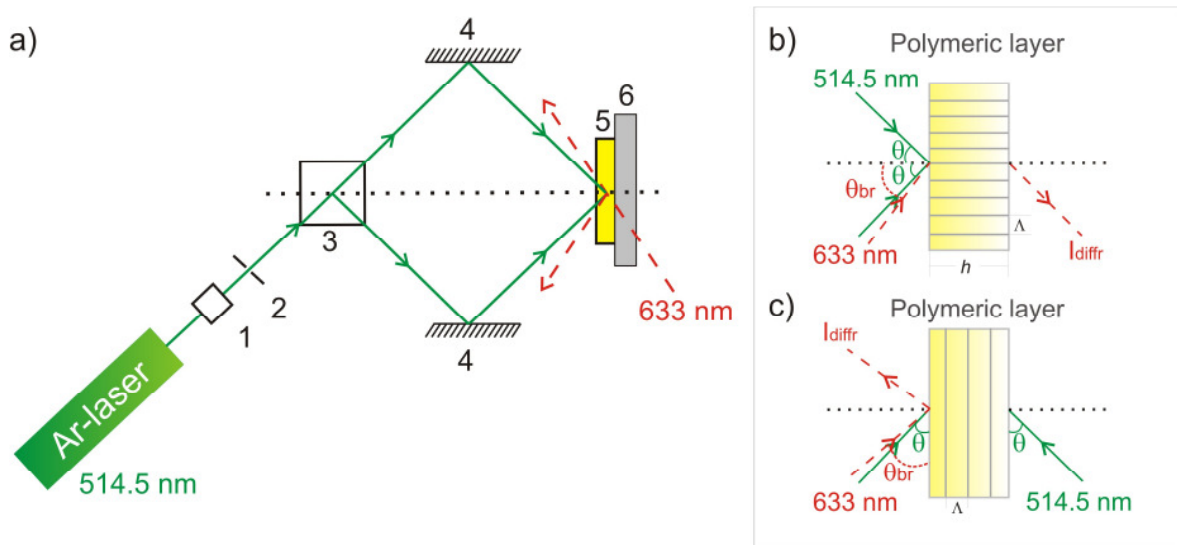

Fig. 4.3. Scheme of the experimental setup for recording and reconstruction of holograms for the case of [a] and [b] transmission gratings and [c] reflection grating in a polymer [(1) collimator, (2) diaphragm, (3) beam splitter, (4) mirrors, (5) glass substrate with a recording layer, (6) precision rotary table]. Recording is performed by an Ar-laser (514.5 nm), reconstruction by a He-Ne laser (633 nm); I_{diffr} denotes the intensity of the diffracted beam, Λ is the grating period, and h is the thickness of the layer.

The experimental setup for recording and reconstructing of holographic gratings is shown in Fig. 4.3 [a]. The reference and object waves are represented by plane waves converging at an angle 2θ in the recording layer and generating an interference pattern. The source of the monochromatic radiation is an Ar-laser with a wavelength of 514.5 nm and a coherent length of about 30 cm. The temporal and spatial coherence values of the source were proven with a Michelson-Young interferometer, correspondingly. Using collimator (1), diaphragm (2), beam splitter (3) and two reflecting mirrors (4), two coherent light beams with an intensity ratio of 1:1 can be extracted. They interfere in the plane of the polymeric sample (5) recording a symmetric phase structure. The simple method of recording by an angular variation between both beams – as indicated in the figure by green lines – makes it possible to exactly control the grating period during the hologram recording. The intensity of each of the input beams has been chosen to be equal to $30\,mW\,/\,cm^2$ for layers with thicknesses of about a few hundreds of microns. A system of different filters is used, if necessary, to block one or both beams as well as to multiple weaken the beam power. The aperture of the incident beams is limited by a diaphragm with 5 mm hole diameter.

In most cases during hologram formation the smallest distance between grating lines is approximately equal to the used light wavelength [128]. It follows that the displacement of photographic material during exposure time should be smaller than a certain percentage of the wavelength. The interferometric stability of the sample is provided by thorough and reliable fastening of the recording polymeric film on the vibration-insulated optical table. Acoustical and thermal perturbations by the ambient air may also cause instabilities of the interference pattern. To reduce the influence of these factors the optical path length (especially between beam splitter and hologram) is usually chosen as small as possible. Decrease of the exposure time has also a positive influence on the mechanical stability reducing perturbations by the environment.

In spite of the irradiation by an Ar-laser at the edge of the material absorption band, it is possible to generate highly efficient holographic gratings in the PQ-PMMA medium by transmission as well as by reflection of laser light [57]. Recording of a transmission hologram applying a symmetrical scheme occurs by interference of object and reference waves, incident on the recording medium from one side under the same angle θ to the normal direction of the film [Fig. 4.3 [b]]. By reconstruction of the transmission hologram a diffracted wave (I_{diffr}) is observed in the transmitted light. The distance between two adjacent intensity maxima of the recorded interference pattern determines the grating period (Λ).

Figure 4.3 [c] demonstrates the principle of the recording and reconstruction of the reflection hologram, when object and reference waves are incident on the medium from opposite sides. The reconstruction of such a grating provides the diffracted wave in reflection. Reflection holograms are widely used in applications of holography and displays. The volume properties (spectral and angular selectivity) of the recorded structure gives a possibilities to use a source with a continuous spectrum (standard incandescent lamp, sun) for the reconstruction of the object wave [Fig. 4.1 [b] , p.36]. Nevertheless, basic measurements are usually carried out at a high-frequency transmission grating. Reflection holograms are used less because of their high sensitivity to the variations of the average refractive index and to the sample deformations occurring during material processing [97,110].

Thus, the recording of the spatial periodical structure can be observed due to the photophysical and photochemical processes in the polymeric medium caused by the interaction of light with the medium. The relaxation of the holographic grating can be detected by the evolution of the light beam diffracted at the photoinduced structure.

The diffraction efficiency (η) of the recorded structure is defined by the fraction of the diffracted wave radiation. This characteristic feature represents an important experimental parameter, which depends on hologram type, medium properties and conditions of recording and reconstruction of the grating. The general definition of the diffraction efficiency is given as the ratio of the diffracted beam intensity (I_{diffr}) to the incident intensity (I_0) and obeys the expression [20,128]:

$$\eta = \frac{I_{diffr}}{I_0}.$$ 4.1

To solve technical and experimental problems another parameter is playing an important goal: the ratio of the intensity of the diffracted beam to the total output intensity behind the holographic grating ($\eta = I_{diffr}/(I_{tr} + I_{diffr})$, I_{tr} is the intensity of the beam transmitted without diffraction) [57]. With this definition of the diffraction efficiency the Fresnel reflection losses are already taken into account.

The absence of absorption can be demonstrated by using a Helium-Neon (He-Ne) laser as reconstruction radiation with a wavelength of 633 nm, for which the PQ-PMMA layer is transparent. A collimated beam of monochromatic He-Ne light is falling on the surface of the hologram which is mounted on the rotary table as part of the optical setup for reconstruction of holograms [Figs.4.3 [b] and [c]]. By turning the hologram relative to the direction of the incident laser beam the maximum light intensity can be achieved to measure the zero-order intensities of the diffracted beams using photodetectors.

The maximum intensity of the diffracted wave is defined by the Bragg condition [88]:

$$2\Lambda \sin\theta = m\lambda,$$ 4.2

with the grating period Λ, the angle θ between the direction of the wave propagation and the grating plane and the wavelength of the incident radiation λ. The magnitude $m = 1,2,3,..$ determines the diffraction order of the periodical

structure of the grating. Equation 4.2 describes for the order $m = 1$ the condition of the principal maximum of the diffracted wave for generating the volume hologram. The deviation from the Bragg's law results in reduced diffraction intensity and determines the selective properties of the hologram.

The Kogelnik formula connects the diffraction efficiency with the amplitude modulation of the refractive index (Δn) of a transmission phase grating as follows [57,88]:

$$\Delta n = \frac{\lambda \cos\theta \cdot \arcsin(\sqrt{\eta})}{\pi \cdot h},$$ 4.3

where h is the thickness of the layer. The ratio between the spatial frequency and the thickness of the layer describes the hologram type. It determines the main properties of the diffractive structure (angular and spectral selectivity, diffraction efficiency) and can be characterized by the Klein parameter (Q) [128]:

$$Q = \frac{2\pi\lambda h}{n\Lambda^2}.$$ 4.4

For Q<1 the hologram is assumed to be optically thin, whereas for Q>10 the hologram is representing a volume and for Q>1000 one gets a three-dimensional highly selective hologram.

Changes of the composition of the polymeric media vary the ability of the diffractive structure recording. Each photorefractive material requires a special amount of energy per volume to generate a stable and efficient hologram. The magnitude of the power for the light exposure (W) can be defined as:

$$W = \frac{P \cdot t_e}{\pi \cdot x_0^2},$$ 4.5

where P is the summarized power of both beams, t_e is the recording time and x_0 is the beam radius. Increasing the power of exposure results in an increase of the modulation of the refractive index till to saturation.

During hologram formation the recording of the gratings occurs till maximal diffraction efficiency is achieved. Thermally amplified PQ-PMMA layers can be fixed by the incoherent irradiation of the PQ-molecules by the absorption band. The homogeneous illumination of the polymer leads to a complete phototransformation of unreacted PQ-molecules which are uniformly distributed in

the sample. An exposure causes decreasing of the optical density for wavelengths in the range of the PQ-absorption band, but the resulting modulation of the refractive index Δn of the grating is preserved. The holographic structure is fixed and stable towards the interaction of outer radiation.

4.2. Characteristics of holograms recorded in PQ-PMMA

4.2.1. Kinetics of holographic grating formation and amplification

Experimental investigations concern first of all the recording of holographic transmission gratings in polymeric layers and the observation of the efficiency and modulation depth of the refractive index under photoinduced processes. During the experiments several samples of this type based on purified PMMA with a PQ-concentration up to 3 mol.% were prepared and series of equal holograms were recorded. Figure 4.4 presents a typical dependence of the modulation of the refractive index on the irradiance (power of exposure per area) during recording of a holographic grating with 3 μm period. The values of Δn are based on the experimentally obtained diffraction efficiency values [Eq. 4.3, p.41]. The refractive-index modulation exhibits a monotonic increase up to a maximum value of Δn that is attained already at a power of exposure of $10\,\mathrm{J/cm^2}$ [Fig. 4.4 [a]]. The photoattachment of the PQ to the polymer and the formation of the phenanthrene structures result in a stable photoinduced pattern.
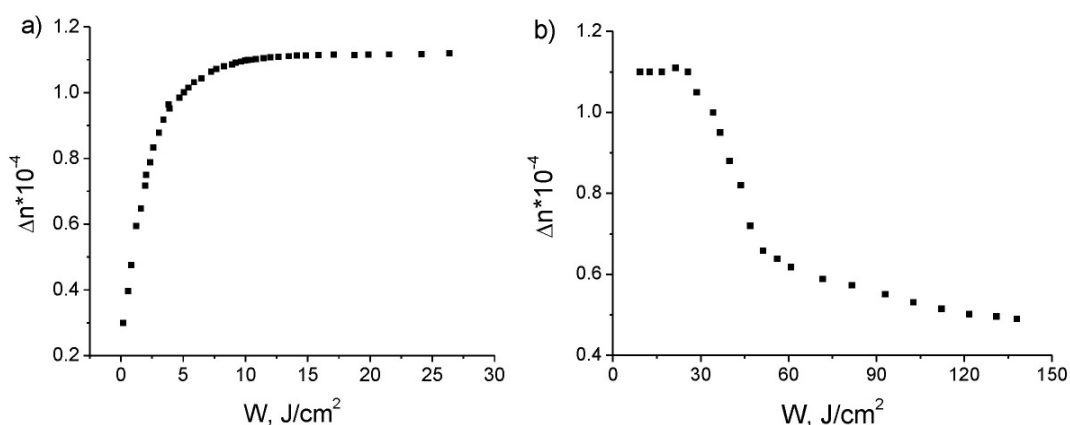

Fig. 4.4. Experimentally determined dependence of the modulation of the refractive index versus power of exposure [a] during recording of the transmission grating till the maximum and [b] slow degradation of the grating [PQ-concentration is 2.5 mol.%, layer thickness is 100 μm, grating period is 3 μm]. The measurements are made with an accuracy of 5 %.

The saturation of the refractive-index modulation is achieved at $\Delta n \approx 1.1 \cdot 10^{-4}$ and starts to decrease again at an irradiance of $30\,J/cm^2$, leading to a slow degradation of the diffractive structure [Fig. 4.4 [b]]. The maximum values of the refractive-index modulation that were obtained during grating recording by the variations of the parameters were $(4 \div 5) \cdot 10^{-4}$.

The main advantage of a PQ-containing holographic media consists of the possibility of their post-exposure amplification. An initially stable but not with maximum efficiency recorded grating can afterwards be enhanced and improved by a subsequent annealing process. After recording, weak holographic structures possess minor defects or distortions. Activation of the diffusion or a corresponding increase of the diffusion rate of PQ-molecules at higher temperatures causes a post-exposure thermal amplification of the grating and an increase of the diffraction efficiency by orders of magnitudes. Post-exposure treatment is usually started several minutes after the recording process, thus excluding any intermediate change of the holographic structure. Measuring the diffraction efficiency directly after the holographic recording and just before the heating process starts confirms that no hologram degradation happens in between.

The processes of thermal enhancement carried out for temperature variations from 55^oC up to 90^oC. The temperature was chosen below the PMMA-glass transition temperature to save the initial rigidity of the polymer, but not lower than 50^oC where the diffusion rate is considerably slower. The values of amplitude modulation of n are increasing ten times due to heating ($\Delta n_{max} \approx 2 \cdot 10^{-3}$). Therefore, this technique provides the recording of highly efficient holograms in the PQ-PMMA samples under investigation.

Previous experiments with the PQ-PMMA medium showed that the spatial distribution profile of the optical parameters (refractive index and absorption coefficient) during recording of the holograms is different from the sine-distribution of the light intensity of the interference pattern [57]. To proof the character of this nonsinusoidal profile, one can observe the numerous diffraction orders (up to 5-6 orders) already at the initial step of grating recording [57,58,93]. This phenomenon is not typical for volume holograms which are characterized by a single nonzero diffraction order only [25]. This nonsinusoidal effect can be explained as a result of

the overlapping of the interferences fields on the same aria of the material with different spatial periods. In other words, by recording of one grating one can note the generation of several gratings with spatial frequencies multiplied by the recorded grating frequency [58]. Experimental investigation of the optical density of PQ-PMMA layers demonstrated the nonlinear behaviour of the PQ-consumption during photoreaction exposure. This nonlinearity results in the distortion of the refractive-index profile and in its deviation from the sinusoidal distribution, as provided by the interference pattern. The occurrence of the multiplied gratings are reducing the 1st-grating maximum of the generated diffractive structure and are limiting the magnitude of Δn, compared with the otherwise possible maximum [42].
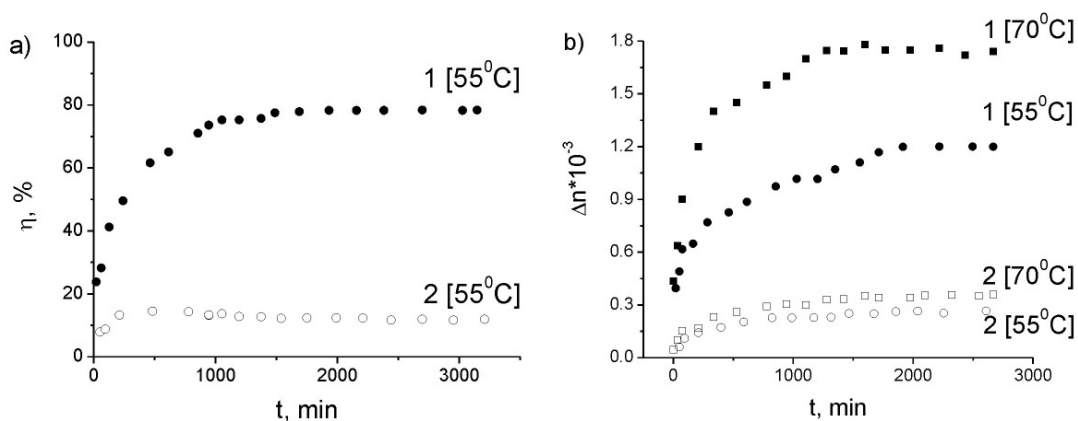

Fig. 4.5. [a] Dependence of the diffraction efficiency and [b] dependence of the amplitude modulation of the refractive index versus annealing time for the transmission gratings with periods of [a] 1.2 µm (1) and 0.6 µm (2) and [b] 2.4 µm (1) and 1.2 µm (2) [PQ-concentration is 2.5 mol.%; layer thickness is 125 µm, power of exposure is 12 J/cm^2]. The measurements are made with an accuracy of 5 %.

Figure 4.5 [a] presents the diffraction behaviour of the dependence of the gratings diffraction efficiency on the annealing time at $55^{o}C$. A rapid strengthening of the hologram occurs for the first grating (1 [$55^{o}C$]) up to a maximum of diffraction efficiency of 80 %. Saturation was reached after 25 hours of heating and remained stable in time. A maximum of the second grating (2 [$55^{o}C$]) of almost one order of magnitude lower was obtained already in the early stages of the grating amplification and stayed constant for a very long time.

The dependences of the modulation of the refractive index on temperatures of the post-exposure annealing of $55^{o}C$ and $70^{o}C$ are demonstrated in Fig. 4.5 [b]. Almost immediately after exposure, Δn of the second holograms (2 [$55^{o}C$] and

2 [70°C]) does not exceed $0.3 \cdot 10^{-3}$. Under heating Δn grows by an order of magnitude with a similar slope as the increase of the diffraction efficiency η. As can be seen in Fig. 4.5 [b], the rate of change of the amplification process depends weakly on temperature. The rise of Δn, approaching saturation, is only slightly faster at 70°C for the first grating (1 [70°C]) as compared with that of the thermal annealing at 55°C (1 [55°C]), whereas no clear difference was observed for the second generated gratings. Series of experiments under different heating conditions (up to 90°C) have proved that a variation of the temperature for the post-exposure annealing does not significantly influence the magnitude of the Δn-maximum. However, the lower the temperature, the slower is in general the amplification process, but the maximal efficiency is the same. This dependence of the enhancement velocity on temperature is associated with the acceleration of diffusive molecular motion, resulting in the development and the amplification of the hologram, but also in its faster destruction. The speed of grating amplification is determined by the unreacted PQ-molecules, uniformly distributed throughout the sample. This process depends on all experimental conditions, like material composition, pre-treatment, annealing temperature and spatial frequency of the hologram.
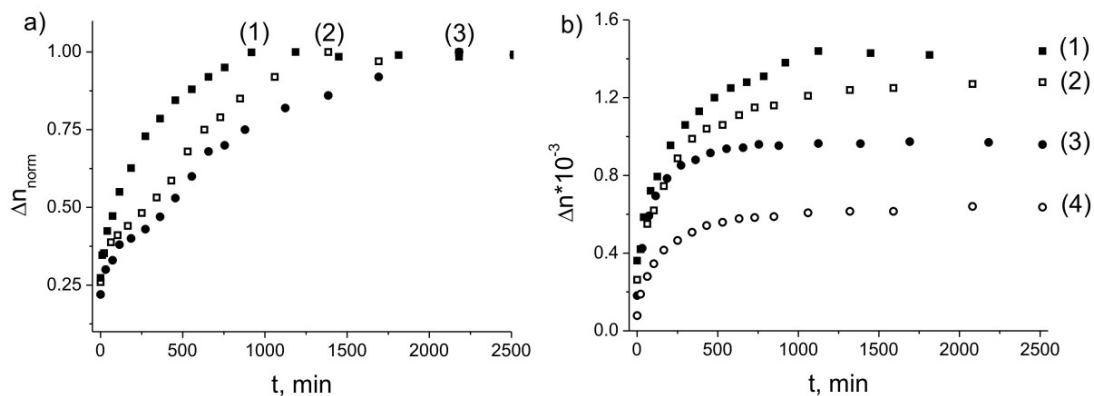

Fig. 4.6. [a] Dependence of the normalized and [b] dependence of the non-normalized modulation of the refractive index on the annealing time at a temperature of 70°C: [a] corresponds to an irradiance of 12 J/cm^2 and various grating periods of 1.5 µm (1), 2 µm (2) and 3 µm (3); [b] corresponds to a grating period of 1.5 µm and different powers of exposure of 12 J/cm^2 (1), 7 J/cm^2 (2), 3.2 J/cm^2 (3) and 1.5 J/cm^2 (4). [PQ-concentration is 2.5 mol.%, layers thickness is 125 µm]. The measurements are made with an accuracy of 5 %.

Variations of the spatial frequency of the hologram are substantially influencing the amplification process. Figure 4.6 [a] presents the behaviour of the normalized to the maximum refractive-index modulation versus time. The small differences of the grating periods are effecting the annealing time of post-exposure hologram amplification. The decrease of the period of diffractive structures causes a reduction of the time for achieving the maximum modulation of the refractive index. Thus, the higher the spatial frequency and temperature of the post-exposure process, the faster the saturation of the efficiency.

A correct selection of the energy of the incident laser light is very important to get optimum Δn-values of the polymeric medium. Figure 4.6 [b] exhibits typical experimental curves for the dependence of the refractive-index modulation under thermal annealing at 70°C and for a $1.5\,\mu\text{m}$ grating period on different power values of exposure. By increasing the irradiance or the time of post-exposure heating, correspondingly, the phase modulation of the transmission holograms is amplified gradually till saturation. These saturation maxima are stronger with increasing power strength of exposure. As can be seen from Fig. 4.6 [b], a variation of the exposure from $1.5\,\text{J}/\text{cm}^2$ to $12\,\text{J}/\text{cm}^2$ and the corresponding enhancement of heating results in an amplification of the Δn-maxima by more than a factor of two, thereby leading to a deeper modulation of the refractive index of the recorded hologram.

Experimentally we detected a nearly negligible volume variation of the PQ-PMMA material during thermal amplification. Moreover, a small shrinkage of the polymeric layers was found as difference of the thickness of exposed and unexposed areas of the sample. This is a result of the initial material compression due to its interaction with light and the following expansion of the polymer by thermal treatment (formation of a surface relief). The advantage of the method of pouring a liquid PQ-PMMA solution on the surface consists in the negligible shrinkage of the material, which is by an order of magnitude smaller than in the case of the block-preparation process based on MMA polymerization. For example, the technique of bulk-polymerization leads to a shrinkage of about 0.03 % even during the recording process, which can easily increase in some cases up to several percents [109]. In contrast, according to our experimental results, PQ-PMMA layers with thicknesses of hundreds of microns do not reveal

any volume modulation during recording of the grating and show shrinkage values of only about 0.002 % during post-exposure amplification at rather high temperatures of $80^{\circ}C$. This negligible shrinkage practically excludes any variation of the photoinduced refractive-index modulation and can also be related with ageing or mechanical stresses of the polymeric material [46,110]. This is similar to the diffusion of elements of the free volume (or the residual solvent) in the direction of minimum (dark area) or of maximum illumination (light area) with small diffusion coefficients and does not distort the kinetics of the PQ-PMMA medium.

4.2.2. Diffusion of PQ-molecules during recording, enhancement and stabilization of holograms

The recording of the interference pattern in polymeric media due to photophysical and photochemical reactions with following amplification of the grating generates sufficient gradients of concentrations. It is possible to detect even slow diffusion processes in polymers by observation of the evolution of a periodical structure. The characteristic length of the grating period can be varied by changing the geometry of the optical scheme. The dependence of the rate of change of the amplification process on the spatial period length defines the diffusion action.

Based on experimental data we conclude that under laser illumination the diffusion of both PQ-molecules and photoproducts results in the formation of the periodical structure in the medium. After the recording process the fabricated grating is stable due to the large size of the macromolecules, which are practically immobile as compared with the much smaller PQ-molecules. The thermal enhancement of the holographic grating is the result of an accelerated process of increased mean velocity at which PQ-molecules diffuse. A possible contribution of photoinduced radicals to the diffusion mechanism causing a regression of the latent image was not observed by us, in contrast to the results obtained in [46]. A diffusion of low-molecular products can also be excluded, because of the absence of processes of dark degradation after recording of the gratings. The observed lack of the diffusion of additive compounds of radicals and low-molecular substances can be associated with the matching of pure and contamination-free solvent and a high degree of PQ-adherence to the polymeric matrix.

The evolution of the diffusion coefficient of PQ-molecules during grating recording is shown in Fig. 4.7 [a]. The change of the diffusion coefficient due to light exposure was obtained by an approximation of the recording kinetics of the holograms. Due to small migrations of PQ-molecules by diffusion it becomes possible to detect extremely low values of D (close to $10^{-16}\,cm^2/s$). The photoattachment of PQ-molecules to the polymeric matrix is responsible for a decrease of its concentration under exposure. The diffusion coefficient for the PQ-molecules amounts to values of $10^{-17}\,cm^2/s$ during illumination. As mentioned already, the magnitude of the diffusion coefficient of the photoproducts during the process of photoattaching is an order of magnitude lower than that of the PQ-molecules and amounts to $10^{-18}\,cm^2/s$. It is a result of two-times larger size of the photoproduct molecules in compare with dye-molecules.
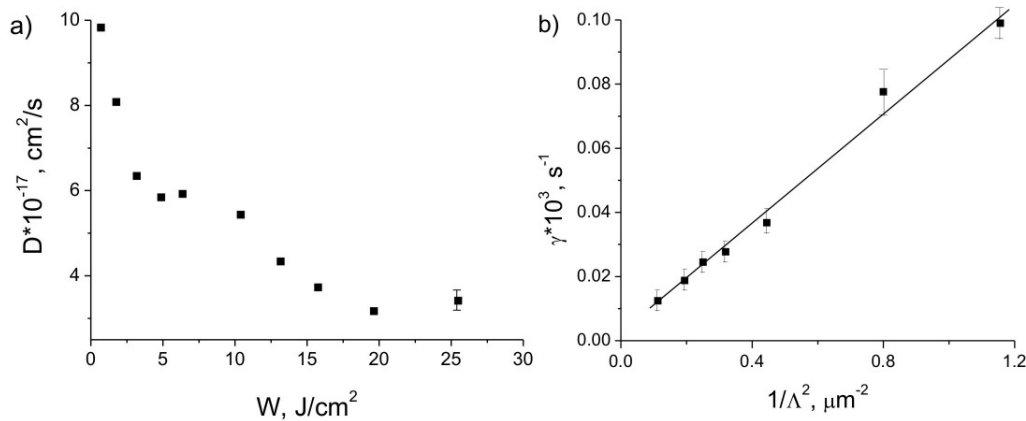

Fig. 4.7. [a] Diffusion coefficient versus power of light exposure W during recording of a grating with a 3 µm period; [b] rate of change of the amplification process γ versus Λ^{-2}, where Λ denotes the grating period [PQ-concentration is 3 mol.%, layer thickness is 100 µm].

The following process of thermal amplification occurs due to the diffusion of unreacted PQ-components and results in their homogeneous distribution within the polymeric layer. The experimental curves of Fig. 4.5 [b], p.44 show the dependence of the modulation of the refractive index on the amplification time. They can be described by an exponential expression, taking into account the diffusion of the PQ-molecules [26,27,58]:

$$\Delta n = \Delta n_0 + H \cdot exp[-\gamma t] \,, \qquad\qquad 4.6$$

where Δn_0 corresponds to the modulation of the refractive index at the end of the diffusion processes, γ is the diffusion-rate constant of the grating amplification, H is a parameter characterizing the contribution of the amplification process. Approximation of the experimental dependence by Eq. 4.6 helps to extrapolate empirical parameters of the thermal amplification process.

The dependence of γ on the grating period indicates its diffusive nature. According to Eq. 3.5, p.23, the dependence of the magnitude of γ on Λ^{-2} has a linear character. The amplification kinetics of the holograms with different periods were approximated by Eq. 4.6. There is the directly proportional dependence of the rate of change of the amplification process on the inversely square of the grating period [Fig. 4.7 [b]]. The linear increase of γ with Λ^{-2} confirms the assumption about the nature of a single-component diffusion process during thermal annealing.

Thereby, the achievement of the maximum of the hologram amplification can be regarded as a uniform distribution of PQ-molecules in the polymeric layer. Thus, the fixation of the periodical structure by incoherent radiation with wavelengths in the range of the PQ-absorption band leads to the complete phototransformation of the unreacted dye-molecules.

To achieve stability of the amplified hologram by the following fixation process without any change of its refractive-index parameters requires the complete enhancement of the previously formed periodical structure. The detection of the degree of the diffusion-amplification process one can carry out by the observation of the Δn-evolution. The values of the refractive-index modulation immediately after the hologram recording (Δn_e) are directly connected to changes of the PQ-concentration (ΔC_{PQ}) and to the refraction coefficients of the components [58]:

$$\Delta n_e = \frac{(n^2+2)^2}{6 \cdot n} \Delta C_{PQ}(t) \cdot [R_{HPQR} - R_{PQ}]. \qquad 4.7$$

To estimate the molar refraction values of the PQ-molecules and the probability for their attachment to the photoproduct molecules, one can use the technique based on the property of refraction additivity to the group contribution [42,129].

Smaller differences between the molar refractions of the initial material and of the photoproduct produce larger amplitude-modulation coefficients. The result of the calculation provides the following values of the refraction coefficients for the photoproduct: $R_{HPQR} = 62.9 \, cm^3 / mol$ and for the PQ-molecules: $R_{PQ} = 61.5 \, cm^3 / mol$ [42,58]. In spite of the small difference of the refraction coefficients of photoproduct and PQ ($\Delta R = 1.4 \, cm^3 / mol$) one can determine the degree of completeness of the diffusion process applying fixation of the hologram by light at different stages of the thermal amplification process. If the distribution of PQ in a layer is homogeneous at the end of the thermal enhancing process, the continuous irradiation with wavelengths in the PQ-absorption band will cause the uniform binding of PQ to the photoproduct. Illumination of the layer will not lead to any changes of the amplitude modulation of the refractive index. In the case of an incomplete diffusion process during the irradiation by incoherent illumination one can observe the transformation of PQ-molecules, which are distributed in the layer volume, to the light-insensitive photoproduct. Meanwhile the values of amplitude modulation of the refractive index will decrease.

The range of possible variations of the refractive-index modulation during the fixation process lies between $0 \le \Delta \le \Delta n_e$ [Eq. 4.7]. During the diffusion amplification process proceeding in the polymeric layer the amplitude modulation of the refractive index is given as:

$$\Delta n_{during} = \frac{(n^2 + 2)^2}{6 \cdot n} \Delta C_{PQ}(t) \cdot [R_{HPQR} - R_{PQ} \cdot \exp[-\gamma(t - t_e)]] \,. \qquad 4.8$$

After complete addition of PQ-molecules to a polymeric matrix the amplitude modulation of n becomes equal to:

$$\Delta n_{after} = \frac{(n^2 + 2)^2}{6 \cdot n} \Delta C_{PQ}(t) \cdot [R_{HPQR} - R_{HPQR} \cdot \exp[-\gamma(t - t_e)]] \,. \qquad 4.9$$

The difference between the two previous expressions [Eq. 4.8 and Eq. 4.9] will provide the reduction of the refractive-index modulation due to a homogeneous fixation process (Δ). By comparing it with Eq. 4.7 one notices that the decrease of the Δ-modulation during the diffusion amplification process depends on the value of Δn_e in the following form:

$$\Delta = \Delta n_e \cdot \exp[-\gamma(t - t_e)]].$$ 4.10

As an experimental proof, several holographic gratings with different amplification ratios under the thermal process at $55^\circ C$ were exposed by homogeneous Ar-laser illumination. Figure 4.8 [a] presents the amplification kinetics of the partially enhanced sample with a 3 μm grating period. A sharp decrease of Δn at the initial time of the homogenous fixation occurs as a result of incomplete thermal amplification of the hologram before irradiation. The large quantity of the unreacted PQ-molecules leads to their transformation to the light-insensitive photoproducts with a directly decreasing refractive-index modulation. The following annealing process at higher temperatures (up to $70^\circ C$) has no influence on the grating efficiency.
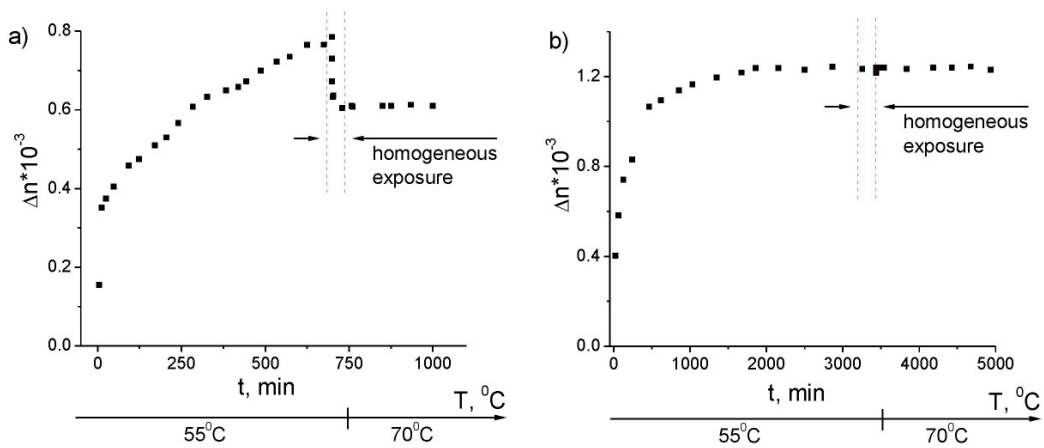
Fig. 4.8. Dependences of the amplitude modulation of the refractive index on the annealing time for samples irradiated by homogeneous Ar-laser radiation [PQ-concentration is 2.5 mol.%, layers thickness is 130 μm, grating period is 3 μm]. Annealing process was occurred under $55^\circ C$ temperature before a homogeneous exposure and under $70^\circ C$ after exposure]. The measurements are made with an accuracy of 5 %.

In Fig. 4.8 [b] one can observe a similar process for the case of a completely amplified holographic grating. The kinetics stays stable under exposure confirming a homogeneous distribution of the PQ-molecules in the polymeric layer at the end of the process. Besides, fixation results in a high stability of the generated periodical structure against the surrounding illumination and produces effective holographic elements with constant optical properties.

Numerical calculations confirmed our experimental data. For the case of an incomplete diffusion process [Fig. 4.8 [a]], Eq. 4.10 leads to the result:

$\Delta_{numer} = 1.72 \cdot 10^{-5}$ with the parameters $\gamma = 4.8 \cdot 10^{-3} s^{-1}$, $\Delta n_e = 1.7 \cdot 10^{-4}$, $t_e = 65\,s$ and $t = 57.2\,h$. An approximation of the experimental results by Eq. 4.10 gives the value $\Delta_{exper} = 1.96 \cdot 10^{-5}$, which is close to the numerical one. Similarly, in the case of a complete diffusion process [Fig. 4.8 [b]] one obtains $\Delta_{numer} = 0$ ($\gamma = 1.11 \cdot 10^{-5} s^{-1}$, $\Delta n_e = 4.03 \cdot 10^{-4}$, $t_e = 65\,s$, $t = 58.2\,h$) that is in a good agreement with experiment, because the decrease of the amplitude modulation of the refractive index was not observed.

Thus, despite of the small difference of the refraction coefficients of PQ and photoproduct, homogeneous exposure enables to fix sufficiently any changes of the amplitude modulation of the refractive index and to realize the diffusion process entirely. The complete grating amplification requires approximately 20-30 hours of annealing at $55^o C$, depending on the grating period. This can be accelerated by applying higher temperatures (at $70^o C$ the grating is amplified already within 10-15 hours). The fixation of the periodical structure after its complete amplification can be done by uniform irradiation. The recorded amplified and fixed grating is temporally stable in case of a variation of the surrounding conditions (increasing temperature, additional illumination).

4.3. PQ-P(MMA) samples and modified copolymer (CP)

High-quality glass-like polymeric materials with their excellent optical properties can be used in various fields, e.g. for telecommunication or as holographic displays and channel formation with the aim of storage of information and data transfer. Most of these applications require high thermal and adhesion properties of the media. The possibility to use thin, transparent and contamination-free polymeric films containing a large concentration of PQ-molecules as dopant results in a low shrinkage effect of the material and a precise modulation of its index of refraction. These particular characteristics guarantee a long-lasting stability of the polymeric compounds during photoinduced structure formation. Usually post-exposure enhancement of the holographic structures is achieved at temperatures of $50 - 80^o C$, limited by the glass transition temperature of PMMA ($105^o C$). An increase of the thermal stability by applying up to $140^o C$ leads to a

lower refractive-index modulation, i.e. to grating degradation, as shown in our previous experiments [57].

To broaden the field of applications we improved the polymeric properties by increasing their thermal stability up to $160-200^{\circ}C$ [117,118,120,130]. The preparation of these new, heatproof polymers was implemented, using a new method of copolymerization of MMA with polar monomers by the technique of homopolymerization. Such monomers include in particular acrylic acid (AA), methacrylic acid (MA), and methacrylamide (MAA). After producing the PMMA basic material layer molding was carried out using pouring of a liquid solution of the polymerized PMMA on glass substrates with injection of a high PQ-concentration. The use of the method of radical polymerization together with high dye-concentration is necessary to achieve the desired large values of the refractive-index modulation, similar to new thermostable recording media with large Δn-values produced by other research groups. This polymerized PQ-PMMA medium is designated in the following as PQ-P(MMA).

4.3.1. MMA based polymer with Acrylic Acid as copolymer

By applying a special polymerization method, a new medium of polymerized PQ-P(MMA) with high PQ-concentration was developed. The initial P(MMA) polymer was prepared by block polymerization of MMA at $60^{0}C$ under nitrogen atmosphere utilising multi-step washing with distilled water and drying at $50^{0}C$ [117]. MMA produced by the Rohm GmbH & Co. (Germany) was purified by distillation at reduced pressure before polymerization. As initiator 2.2'-azo-bis-isobutyronitrile (AIBN) was used. We succeeded to inject PQ into the polymerized polymer with high concentration (up to 4 mol.%), a technique which was not demonstrated so far in previous research work. The mixture of PMMA, PQ and dichloroethane as solvent was casted on the glass substrate followed by evaporation of the solvent and drying of the produced layers.

From previous experiments it is known that materials based on polymerized PQ-P(MMA) possess a minor refractive-index modulation together with quite reduced thermal and adhesion properties [130]. It is very difficult to use PQ-P(MMA) recording media in conjunction with silicate glass and to subject such polymeric compounds to high temperatures. One way to eliminate these problems

can be to modify P(MMA) in order to improve its thermo-mechanical characteristics, in particular to enhance its heat resistance and to improve the adhesion to glass, but at the same time to save its spectral transparency.

We have developed a new modified polymeric medium by radical copolymerization of MMA with acrylic acid (AA). Radical block copolymerization was carried out in a glass test tube fitted with a backflow condenser. Using a molar ratio of (AA : MMA) = 1 : 1, polymerization proceeded in a current of nitrogen at a temperature of $60^{\circ}C$ during 4 hours period. As an initiator AIBN was used. After completion of the synthesis the obtained polymeric sample was grinded at room temperature and washed with water and ethanol to remove unreacted monomers and the unconsumed AA-homopolymer. Dried samples were dissolved in dimethylformamide (DMF). The solution was passed through a Schott filter, after which the product of copolymerization is deposited in water. A small quantity of P(MMA) may possibly remain on the filter, which is not soluble in DMF. Some AA-homopolymer stayed in the CP precipitant. The composition of CP was determined by acid-base titration of carboxyl groups in an organic solvent. MMA copolymer with AA was solved in acetic acid contained in the glass tube [117]. The polymeric samples were obtained by pouring the liquid solution of MMA+AA and PQ on the glass substrates with following drying at $70^{\circ}C$. The film thickness was varied from 70 µm up to 100 µm for all types of polymers modifications.
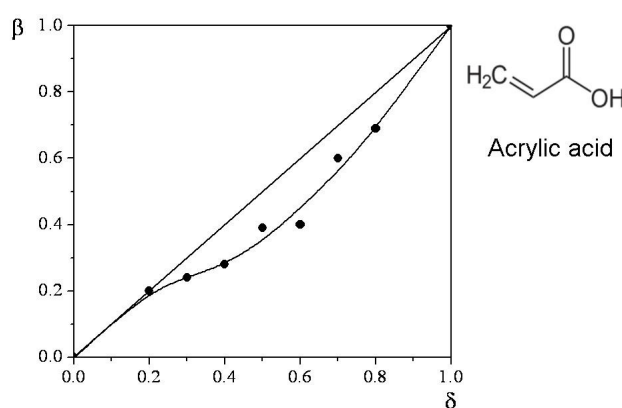

Fig. 4.9. Content of the AA-links in the copolymerization product (β) in dependence of the molar fraction of polar comonomer (MMA+AA) in the monomer mixture (δ).

The choice of the synthesis process influences the generated chemical structure and the characteristics of the formed comonomer layer and can also

change the optical parameters of the material. The determination of the composition of the CP in dependence on the composition of the monomer mixture allows to estimate the reactivity of the monomer during the copolymerization reaction. Experimental results of the copolymer and monomer compositions are shown in Fig. 4.9, where δ is the molar fraction of polar comonomers in the mixture of monomers and β is the molar fraction of polar comonomers in the copolymer. The equality of δ and β represents the "ideal" copolymerization process, where the additive reaction of polymerization occurs completely. For the system of MMA+AA the complete synthesis happens for $\delta < 0.3$. Increasing the δ-values results in the enrichment of the copolymer CP by MMA-links and decreasing the quantity of the AA-links. Therefore, to get optimal optical and thermal properties the best composition is obtained for choosing $\delta = 0.2$.
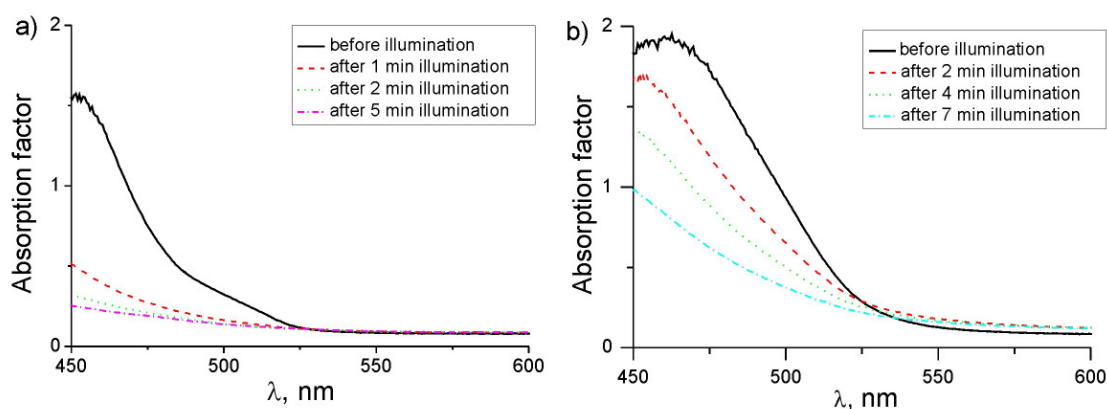

Fig. 4.10. Spectral dependences of absorption [a] for polymerized PQ-P(MMA) and [b] for a modified copolymer PQ-P(MMA+AA) under Ar-laser illumination [PQ-concentration is 4 mol.%, input intensity is $60 \, \mathrm{mW/cm^2}$ at 514.5 nm wavelength].

Figure 4.10 presents spectral evaluations of both media, PQ-P(MMA) and PQ-P(MMA+AA), under illumination in the VIS range. Polymers were illuminated by an Ar-laser (514.5 nm, $60 \, \mathrm{mW/cm^2}$). Comparing these results with the spectra of PQ-PMMA without polymerization [Fig. 4.2, p.37] one can see a similarity of the active absorption band approximately up to a wavelength of 520 nm. In spite of the similar spectral behaviour of both materials, the absorption of PQ-P(MMA) decreases faster than that of its copolymer with AA. For PQ-P(MMA) we need just 5 min of irradiation with a light intensity of $60 \, \mathrm{mW/cm^2}$ to make it completely transparent at 514.5 nm wavelength, while for the copolymer we achieved only about 50 % of phototransformation for the same exposure conditions.

Holographic gratings in PQ-P(MMA) and PQ-P(MMA+AA) media were recorded and reconstructed using the same scheme as presented in Fig. 4.3, p.38. Formation and evolution of the periodical structure were measured to investigate the optical and thermal properties of the polymers [117,118]. The concentration of the PQ-molecules was 4 mol.%, the thickness of the layers was 90 µm and the grating period was 0.6 µm. The values of the diffraction efficiency were measured during the process of grating recording by detecting the diffracted beam intensity. The kinetics of η for both materials are shown in Fig. 4.11.
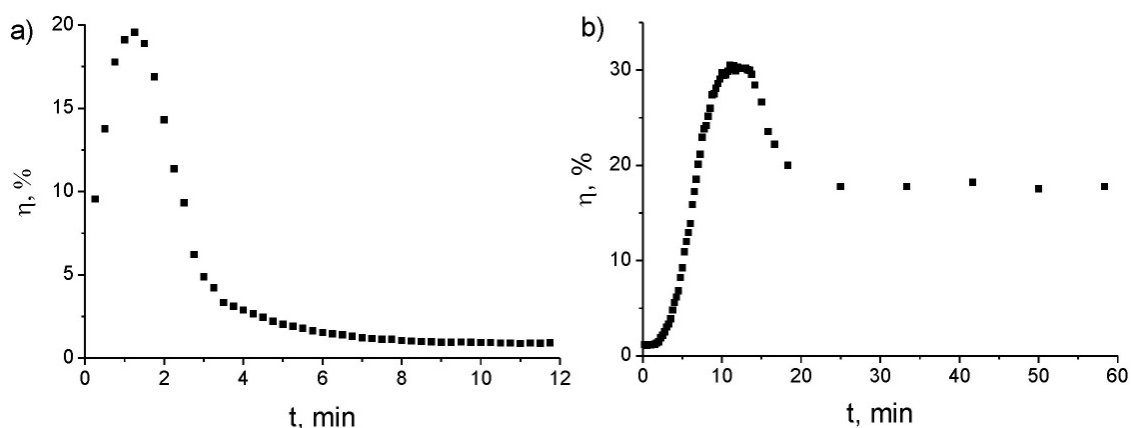
Fig. 4.11. Diffraction efficiency kinetics [a] of polymerized PQ-P(MMA) and [b] of copolymer PQ-P(MMA+AA) versus recording time. The gratings with a period of 0.6 µm are written and read out by an Ar-laser (514.5 nm). The measurements are made with an accuracy of 5 %.

With the new PQ-P(MMA+AA) medium values of the diffraction efficiency up to 32 % were obtained within 600 s of recording time followed by a slight reduction of the efficiency till saturation has been reached near 20 % (about the same as the maximum efficiency of PQ-P(MMA)) [Fig. 4.11 [b]]. The magnitudes of efficiency during recording are higher for CP with AA than for PQ-P(MMA) [Fig. 4.11 [a]]. The maximum values are reached faster for PQ-P(MMA+AA) CP (about 60-80 s), but continuous illumination of this polymer results in an exponential grating degradation. The refractive-index modulation Δn during hologram recording for both cases covers the range of 10^{-4}.

The difference of the behaviours in spectra and kinetics can be explained by different photochemical reactions taking place in the different polymeric media. For PQ-P(MMA) samples one observes an increasing diffraction efficiency as a result of the additive of semiquinone radicals to the macromolecules. In the case of the

copolymer the situation is different [117]. In PQ-P(MMA+AA) the formation of hydrogen bonds occurs due to the reacting macromolecules, which results in the following two competing processes contributing differently to the photoinduced grating formation:

$$HPQ^\bullet + R^\bullet \rightarrow HPQR$$

and

$$HPQ^\bullet + HPQ^\bullet \rightarrow recombination\,products\,.$$

The delay of the PQ-diffusion in the CP is a result of the formation of hydrogen bonds by AA-links and the reduced mobility of the macromolecules. This is responsible for the reduced interaction probability of the PQ-molecules with the copolymer and the only partial attachment of PQ to MMA+AA [118]. Thus, the gratings can only be formed by CP with lower reaction velocity, therefore, however, ensuring a long grating storage.
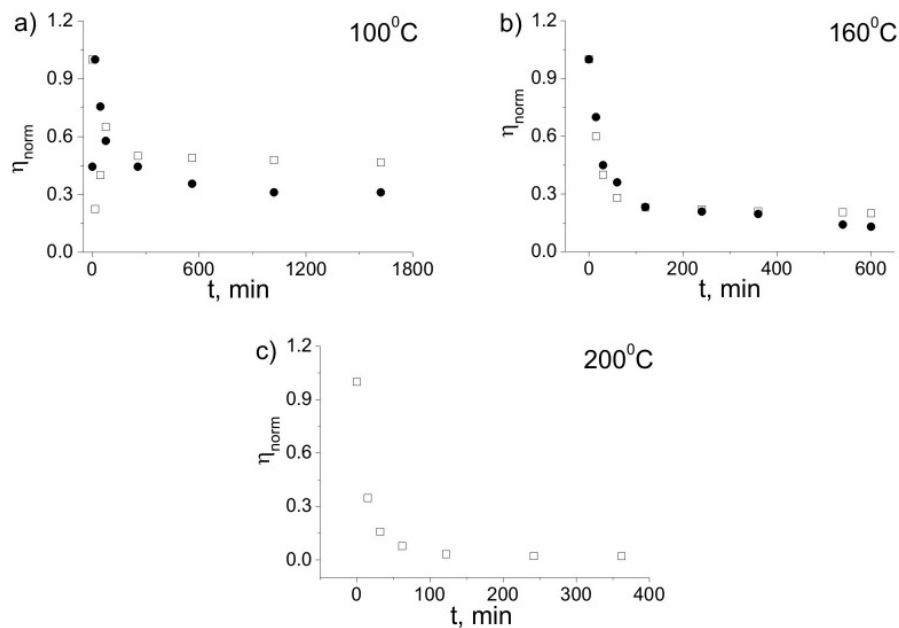
Fig. 4.12. Dependence of the diffraction efficiency normalized to the maximum values on heating time at temperatures of [a] $100°C$, [b] $160°C$ and [c] $200°C$. Fill circles correspond to PQ-P(MMA) and hollow squares correspond to the copolymer PQ-P(MMA+AA). The measurements are made with an accuracy of 5 %.

A thermal analysis of PQ-P(MMA) as well as of the copolymer PQ-P(MMA+AA) is presented in Fig. 4.12. Polymeric layers were annealed by temperatures in the range of $100 - 200°C$. During thermal heating, a short-term amplification of the diffraction efficiency was observed due to the fast PQ-diffusion, whereas the

longer term reduction of η is a result of the slow diffusion of the large photoproduct molecules. Initial η-values are higher for CP layers in comparison with PQ-P(MMA) for the same process conditions of recording and annealing. A temperature increase up to $160^{o}C$ leads for both samples to a similar tendency of grating degradation. This is the highest temperature so far, for which the evolution of gratings in polymerized PQ-P(MMA) has been observed. Annealing in the range of $170-200^{o}C$ results in a complete destruction of the PQ-P(MMA) material and generates only a weak holographic structure in its copolymer. However, even at $200^{o}C$ the values of diffraction efficiency for PQ-P(MMA+AA) were dropping to zero within 300 minutes [Fig. 4.12 [c]].

The adhesion properties of the polymerized polymeric and copolymeric films have been investigated by taking into account the action of the mechanic force required to remove the polymeric film from the glass substrate. This can be observed in the glass bulb during the synthesis process, as well as during drying and subsequent formation of the polymeric film in a Petri dish. The experiments demonstrated that the copolymer has better adhesion properties to silicate glass compared with the MMA homopolymer. Besides, in all cases adherence was worse than in purified PQ-PMMA.

4.3.2. Non-local response in polymerized material

The decrease of the spatial period of holographic gratings recorded in non-polymerized PQ-PMMA layers results in a faster grating amplification, but has no influence on the achieved maximum values of Δn [Fig. 4.6 [a], p.45]. A similar experiment was made for block synthesized PQ-P(MMA) and for its copolymer with AA. The time t_{max} (in s) for achieving the maximum diffraction efficiency versus the angle 2θ between the interfering beams is shown in Fig. 4.13. Whereas for the case of non-polymerized PQ-PMMA this dependence is linear, for polymerized PQ-P(MMA) [Fig. 4.13 [a]] and for PQ-P(MMA+AA) [Fig. 4.13 [b]], the dependence is different. The decrease of time t_{max} with increasing angle 2θ (i.e. decreasing of the grating period) is observed till to the critical angle for which the diffraction efficiency reaches its maximum within shortest time ($2\theta = 80^{0}$). After that angle, t_{max} and the value of the diffraction efficiency grow again for both

kinds of material. Fresnel reflection was taken into account for each case; therefore, its influence on this behaviour is excluded.
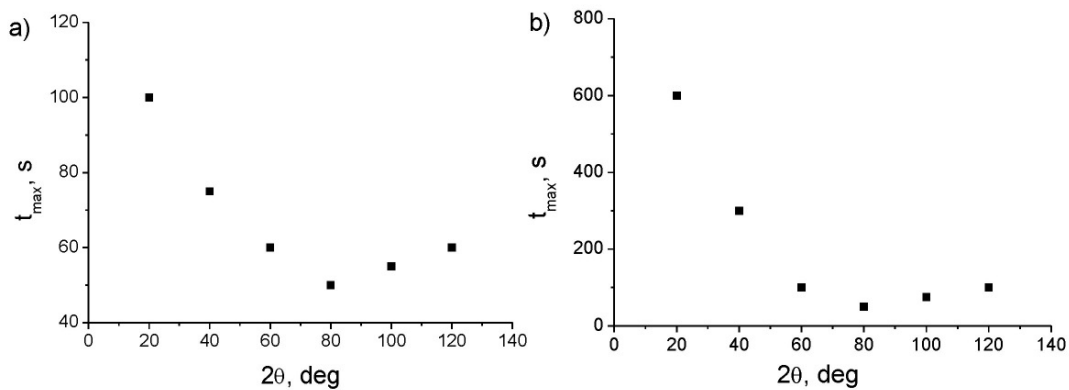

Fig. 4.13. Dependence of the time t_{max} for achieving the maximum diffraction efficiency on the angle 2θ between the interfering beams for holographic gratings recorded [a] in PQ-P(MMA) and [b] in PQ-P(MMA+AA). The measurements are made with an accuracy of 5 %.

Accordingly, one can obtain from the experiment the particular angle between the incident beams for which the time, necessary to reach the maximum of diffraction efficiency, is minimal. This non-typical behaviour of the grating kinetics suggested to us an idea of a non-local response presented in polymerized material [119]. Under illumination of the photopolymeric material the monomer is activated. Polymeric chains can be generated in a bright illuminated region, growing slowly into the nearest dark region. This spreading of the chains leads to a "smearing" (averaging) of the recorded refractive-index profile and is responsible for a non-local material response [131-134]. This situation can be modelled by a one-dimensional diffusion process of grating formation [55,131,134-136]. The mathematical description of the redistribution process of molecules exhibits the existence of the non-local, nonlinear properties of polymers and provides a possibility to find out the non-local response length of PQ-components [119].

An experimental observation of the temporal behaviour of the diffractive structure helps to simulate numerically the diffusion mechanism in the PQ-P(MMA) material and in its copolymer. We assume that modified photopolymers possess diffusion properties of two components (of the mobile substance (PQ) and the rather immobile photoproduct molecules) [57,117]. The model presented in the following is based on the Sheridan and Lawrence's theory [131,132]. It describes the contribution of the non-local response by a one-dimensional diffusion theory.

According to Zhao and Mouroulis [134] the change of the diffusion coefficient has negligible influence on the grating formation in a polymerized photopolymer and can be assumed as a constant parameter of the model.

The expression $\partial C(x,t)/\partial t$ that describes the change of the PQ-concentration in time and space (according to the second Fick law for the one-dimensional case, when the diffusion coefficient D is a constant) can be written in the following way [131]:

$$\frac{\partial C(x,t)}{\partial t} = \frac{\partial}{\partial x}[D\frac{\partial}{\partial x}C(x,t)] - \int\limits_{-\infty}^{+\infty} R(x,x') \cdot F(x',t)C(x',t)dx'],$$ 4.11

where $F(x',t')$ is the copolymerization rate and, $R(x,x',t,t')$ defines the non-local response (the change of the concentration at the point $\{x',t'\}$, in case, the material was exposed at the point $\{x,t\}$). According to [131] the non-local response of the medium can be described using a non-local response length $\sqrt{\sigma}$ by:

$$R(x-x') = \frac{\exp[-(x-x')^2/2\sigma]}{\sqrt{2\pi\sigma}}.$$ 4.12

The modulation of the photoproduct concentration $[\partial N(x,t)/\partial t]$ can be found from:

$$\frac{\partial N(x,t)}{\partial t} = \xi \cdot I \cdot C(x,t),$$ 4.13

where ξ is the constant of copolymerization. During the recording process the light intensity distribution in the layer is given by:

$$I(x,t) = I_0 \cdot (1 + V \cdot \cos[fx]),$$ 4.14

with initial intensity I_0, fringe visibility V and spatial frequency of the grating f $[f = \frac{2\pi}{\Lambda}]$. The rate of photoattachment (probability) is proportional to the beam intensity and equal to:

$$F(x,t) = F_0 \cdot (1 + V \cdot \cos[fx]),$$ 4.15

with $F_0 = \xi \cdot I_0$. The solution of Eq. 4.11 can be written as a Fourier series:

$$C(x,t) = \sum_{j=0}^{\infty} C_j(t) \cdot \cos[ifx].$$ 4.16

We shall consider only two first harmonics:

$$C(x,t) = C_0(t) + C_1(t) \cdot \cos[fx].$$
$$\text{4.17}$$

Substituting this equation in Eq. 4.11 one can derive the following expressions for the concentration of the first two harmonics during recording of the grating:

$$
\begin{cases}
\dfrac{\partial C_0(t)}{\partial t} = -F_0 \cdot C(t) - \dfrac{F_0 V}{2} C_1(t) \\[2mm]
\dfrac{\partial C_1(t)}{\partial t} = -F_0 \cdot V \cdot \exp[-\dfrac{f^2 \sigma}{2}] \cdot C_0(t) - F_0 \cdot \exp[-\dfrac{f^2 \sigma}{2} + R] \cdot C_1(t).
\end{cases}
$$
$$\text{4.18}$$

After integration of Eq. 4.13 and substitution of Eq. 4.18 in it one gets the modulation of the photoproduct concentration:

$$N(x,t) = N_0(t) + N_1(t) \cdot \cos[fx] + N_2(t) \cdot \cos[2fx] + \ldots .$$
$$\text{4.19}$$

For the first two harmonics one obtains accordingly:

$$
\begin{cases}
N_0(x,t) = \displaystyle\int_0^t [F_0 \cdot C_0(t) + \dfrac{F_0 V}{2} C_1(t)]\, dt \\[3mm]
N_1(x,t) = \displaystyle\int_0^t [F_0 \cdot V \cdot \exp[-\dfrac{f^2 \sigma}{2}] \cdot C_0(t) + F \cdot (\exp[-\dfrac{f^2 \sigma}{2} + R] \cdot C_1(t))\, dt.
\end{cases}
$$
$$\text{4.20}$$

If the change of the concentrations is relatively small, the modulation of the refractive index of volume holographic gratings can be derived as the diffusion contribution of both processes using the Lorentz-Lorenz formula [96]:

$$\Delta n = \dfrac{(n^2 + 2)^2}{6 \cdot n} \sum_i R_i \Delta C_i ,$$
$$\text{4.21}$$

where R_i and ΔC_i are the refraction coefficient and the change of concentration of the i-th components (i = PQ or photoproduct). The diffraction efficiency η for volume reflection holograms under the Bragg condition can be calculated using the Kogelnik formula [Eq. 4.3, p.41].

To analyze the influence of the non-local response of the medium on the grating formation process one can switch off or switch on this effect in the model. In the theoretical calculations the following parameters have been used: refractive index $n = 1.5$, wavelength $\lambda = 514.5$ nm, diffusion coefficient $D = 10^{-17} \text{cm}^2 / s$, input

intensity of each beam: $I_0 = 200 \, mW / cm^2$, constant of copolymerization $\xi = 5{,}67 \cdot 10^{-5} \, W^{-1}s^{-1}cm^2$ [119].
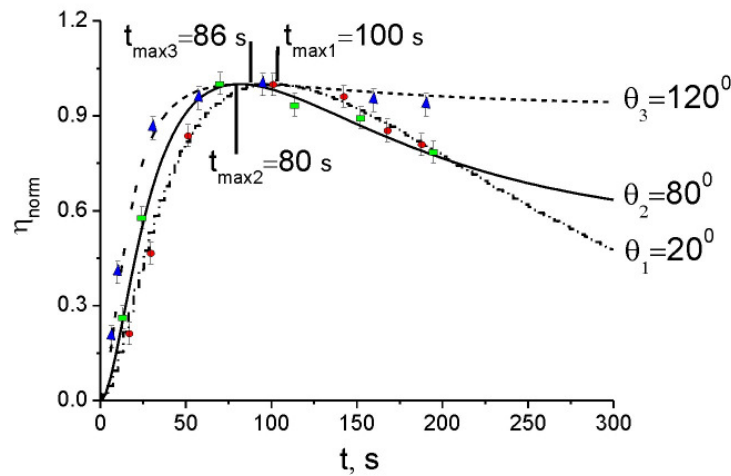

Fig. 4.14. Experimental (points) and theoretical (lines) dependences of the diffraction efficiency normalized to the maximum versus time for reaching the maximal values for incidence angles $20°$, $80°$ and $120°$, which correspond to the grating periods of 1.5 µm, 0.4 µm and 0.3 µm, respectively. The initial PQ-concentration is 2.5 mol.% and the non-local response length amounts to $\sqrt{\sigma} = 31$ nm.

Figure 4.14 shows the experimental (points) and theoretical (lines) curves of the diffraction efficiency versus the time for reaching the maximum of η corresponding to a variation of input angles from 20° to 120°. Theoretical simulations confirm that an increase of the incidence angle leads to a decrease of the time necessary for reaching the maximal diffraction efficiency up to a certain interaction angle. Above this particular angle of incidence the corresponding times increase again. In the case of PQ-P(MMA) this time decreases from 100 s (angle 20°) till 80 s (80°) and then increases up to 86 s (120°) again. Besides, one can note that the grating with the incidence angle of 120° is the most stable in behaviour confirming the optimum recording time in the range of 80 s.

Figure 4.15 shows the theoretically calculated normalized to the maximum time necessary for achieving the maximal diffraction efficiency versus the angle between the beams for different fitted values of the non-local response length of PQ. The general form of the theoretical curve coincides with the experimental one [Fig. 4.13, p.59]. The agreement of the experimental and theoretical results justifies to suppose that the existence of an extreme of the time for reaching the maximal diffraction efficiency versus the angle between the beams is due to a non-

local response of the PQ-P(MMA) polymeric layer and its copolymer. Fitting the averaged curve of the non-local response length of phenanthrenequinone leads to a value of 31 nm for PQ-P(MMA) and of 70 nm for PQ-P(MMA+AA).
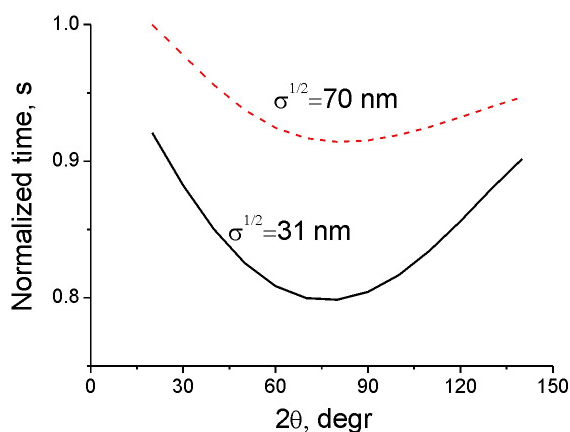

Fig. 4.15. Theoretical dependence of the time necessary to achieve the maximum diffraction efficiency on the angle between the interfering beams (2θ) for different values of the non-local response length $\sqrt{\sigma}$.

4.3.3. Copolymers of MMA with Methacrylamide and Methacrylic Acid

The next step for the improvement of adhesion and thermal properties of PQ-P(MMA) media was its modification by MMA-copolymerization with polar monomers [methacrylamide (MAA) and methacrylic acid (MA)]. The choice of the method of copolymer synthesis was determined by the ability of the comonomer to dissolve in the MMA-monomer. The MA is soluble in MMA, therefore its copolymerization can be performed by a strong intermolecular block interaction in the MAA-element. This makes it indissoluble in the monomer due to the formation of hydrogen bonds between carbonyl and amide molecules groups. Radical copolymerization of MMA with MAA occurs in a 40 % solution of the monomer mixture with 1,4-dioxane at $80^{\circ}C$ in the presence of AIBN as initiator. The duration of synthesis is 4 hours; the concentration of AIBN amounted to 10 % of the mass of the monomer mixture. The molar fraction of MAA and MA in the monomer mixture (δ) was varying from 0.2 up to 0.8.

The polymeric samples of both copolymers were prepared from a 10 % solution in acetic acid. PQ was added in the quantity of 4 mol.% after its complete dissolution. The solution was poured on smooth glass plates and dried at $80^{\circ}C$ to

remove the solvent. The average thickness of the achieved polymeric films was 90 µm.
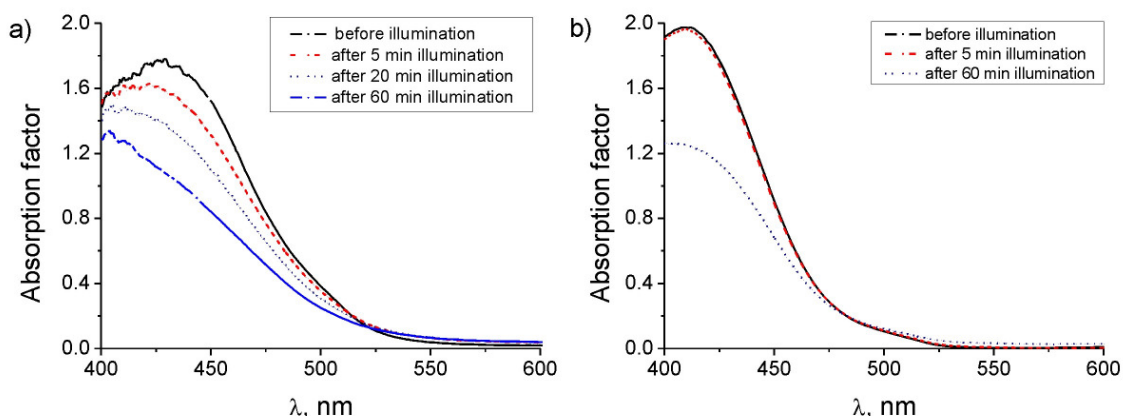

Fig. 4.16. Absorption spectra before and during illumination of copolymers [a] PQ-P(MMA+MAA) and [b] PQ-P(MMA+MA) under Ar-laser illumination [PQ-concentration is 4 mol.%, input intensity is $60\,mW/cm^2$ at 514.5 nm wavelength].

Figure 4.16 exhibits the absorption spectra versus exposure for P(MMA+MAA) and PQ-P(MMA+MA) copolymers. Both media were illuminated during 1 hour and are characterized by a slow photoattaching reaction of the PQ-molecules to the polymeric matrix. The same situation was observed experimentally for various possible variations of molar fraction of MAA and MA in the monomer mixture.
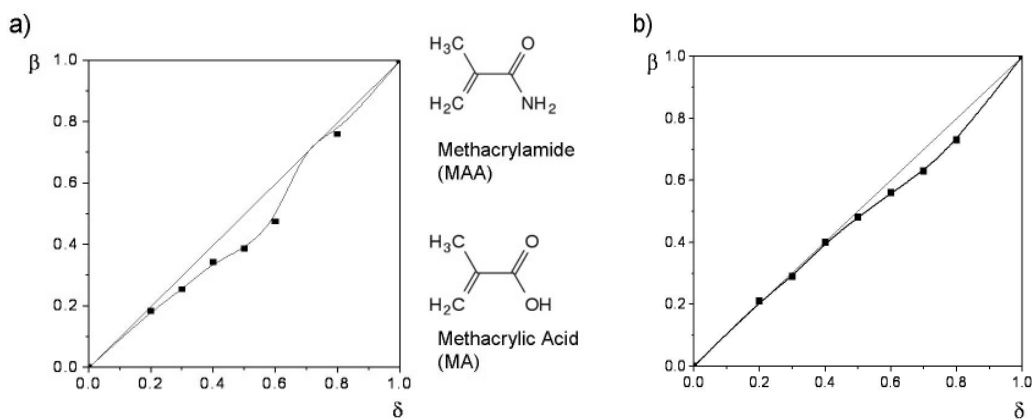

Fig. 4.17. Content [a] of MAA-links and [b] of MA-links in the copolymerization product (β) in dependence on the molar fraction of the polar comonomer (MAA or MA) (δ) in the mixture of the monomers.

Experimental data for the dependence of the copolymeric composition on the composition of the monomer mixture in PQ-P(MMA+MAA) and PQ-P(MMA+MA) are shown in Fig. 4.17. For the system MMA+MAA the deviation of the experimental curve from the theoretical diagonal is significant. For small values of

δ till 0.2-0.3 the correlation between MMA and MAA-links is practically identical to that of the initial monomer mixture and to the mixture with CP. It starts to deviate strongly at higher values [Fig. 4.17 [a]]. The maximum deviation was obtained for δ between 0.4 and 0.6. At these values a deficiency of methacrylamides links in CP was observed. At higher content of MAA the composition of CP gets closer to the composition of the comonomer mixture.

In a system of MMA+MA at δ varying from 0.2 to 0.4 the composition of the copolymer is chemically similar to that of the monomer mixture, i.e. the copolymerization results in an azeotropic mixture [Fig. 4.17 [b]]. With further increase of the MA content in the monomer mixture from 0.4 up to 0.8 one observes deviations of the CP-composition mixture from an azeotropic one. The formation of MMA+MA copolymer with a statistical distribution of these compounds supports the depletion of the CP-mixture by the MA-links for $\delta > 0.4$.

Series of experiments of hologram recording with different δ-values were performed by analogy to previous investigations of copolymers [Fig. 4.18]. Both copolymers possess a low modulation of the refractive index. Generation of the diffractive structure in the PQ-P(MMA+MAA) medium was realized in the range of δ between 0.2 and 0.4, whereas for the copolymer with the MA-content the modulation of the refractive index occurs for $\delta \leq 0.3$. These results are correlated with the type of copolymerization, i.e. gratings can be recorded, when the compositions consisting of copolymer and monomer are forming a chemically related mixture, showing an azeotropic behaviour. For both components the maximum achieved values of the diffraction efficiency are in the range of $\eta \approx 0.04 - 1\,\%$, showing a photoinduced structure, which is weak in comparison with previous polymeric media.
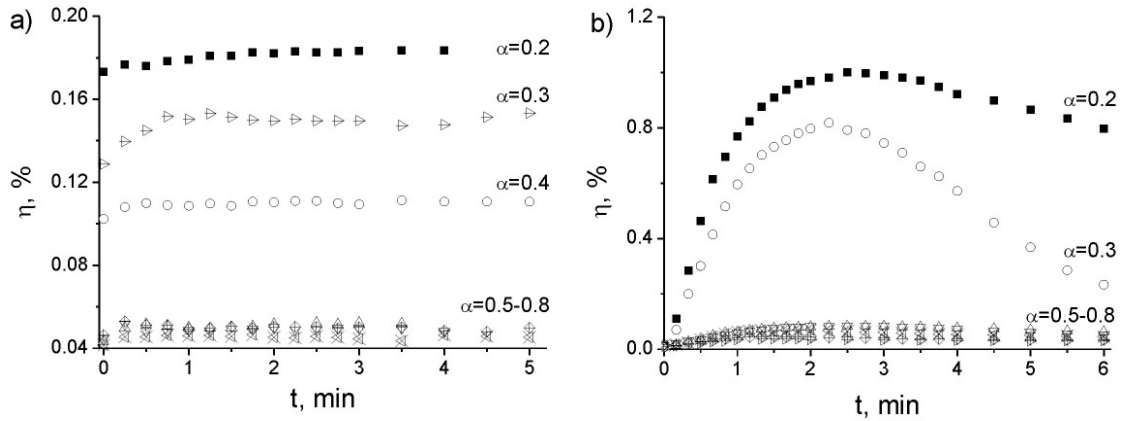
Fig. 4.18. Diffraction efficiency dependences versus recording time [a] in PQ-P(MMA+MAA) and [b] in PQ-P(MMA+MA) copolymers under Ar-laser illumination [PQ-concentration is 4 mol.%, input intensity is 60 mW / cm^2 at 514.5 nm wavelength]. The measurements were made with an accuracy of 5 %.

Further gratings have to be annealed in order to further increase their thermal stability. Diffractive structures were generated by applying temperatures up to 160°C. However, further heating results in a complete destruction of the hologram. Thus, copolymers with MAA and MA contents show a weak grating formation with limited optical and thermal characteristics in comparison with previous CP-content. The positive and important quality of copolymeric films is their advanced adhesion property, producing a tight connection between the material and glass substrate.

4.4. Conclusion

Polymeric materials based on a PMMA matrix containing distributed PQ-molecules are fabricated for the purpose of optical recording by generating holographic diffractive structures under Ar-laser illumination. Additionally, using a new technology of sample preparation by injecting a high PQ-concentration (up to 4 mol.%), diffractive structures with almost 80-90 % efficiency were generated in polymers of thicknesses of hundreds of microns. Pouring of the liquid solution on glass substrates with following drying together with a high concentration of dye results in a deep modulation of the refractive index during photoinduced structure recording ($\Delta n \approx 5 \cdot 10^{-4}$). A moderate layer thickness mainly excludes shrinkage and relief formation. Recording and enhancement of the gratings under different

conditions show the independence of the achieved Δn-values on the spatial period, but lead to a bigger modulation of Δn by increasing the injected energy. The investigation of the process of thermal enhancement proved its enhancing influence on the periodical structures amplifying the refractive-index modulation by an order of magnitude ($\Delta n \approx 10^{-3}$). Homogenous irradiation stabilized the recorded grating making it insensitive to surrounding illumination and increasing the shelf-life of the holograms.

The improvement of the optical parameters of the polymeric samples for their broader applications was obtained by block polymerization of the MMA monomer producing copolymeric media. Modified PQ-P(MMA) materials as well as PQ-P(MMA+AA) possess a relatively large value of diffraction efficiency during recording [$\eta = 20 - 30\%$] with refractive-index modulation in the range of 10^{-4}. The thermostable PQ-P(MMA+AA) medium enables to save grating structures by heating up to temperatures of maximal $200^{\circ}C$. These particular properties make copolymers very attractive for their application in the field of telecommunication and fabrication of displays, where high stability and resistance towards high temperatures plays a major role.

In spite of these advantages the insufficient adhesion of the modified material is responsible for the rather complicated process of pouring of the polymeric solution with high PQ-concentration on the silicate glass substrate. The fast degradation of the recorded gratings and the behaviour of the non-local response results in somewhat blurred and unsharp pictures with lower refractive-index modulation and shorter grating stability as compared with purified PQ-PMMA monomer media. Modified copolymers with methacrylamide and methacrylic acid reveal a slower process of phototransformation due to PQ-molecules with a weaker modulation of the refractive index. The formation and evolution of the holographic gratings in copolymers are complicated processes due to the existence of intermolecular hydrogen bonds together with competing reaction contributions of cross and square recombination of polymeric radicals. Besides, previous research works indicate the strong influence of the polymerization process on the surface relief formation destroying the recorded image.

Comparing the optical properties of all developed PQ-containing polymeric media leads to the conclusion to continue the investigations of the self-trapping

formation in purified monomer PMMA with high PQ-concentrations. The photoinduced change of the refractive index in PQ-PMMA achieved already without extra annealing is sufficient to generate stable self-written channels in nonlinear polymeric media by light interaction. Because of the relatively large molecular size of the doping agents post-diffusion dark processes of this material are ruled out. Also, depending on the applied temperature the gratings, formed in this material, are stable for tens of years. Moreover, PQ-PMMA photopolymers do not show any effects of surface deformation and non-local behaviour during recording of grating structures forming effective distinct holograms.

Chapter 5   Self-Trapping in Polymers Based on PQ-PMMA

5.1. Numerical modeling of (1+1)D laser-beam self-trapping in polymeric layers
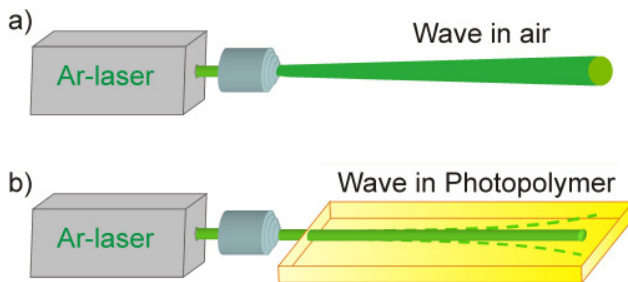

Fig. 5.1. [a] Propagation of a laser wave in air and [b] generation of self-trapping in a photopolymer.

In the previous chapters we mentioned that nonlinear wave propagation and diffraction of a light beam in nonlinear materials are effectively compensated by the effect of self-trapping [3,6]. In order to investigate this phenomenon occurring in light-sensitive PQ-PMMA media, the behaviour of a light beam focused on the front surface of the sample was examined. Compared to a uniform linear medium, where an optical beam strongly diverges [Fig. 5.1 [a]], the propagating laser beam forms in the PQ-PMMA polymer a nonlinear area with higher refractive index in direction of the light propagation. The correlation between the intensity of the input beam and its diameter results in a decrease of the diffraction properties of the beam and in a concentration of the light beam in the formed channel. If the thus captured beam is able to save its characteristic properties for a certain period of time, a homogeneous channel waveguide located along the propagation axis is generated in the area with the modified refractive index [Fig. 5.1 [b]]. This self-channeling can be formed in one-dimension as well as in the volume of a nonlinear media. The next step of our research is to investigate numerically and also experimentally the photoinduced generation of the (1+1)D-self-trapping process. The light propagates with a finite spatial cross section, whereby the self-focused beam travels without divergence in the PQ-PMMA medium.

5.1.1. Theoretical approach of the light propagation in polymers

The self-channeling of a laser beam in the PQ-PMMA layer occurs due to the nonlinear action of the change of the refractive index. The distribution of light corresponding to a coherent electromagnetic illumination is described by Maxwell equations. To characterize the propagation of a laser beam in a polymeric medium one can use the scalar Helmholtz equation [12]:

$$\nabla^2 E + \overset{\wedge 2}{K} E = 0,$$ 5.1

with $\hat{K} = k_0 \cdot \widehat{n}$, where $k_0 = 2\pi / \lambda_0$, λ_0 is the free-space wavelength, $\widehat{n} = n(x,z,t) - i\kappa(x,z,t)$ is the complex refractive index with the nonlinear coefficient of the extinction $\kappa(x,z,t)$. The magnitude $\widehat{n}$ includes the absorption of the medium and the real part of the refractive-index coefficient $n(x,z,t) = n_0 + \Delta n$, n_0 is the initial refractive index, and Δn is the photoinduced variation of the refractive index.

In the case of (1+1)-D Eq. 5.1 has the solution:

$$E = A(x,z) \cdot \exp[-ikz],$$ 5.2

with the complex amplitude of the light wave $A = a \cdot \exp[i\varphi]$ and wave number $k = k_0 \cdot n_0$. Equation 5.1 yields the diffraction equation for the distribution of the beam along the coordinate z in the polymeric layer:

$$\frac{\partial^2 A}{\partial x^2} - 2ik\frac{\partial A}{\partial z} - Ak^2 + K^2 A - ik\alpha A = 0,$$ 5.3

where $K = k_0 \cdot n$ and α is the absorption coefficient of the medium that is equal to $\alpha = \alpha_{mol} \cdot C_{PQ}$, C_{PQ} is the PQ-concentration and α_{mol} is the molar absorption cross-section [137]. In consideration of variations of the PQ-concentration under illumination the absorption coefficient depends on coordinates and time [$\alpha = \alpha(x,z,t)$]. One notices that Eq. 2.11, p.16 is a generalization of the obtained Eq. 5.3 with zero absorption of the medium ($\alpha = 0$).

The solution of Eq. 5.3 can be found by using the split-step method [138,139]. For this purpose we write Eq. 5.3 in the form:

$$\frac{\partial A}{\partial z} = -\frac{i}{2k}\frac{\partial^2 A}{\partial x^2} + \frac{i}{2k}A(k^2 - K^2) - \frac{\alpha A}{2}.$$

5.4

According to the split-step method the complex amplitude A is assumed to be the sum of a linear (A_L) and a nonlinear (A_{NL}) part:

$$A = A_L + A_{NL}.$$

5.5

By separating the linear [Eq. 5.6 [a]] and the nonlinear [Eq. 5.6 [a]] parts of Eq. 5.3 one obtains:

$$\frac{\partial A_L}{\partial z} = -\frac{i}{2k}\frac{\partial^2 A}{\partial x^2}$$

5.6 [a]

and

$$\frac{\partial A_{NL}}{\partial z} = \frac{i}{2k}A[k^2 - k_0^2 n^2(x,z,t)] - \frac{\alpha A}{2}.$$

5.6 [b]

The nonlinear part has an analytical solution, but the linear one can be calculated only numerically. If we assume a small step along the z-direction, then the two parts can be treated separately with only a relatively small numerical error. Thus, for the nonlinear part the solution has the form:

$$A_{NL_J} = A_{NL_{0J}} \cdot \exp[(\frac{i}{2k}(k^2 - k_0^2 n^2(x,z,t)) - \frac{\alpha}{2})\Delta z],\ j = 1,2.$$

5.7

For the linear part the fast Fourier transform (FFT) is applied, which is an efficient algorithm to compute the discrete Fourier transform (DFT) and its inverse. For the direct Fourier transformation we substitute the Fourier function by the following expression:

$$A_L(z,x) = \int_{-\infty}^{\infty} A_L^*(z,\omega_x) \cdot \exp[-2\pi i\omega_x x]\ d\omega_x,$$

5.8

where ω_x is the projection of the Fourier-transformation frequency on the x axis. Finally, the solution of the linear part is:

$$A_{L_j}^* = A_{L_{0j}}^* \cdot \exp[\frac{2i\pi^2\omega_x^2\Delta z}{k}].$$

5.9

5.1.2. Simulation of the diffusion mechanism

The diffusion process in the PQ-PMMA photopolymer can be described by two diffusion mechanisms: the first one is the diffusion of unreacted PQ-molecules, the second one is the diffusion of the photoproduct. In the one-dimensional case the change of the PQ-component is described by the following expression [121]:

$$\frac{\partial C(x,z,t)}{\partial t} = D(x,t)[\frac{\partial^2}{\partial x^2}C(x,z,t) + \frac{\partial^2}{\partial z^2}C(x,z,t)] - \varepsilon \cdot I(x,z) \cdot C(x,z,t) , \qquad 5.10$$

where $C(x,z,t)$ is the change of the PQ-concentration by diffusion with the diffusion coefficient $D(x,t)$ and the coupling rate ε. The diffusion coefficient is defined by a formula derived from the free-volume theory. Accordingly, $D(x,t)$ is represented by an exponential decrease, which is caused by an increasing change of the photoproduct concentration:

$$D(x,t) = D_0(1 - \exp[-c_d\frac{C_0}{N(x,z,t)}]) , \qquad 5.11$$

where C_0 is the initial PQ-concentration before illumination, $N(x,z,t)$ is the change of the concentration of the photoproduct, D_0 is the initial diffusion coefficient and c_d is the diffusion constant that was found experimentally according to [131]. Taking Eq. 5.11 into account, one can assume that not all PQ-molecules contained in the illuminated part of the layer are involved in the photoreaction process.

Equation 5.11 can be solved in the same way as it was done for Eq. 5.4, p.71 using the split-step method by separation into a linear [Eq. 5.12 [a]] and a nonlinear [Eq. 5.12 [a]] part:

$$\frac{\partial C_L(x,z,t)}{\partial t} = D(x,t)[\frac{\partial^2}{\partial x^2}C(x,z,t) + \frac{\partial^2}{\partial z^2}C(x,z,t)] \qquad 5.12\ [a]$$

and

$$\frac{\partial C_{NL}(x,z,t)}{\partial t} = -\varepsilon \cdot I(x,z) \cdot C(x,z,t) . \qquad 5.12\ [b]$$

Here the nonlinear part has the solution:

$$C_{NL} = C_0 \cdot \exp[-\varepsilon I(x,z)\Delta t] \,, \qquad\qquad 5.13$$

and the linear one yields (using FFT):

$$C_L^* = C_0^* \cdot \exp[-4\pi D(\omega_x^2 + \omega_z^2)\Delta t] \,, \qquad\qquad 5.14$$

where ω_x and ω_z are the projections of the frequencies obtained by their Fourier transformation on the x and z axes.

The change of the PQ-concentration can be written as the difference between the present (C) and the initial (C_0) concentrations:

$$\Delta C = C - C_0 \,, \qquad\qquad 5.15$$

whereas the change of the photoproduct can be found from [121]:

$$\frac{\partial N(x,z,t)}{\partial t} = \varepsilon \cdot I \cdot C(x,z,t) \,. \qquad\qquad 5.16$$

Based on the values for the variations of the concentrations of the photoproduct and the PQ-molecules, inserting their refraction coefficients (R_{HPQR} and R_{PQ}) and using the Lorentz-Lorenz formula, the following expression for the change of the refractive index is obtained [42,96]:

$$\Delta n_{PQ} = \frac{(n^2+2)^2}{6 \cdot n}[R_{HPQR} \cdot N(x,z,t) - R_{PQ} \cdot C(x,z,t)] \,. \qquad\qquad 5.17$$

5.1.3. Results of the theoretical modeling

The simulation of the self-trapping mechanism in the PQ-PMMA medium was calculated numerically by using the Mathlab program. For the theoretical treatment we used a Gaussian distribution for the intensity $[I = I_0 \exp[-(x^2/x_0^2)]]$ and the following parameters, obtained from previous experiments [42,57,119-121] refractive index $n = 1.5$, wavelength in vacuum $\lambda_0 = 514.5\,nm$, difference between the refraction coefficients of photoproduct and PQ $\Delta R = 1.4\,cm^3/mol$ [42,58], initial concentration of PQ-molecules in the polymeric layer $C_0 = 1.4\,mol.\%$, molar absorption cross-section $\alpha_{mol} = 10^5\,cm^2/mol$, diffusion coefficient $D = 10^{-17}\,cm^2/s$, diffusion coefficient constant $c_d = 10^{-2}$, absorption coefficient α (which varies

thereby in the range of about a few tens of cm^{-1}), and coupling rate $\varepsilon = 10^{-5}\,\text{W}^{-1}\text{s}^{-1}\text{m}^2$ (which was found theoretically from a simulation calculation of the holographic grating formation) [121].

A series of numerical simulations for various cross-sections of the input beam have been performed showing a similar behaviour of the beam for all cases. As typical dimension for the laser-beam we used an input radius $x_0 = 6\,\mu\text{m}$ (at the 1/e mean) for the presented model, corresponding to the beam full width at half maximum of about 10 μm (FWHM). To prove our prediction about self-trapping in the polymer we need to generate a channel with a length several times longer than the self-focussing length, the so-called, "Rayleigh length" [74]. Inserting a one-dimensional Gaussian beam in Eq. 2.8, p.15 one can derive the following expression for the Rayleigh length: $L_R = 2\pi x_0^2 n / \lambda_0$. For the PQ-PMMA layer it amounts to about 0.7 mm [$x_0 = 6\,\mu\text{m}$, $\lambda_0 = 514.5\,\text{nm}$ and $n = 1.5$]. In the following numerical simulations were performed with a value of 5 mm for the channel length and with an input-beam intensity of $I_0 = 1\,\text{W/cm}^2$, required to achieve the necessary change of the refractive index.
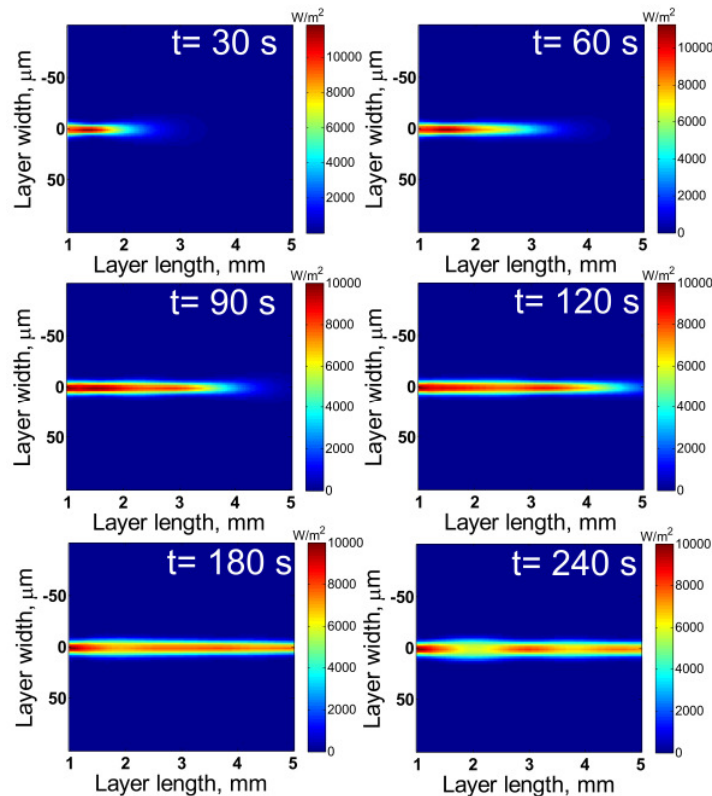

Fig. 5.2. Simulation calculations of the self-trapping formation in the PQ-PMMA polymeric layer in dependence on the recording time [from 30 s to 240 s].

Using the theory presented above, the formation process of beam focusing can be described as a consequence of the compensation of the divergence of light by the nonlinear response of the polymeric medium. Figure 5.2 shows an example for the formation of self-trapping in a polymeric layer by the light intensity distribution. The self-trapping process develops within 2.5-3 min. Further illumination longer than 4 min leads to an overfocusing of the laser beam. One assumes that the formation of the self-trapping channel in the PQ-PMMA polymeric layer for the predicted parameters (e.g. an input intensity of about $1 \text{W}/\text{cm}^2$) requires a recording time of about 120-180 s.

The distributions of the change of the refractive index in a polymeric layer after different times of illumination are shown in Fig. 5.3. The variation of the amplitude of the refractive index reaches its maximum (of about $\Delta n = 4 \cdot 10^{-4}$) at the front of the polymeric layer. The channel is formed gradually and achieves the maximum of Δn within the sample. The simulated values of the maximal refractive-index change are in good agreement with the experimental results of the recorded periodical structures (chapter 4.2).
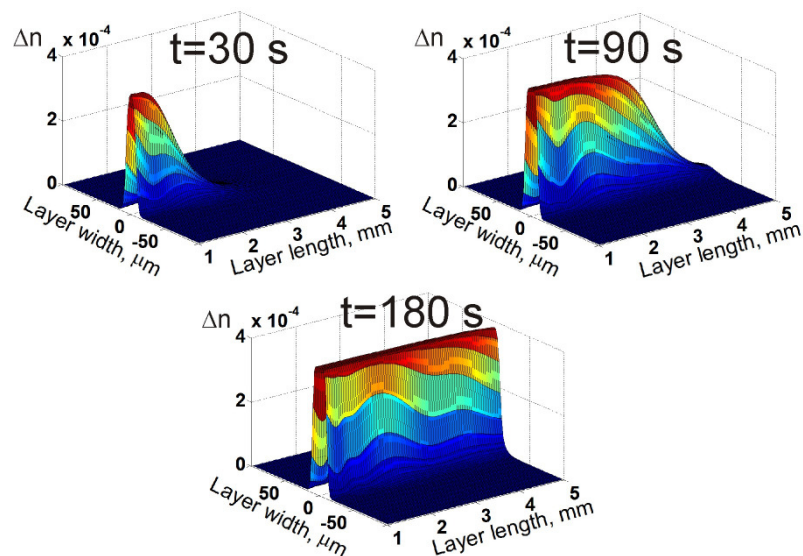

Fig. 5.3. Simulation of the refractive-index change versus illumination time [t=30 s, 90 s and 180 s].

The change of the cross-section of the output beam under laser radiation is illustrated in Fig. 5.4. Three temporal phases can be separated. The first phase (several seconds) corresponds to the case, when the beam cannot escape from the medium due to strong absorption. The second phase (until ~ 2 min) corresponds to a sharp decrease of the radius of the output beam. The third phase

(several minutes) corresponds to a slow asymptotic constriction of the output beam. At 125 s the output radius becomes equal to the input one ($x_0 = 6\,\mu m$), and a straight channel in the polymeric layer is generated. Subsequent laser radiation leads to a further reduction of the self-trapping channel width.
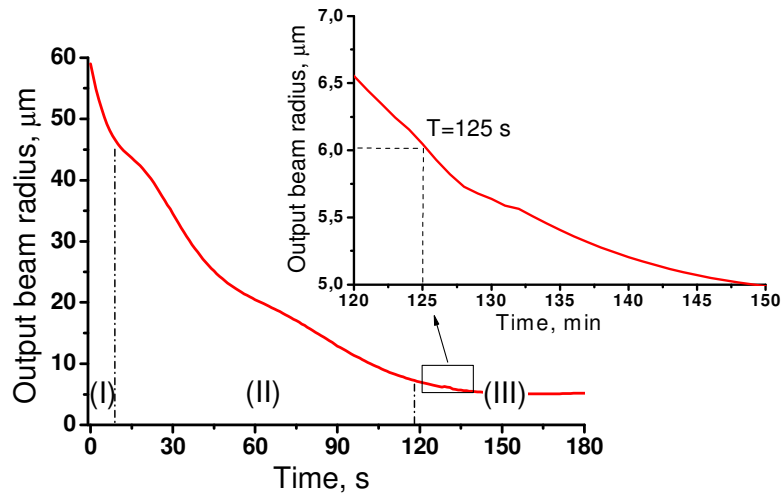

Fig. 5.4. Numerically calculated dependence of the output-beam radius versus recording time.

Figure 5.5 [a] shows the variation of the beam radius along the polymeric layer during illumination. At first the natural divergence of the beam dominates. Then the increase of Δn together with a rapid reduction of absorption in the central part of the beam profile leads to a contraction of the beam radius. Afterwards a further illumination forms a channel by compensating the natural divergence.
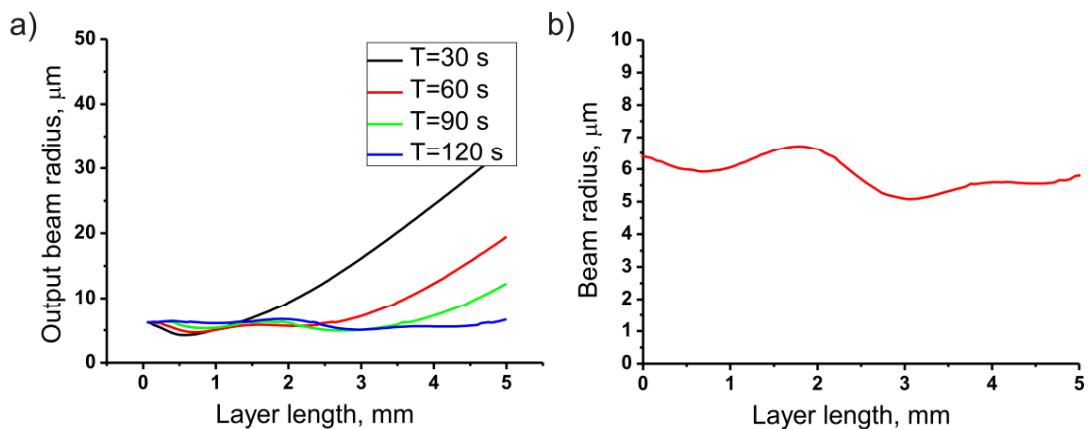

Fig. 5.5. [a] Evolution of the output-beam radius depending on the length of the layer for different illumination times of 30 s, 60 s, 90 s and 120 s and [b] analogous dependence for a fixed recording time of 120 s.

It is possible to retrace the evolution of the beam radius at the time of the self-trapping formation (i.e. at 120 s) [Fig. 5.5 [b]]. For a sample with a length of 5 mm the beam radius shows small variations. In the middle of the layer the beam radius exhibits some deviations but approaches an almost constant value of about 5.5 µm at the end of the sample. In contrast, natural divergence would lead to a beam radius of ~ 70 µm on the 5 mm-length.

In summarising, the generation of self-trapping of light beams in photopolymers based on PMMA doped with PQ-molecules has clearly been proven. The calculated change of the refractive index reached values as large as $\Delta n = 4 \cdot 10^{-4}$. Beam propagation over a length of 5 mm (that is ten times larger than the Rayleigh length) is sufficient to demonstrate unambiguously the self-trapping effect.

5.2. Experimental demonstration of self-trapping in PQ-PMMA layers

After a theoretical model for the self-trapping formation was derived, an experimental proof is definitely required. These experiments were carried out by using the newly developed PQ-PMMA layers. In previous chapters it was demonstrated that a sufficient variation of the refractive index and the formation of an efficient diffractive structure has been obtained. The high thermal stability of the PQ-containing polymeric layers recommends such photorefractive media as very suitable candidates for the self-channeling processes. In this chapter we demonstrate for the first time experimental results which prove the self-trapping of a laser beam in photosensitive PQ-PMMA polymeric materials.

The polymeric layers were prepared by applying the technology as developed by us and described above [i.e. dissolution of PQ and PMMA in chloroform as solvent, pouring this liquid onto a glass substrate and subsequently drying it slowly in a Petri dish at a temperature of $100^{\circ}C$ for 20 hours]. As was described already, the PMMA, carefully purified of the monomer, was used without exploiting the effect of polymerization. Experiments for self-trapping generation were made for a series of samples with a layer thickness of 400 µm and a PQ-concentration of 2.5-3 mol.%.

To generate a waveguiding structure in the polymer an Ar-laser was used [Fig. 5.6 [a]]. The laser power required to form a channel is found experimentally

to be in the range of milliwatts. That is an order of magnitude higher than the values obtained previously from the theoretical model. The laser beam was focused on the front surface of the polymeric layer using a microscope objective with a focal length of 16 mm. The PQ-PMMA sample was placed on a mechanical stage which allows to control the position of the input beam. The beam diameter at its waist behind the microscope objective was 16 µm (FWHM). A CCD-camera was used to detect visually the self-trapping formation.
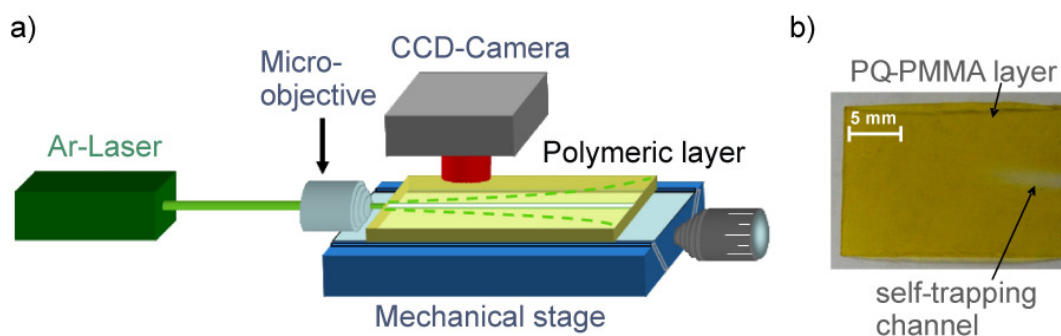

Fig. 5.6. [a] Schematic setup for formation of a self-trapped channel using Ar-laser illumination and a microscope objective; [b] self-trapping in a PQ-PMMA polymeric layer (top view).

The polymeric layers have a yellow colour with an absorption band up to about 530 nm. Under Ar-laser illumination (514.5 nm) the colour changed from yellow to almost transparent, which means that all photosensitive PQ-molecules join the polymeric matrix with subsequent formation of light-sensitive photoproducts. The self-induced waveguiding structure in the PQ-PMMA medium is shown in Fig. 5.6 [b].

The experiment was carried out with several identical samples. The illumination of the samples with a power of 8 mW was made for periods of 60 min. The generation of the planar straight channel induced by the incident light itself was observed in the PQ-PMMA layer during an irradiation period of 12 min [Fig. 5.7]. The photoattachment of PQ-molecules to the polymeric matrix resulted in a necessarily nonlinear change of the refractive index by which a stable waveguiding structure was produced by the Ar-laser illumination. The formed channel has a length up to 4-5 mm after an exposure time of 6-10 min. By further illumination (15-60 min) the distortion of the self-trapping channel started. This happens due to the absorption of PQ-molecules in the peripheral areas of the channel, leading to a multiple broadening of the channel and to a loss of the self-trapping property.
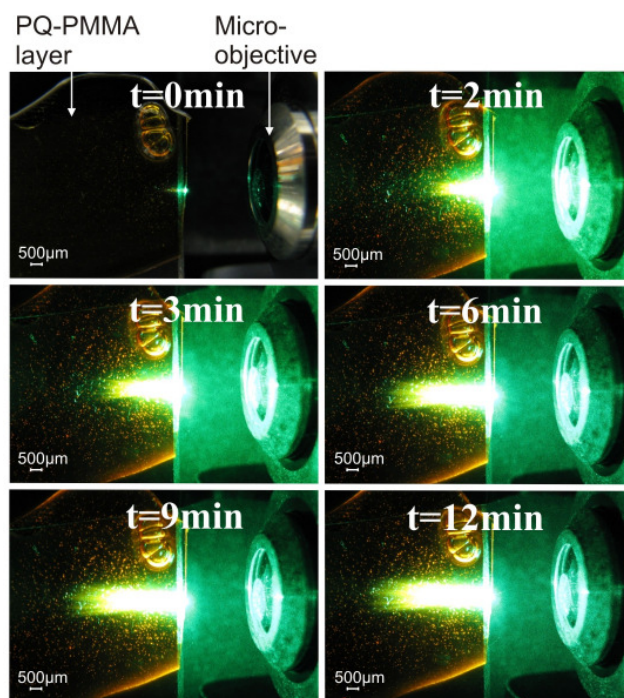
Fig. 5.7. Experimental self-trapping formation in the PQ-PMMA layer by Ar-laser illumination during 12 min [laser power is 8 mW, PQ-concentration is 2.5 mol%, layer thickness is 400 µm].

In spite of the small-input beam diameter (16 µm) the width of the achieved channel was about 500 µm [Fig. 5.7]. The additional investigation of the Plexiglas PMMA material without PQ-molecules under Ar-light illumination revealed a high divergence of the propagating beam [Fig. 5.8]. This led us to suggest that as a result of the high input power at the beam focus the polymeric absorption material starts warming up with the consequently large increase of scattering of light.
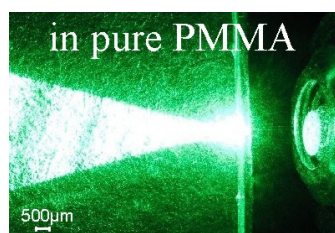

Fig. 5.8. Ar-laser-light propagation in a pure PMMA medium through the micro objective with a magnification factor of 10 and a focal length of 16 mm [light power is 8 mW].

The activation of the warming-up effect in the PQ-PMMA film results in the formation of a thermal-lens and increases the divergence of the laser beam, starting just after beginning of the illumination. Normally Plexiglas is almost transparent for Ar-laser radiation, being subjected to the natural diffraction of light. According to the parameters of the laser and the microscope objective, the light divergence in the PMMA layer should be equal to 10-12 mrad. The thermal lens formed in the layer increases the light divergence even under the

influence of minor absorption ($\alpha \approx$ a tens of cm^{-1}). However, the high intensities in the focal region ($I \approx 1kW / cm^2$) lead to a broader distribution of light [Fig. 5.8].

The injection of the light-sensitive PQ-components into the polymeric matrix causes the photoproduct formation and generates a straight channel [Fig. 5.7]. The process of fast heating appears at the point of maximum input intensity till the PQ-phototransformation is completed and proceeds within the layer. The formation of the self-channeling with significant cross-section can be associated with two competitive mechanisms: thermal beam expansion together with the variation of the photoinduced nonlinear refractive index.

Thereby, experimental results indicate the possibility of the formation of straight waveguides in PQ-PMMA media. The broadening of the channel can be associated to the activation of the thermal defocusing in the material due to the high input power. This defocusing effect is compensated by the effect of nonlinear self-focusing of the light beam generating a waveguide structure. Making the assumption of the thermal expansion of self-trapping we decided to prove it theoretically. An improvement of the previously derived numerical model by including the thermal effect can be implemented by taking the heat-conduction equation into consideration.

5.3. Broadening of the self-trapping channel due to thermal defocusing in PQ-PMMA polymers

5.3.1. Mechanism of light-channel expansion

The special characteristic of the light-beam distribution in polymeric materials is a nonlinear change of the absorption coefficient during the PQ-photoattachment process. Thus, along with the variation of n caused by the photoreaction of PQ (Δn_{PQ}), a thermal change of the refractive index (Δn_T) is closely connected with this and has to be taken into account for any simulation calculation. Under steady-state conditions the influence of the thermal effect on the change of the refractive index can be calculated as [140]:

$$\Delta n_T = \frac{\alpha I t}{C_\rho} \frac{\partial n}{\partial T},$$
5.18

where α is the absorption coefficient of the medium, I is the beam intensity, t is the effective interaction time, C_ρ is the heat capacity of the unit volume, called also the volumetric heat capacity, and $\partial n / \partial T$ is the thermooptical coefficient. Since the medium is normally hotter on the beam axis, compared with the outer regions, a transverse gradient of the refractive index is caused, called the thermooptical effect, which is quantified by the coefficient $\partial n / \partial T$. Index changes can be caused by the temperature dependence of the refractive index and by the thermally induced mechanical stress (photoelastic effect). Both mechanisms can lead to bulging of the end faces of the gain medium, causing the effect of thermal lensing, which plays a significant role in laser resonators.

In the case of an excitation by short pulses (in the range of nanoseconds) the effective interaction time is determined by the pulse duration ($t = t_{pulse}$). For an irradiation with a continuous-wave laser the interaction time is defined by the thermal relaxation time $t = t_{rel} = L^2 / (4\pi^2 a_T)$, where L is the area of interaction and $a_T = k_T / C_\rho$ is the thermal diffusivity coefficient (which is defined as the thermal conductivity k_T divided by the product of the density ρ and the specific heat capacity c_T, which is identified as the volumetric heat capacity $C_\rho = c_T \cdot \rho$). In the general case the effective interaction time is determined by the expression $t = t_{rel}[1 - \exp(-t_{pulse} / t_r)]$. In a medium with $\partial n / \partial T < 0$, there is a defocusing effect caused by the temperature, which eliminates the process of self-focusing [8]. In rare cases, when $\partial n / \partial T > 0$, one can observe the reverse situation, i.e. a heating of the medium generates self-focusing.

The variation of the refractive index due to warming can be essentially higher at a certain area in the polymeric layer and can compensate accordingly the Δn - change caused by photoattaching. The position of this area corresponds to the maximum light intensity and results in a channel widening. To investigate the complete change of the refractive index in the PQ-PMMA material during self-trapping generation, we included the mechanism of thermal nonlinearity in the numerical simulations.

The change of the temperature (ΔT) in the illuminated area can be calculated using the heat conduction equation along the two orthogonal coordinates x and z [141]:

$$\frac{\partial \Delta T}{\partial t} - a_T \left(\frac{\partial^2 \Delta T}{\partial x^2} + \frac{\partial^2 \Delta T}{\partial z^2} \right) + b \Delta T = \frac{\alpha I}{C_\rho}, \qquad 5.19$$

where b is the coefficient of the heat transfer and $C_\rho = c_T \cdot \rho$ is the volumetric heat capacity with the specific heat capacity c_T and the density ρ of the material, as mentioned above.

The solution of Eq. 5.19 provides the value of ΔT (temperature difference between the waveguide structure and the surrounding material), which can be calculated by separation of the linear [Eq. 5.20 [a]] and nonlinear [Eq. 5.20 [b]] parts of Eq. 5.19 applying the split-step method [139]:

$$\frac{\partial \Delta T_L}{\partial t} = a_T \left(\frac{\partial^2 \Delta T}{\partial x^2} + \frac{\partial^2 \Delta T}{\partial z^2} \right) - b \Delta T \qquad 5.20 \ [a]$$

and

$$\frac{\partial \Delta T_{NL}}{\partial t} = \frac{\alpha I}{C_\rho}. \qquad 5.20 \ [b]$$

The change of the refractive index due to the heating (Δn_T) results in the thermal defocusing of the beam and can be calculated by the following expression:

$$\Delta n_T = \frac{\partial n}{\partial T} \Delta T, \qquad 5.21$$

where $\partial n / \partial T = -1.3 \cdot 10^{-4} \, K^{-1}$ is the thermooptical coefficient of PMMA [142]. Because of the negative value of the thermooptical coefficient the thermal change of the refractive index leads to an absolute magnitude with opposite sign as compared with the magnitude of Δn_{PQ} (contributions of the change of refractive index due to the PQ-reaction with subsequent photoproduct formation [Eq. 5.17, p.73]). This results in a thermal defocusing of the light beam with the corresponding channel broadening. The sum of the two contributions to the change of the refractive index (Δn_Σ) is decreasing according to:

$$\Delta n_\Sigma = \Delta n_{PQ} + \Delta n_T. \qquad 5.22$$

5.3.2. Numerical simulation of channel broadening

These calculations are based on the PQ-PMMA parameters used in the experiment presented above: laser input power 8 mW, input-beam radius $x_0 = 9.6$ µm (at 1/e mean) and the initial PQ-concentration 2.5 mol.%, $n = 1.5$, $\lambda_0 = 514.5$ nm, $\Delta R = 1.4\,\text{cm}^3/\text{mol}$ [42]. The absorption coefficient α varies in the range of about tens of cm^{-1}. For the solution of Eq. 5.20 [a] the thermal diffusivity coefficient was assumed to be $a_T = 10^{-7}\,\text{m}^2/\text{s}$ and a heat capacity of $C_\rho = 1.7 \cdot 10^6\,\text{J/(m}^3 \cdot \text{K)}$ was used, which were corresponding to the properties of the PQ-PMMA material [142-144]. The magnitude of the heat-transfer coefficient was found to be inversely proportional to the velocity of the heat propagation in the polymeric medium. In the numerical calculations $b = 0.2\,\text{s}^{-1}$ was chosen for a polymeric layer thickness of 400 µm [141,142].
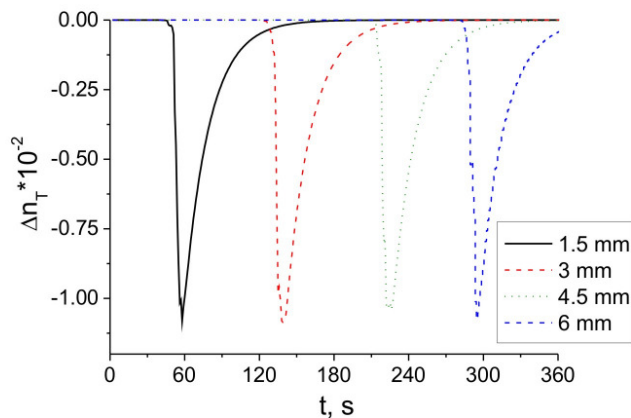

Fig. 5.9. Distribution of the thermal changes of the refractive index in dependence on the illumination time for different lengths of the polymeric layer [1.5 mm, 3 mm, 4.5 mm and 6 mm].

The obtained changes of the refractive index Δn_T due to thermal defocusing in dependence on the illumination time for different layer lengths are presented in Fig. 5.9. The decrease of the change of the thermal refractive index reaches values of $\Delta n_T = -1 \cdot 10^{-2}$. The negative value of Δn_T substantially exceeds the positive change of the refractive index $\Delta n_{PQ} \approx 10^{-4}$ [121]. The superposition of both processes leads in total to a negative change of the refractive index at the local point where the laser has higher intensity. The interplay of thermal

defocusing and nonlinear properties of the medium causes a channel widening at this point.
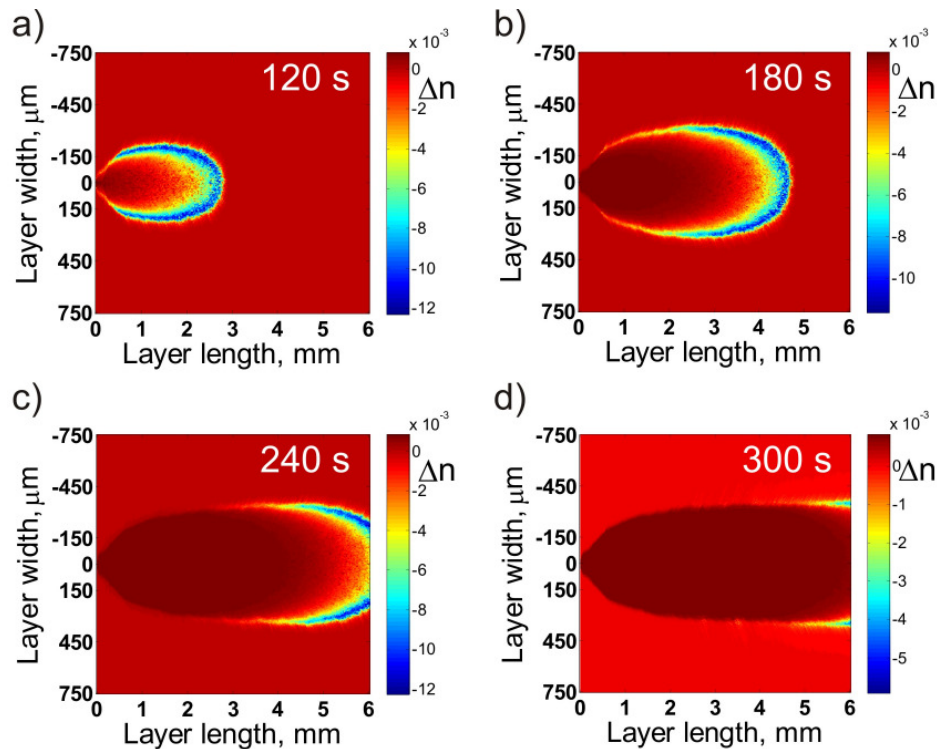

Fig. 5.10. Formation of the refractive-index profile for illumination times of [a] 120 s, [b] 180 s, [c] 240 s and [d] 300 s.

The numerical evolution of the total refractive-index profile is shown in Fig. 5.10. As mentioned above already, one can observe that in spite of the small input beam diameter (16 µm) the resulting channel has a large width of about 500 µm. The influence of the thermal change of the refractive index occurs immediately when the polymeric layer is hit by the laser beam, thus substantially expanding the self-trapping channel. At the point where the channel is already formed the temperature of the polymer is reduced and the total refractive index becomes positive. This allows already illuminated and chilled areas to be used as waveguiding structures. The complete formation of a self-trapping channel in the PQ-PMMA layer of a length of 6 mm was generated within 5-6 min of illumination with an input beam power of 8 mW. The obtained numerical result corresponds to our previous experimental observation of the formation of a straight channel [Fig. 5.7, p.69].
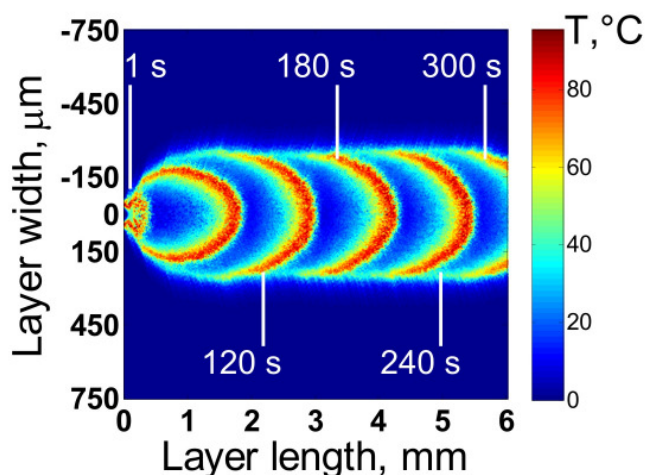
Fig. 5.11. Evolution of the spreading of temperature in the polymeric layer during an illumination period of 300 s.

Thus, the mechanism of channel formation and broadening can be described like a heat wave propagating together with a light wave through the polymer [Fig. 5.11]. At the point of maximum intensity the formation of a thermal lens occurs with subsequent activation of the thermal defocusing effect. The main broadening of the channel is observed during the first 15 s after starting the illumination process. At the place of the maximal beam intensity the temperature of the polymeric layer achieves a peak value of about 100°C (for input beam power of 8 mW) due to the thermal absorption of the PQ-PMMA material. After finishing the PQ-photoaddition process the layer becomes transparent to the laser light and the illuminated area cools down. At this time the warming-up process is stopped. The area of the maximal temperature, a heat wave, moves forward together with the propagating light-beam with a velocity determined by the speed of the reaction of the PQ-photoattaching process to the polymeric matrix.

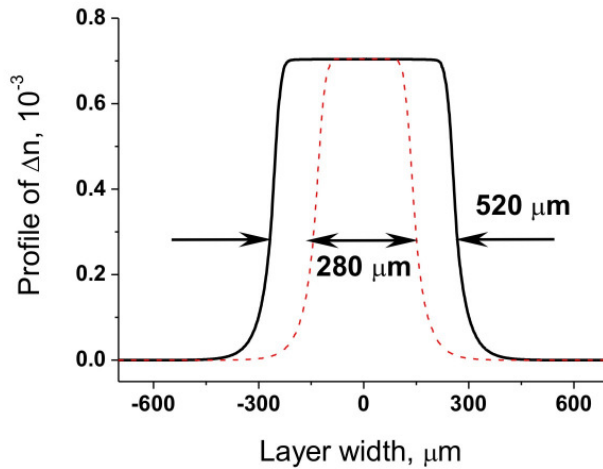### 5.3.3. Control of the width of the generated waveguide

Fig. 5.12. Simulation of the refractive-index profiles for input powers of 2 mW (dotted line) and 8 mW (solid line).

In consideration of the dependence of the thermal defocusing on the beam power, we examined the possibility of the self-trapping formation using specific cross-section parameters of the channel. A numerical simulation of channel formation provides a possibility to control the development of the channel width and allows to produce waveguiding structures of desired dimensions.

Figure 5.12 demonstrates the results of the numerical calculation of the profile of the refractive-index change for input powers of 8 mW and 2 mW. The diameter of the channel is reducing by a factor of about 0.5, if the power decreases by a factor of 4.

After the theoretical simulation of the self-trapping has been made, an experimental improvement of the formation of channels with various widths was required. The experiment was carried out by using the same PQ-PMMA layers and experimental setup as in the previous self-trapping-formation experiment [Fig. 5.6, p.78]. The formed channel has been detected as an area with practically absent absorption. The results of photometric measurements of the formed self-trapping channel gave us the possibility to plot the cross-section of the distribution of the refractive index in the polymeric layer and to determine the diameter of the generated channel. The formation of the waveguiding structures for two different input-beam powers (8 mW and 2 mW) is shown for both cases in Fig. 5.13 together with the Δn-distributions normalized with respect to the maximum values of the refractive-index profiles. At the input beam power of 8 mW the channel broadens out to a width of 510 µm (FWHM), whereas it achieved the width of 285 µm for the lower input power of 2 mW. The experimental results coincide with

the theoretical ones with only small deviations due to the good agreement between the theoretical and experimental parameters.
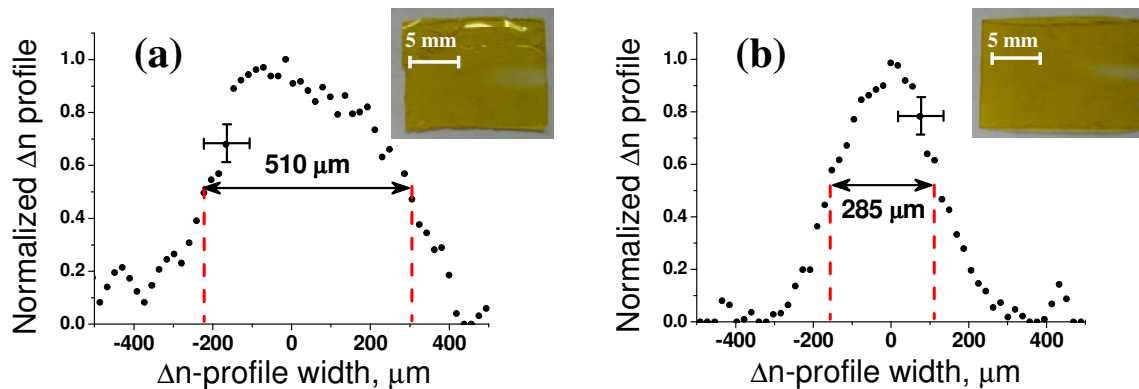

Fig. 5.13. Measured normalized refractive-index profiles for input beams with a power [a] of 8 mW and [b] of 2 mW.

5.4. Conclusion

In this chapter the possibility of the self-trapping channel formation by a (1+1)D beam in a polymethylmethacrylate matrix containing PQ-molecules is shown experimentally and theoretically for the first time. It is proven that this reaction is due to the change of the photoinduced nonlinear refractive index. An analytical description connected with a numerical calculation of the propagation of self-trapped laser beams in PQ-PMMA polymeric layers was shown. A theoretical model for the spatial distribution of boundary optical waves was described depending on the experimentally obtained characteristic beam parameters.

The calculated self-trapped beam radius was 6 μm, and the formation of self-trapping was observed between 120 s and 180 s after starting the illumination, applying a beam intensity of $1 W / cm^2$ of 514 nm wavelength, respectively. By simulation calculations a maximum value of $4 \cdot 10^{-4}$ for the refractive-index change was obtained. A self-trapping effect with a propagating length of 5 mm (exceeding several times the Rayleigh length) was confirmed.

The self-trapping of a laser beam in a PQ-PMMA layer was generated by using an Ar-laser. A width of the channel in the polymer of 500 μm was achieved with an incident beam of 16 μm diameter and remained constant along a distance of 4-5 mm. According to the mechanism of self-trapping the focused laser beam should

propagate through the nonlinear media keeping its cross-section parameters constant without broadening. It was confirmed numerically by using the diffraction equation for the beam distribution, including the effects of diffusion and absorption of the medium. The effect of self-trapping widening was explained by the thermal defocusing of a light beam due to an input power large enough for the generation of self-channeling.

The numerical model of the description of the propagation of a laser beam in PQ-PMMA media was improved by taking the heat-conduction equation into consideration. Heating produces a negative change of the refractive index in the photopolymer, which leads to the reduction of the resulting Δn and to channel widening. The formation of a self-trapped channel with a length of 6 mm was observed by applying Ar-laser illumination for a duration of 5-6 min. This is in good agreement with the experimental results. The effect of thermal beam expansion together with the nonlinearity of the medium are responsible for the self-trapping mechanism. Moreover, a way was found to control the diameter of the generated channel by varying the input power of the laser beam. The experimental results were confirmed by the theoretical modeling of the self-trapping process. For a width of 16 μm of the input beam and an input power of 8 mW a channel width of 510 μm was obtained experimentally and of 520 μm theoretically. For a lower power of 2 mW the theoretical width is 280 μm compared to an experimental value of 285 μm.

Chapter 6   Applications of PQ-PMMA Optical Media

Photorefractive polymeric media with good photosensitivity, long storage time and easy fabrication make it possible to create optical elements having unique properties including diffractive optical elements and reflection and transmission holograms [18-20,107]. They can be applied for the fabrication of optical holographic memories, image storage devices, in multiplexing holography and three-dimensional displays [24,145-148]. High capacity, high density and fast readout rates, that are required for new computer and internet technologies, can be attained by two- and three-dimensional holographic information record, applying these media also for the rapidly proceeding development of CD/DVD technologies [116,149-151].

The low-price production process and the manufacturing of high-precision components suppose it profitable to use PQ-containing medium for the realization of interference filters with high-spectral selectivity and for the fabrication of multiple-channel optical demultiplexers for astronomy, spectroscopy and communication technology [28,113,115]. PQ-PMMA media are used for the production of filters operating with at wavelengths of 1550 nm [109-111] as well as in some optical holographic instruments for data storage [25,40,41,102,117-120]. The wide field of their possible practical application is given by the possibility to mold stable polymeric samples with required dimensional parameters and desired shapes. These PQ-PMMA media are characterized by minimal shrinkage and scattering effects together with a large dynamic range of the refractive-index modulation. Using holography, light that is reflected by a sample interferes with the reference light, leading to an interference pattern, i.e. a hologram, by which for instance cell structures can be newly presented in different depths and with different optical characteristics such as transmission, reflection and refraction index.

PQ-PMMA polymeric layers possess high-optical qualities and open new applications for multiplexing hologram formation [23,107,108,114]. Widening of the angular selectivity of the photoinduced structures recorded in polymers by optical image multiplexing allows the application of the diffractive elements as holographic

concentrators of the radiation energy to improve the efficiency of solar cells. The ability to generate waveguiding structures in PQ-containing samples is important for the optimization of the optical interconnection wiring and for splicing of fibers [100]. It is a potentially useful technique in the wide range of the development of fiber-optical systems, optical interconnects and waveguide couplers. Fixation of efficient and stable gratings in the PQ-PMMA polymer enables to produce optical beam splitters for controlling the beam.

In general, optical devices based on the PQ-PMMA possess high reliability, a wide range of operation temperature and a broad angular acceptance. The whole set of these parameters makes it possible to replace complex optical systems for the interaction of monochromatic light by simple volume phase holograms recorded in PQ-PMMA materials with definite parameters. In addition, the self-trapping generation of gratings opens new feasibilities for optical communication processes using waveguiding channels for light transfer and as light splitters.

6.1. PQ-PMMA polymers for head-up displays

Stable volume holograms written into photopolymeric layers can serve as mirrors, mode selectors, deflectors, filters and splitters. Moreover, they have a wide application in automobile head-up displays (HUDs) as holographic screens [152-154]. The HUDs have been used for many years in military aircraft cockpits and are now being installed also in civil aircrafts and vehicles [154]. The main utilization of HUD is to provide the driver with all necessary information (symbols and/or images) concerning traffic conditions in the form of virtual pictures by reflecting images off a transparent surface in the line of sight of the user. Vehicle windshields consist usually of two glass plates cemented with polyvinylbuteral (PVB). According to the technical specifications of the autoclave manufacturer Tamglass, the production of a HUD is proceeded during about 2 hours at temperatures of $140^0 C$ under a pressure of 13 bar.

After developing new PQ-P(MMA+AA) polymeric media with high thermal stability (up to $200^0 C$) we designed a new HUD screen for vehicle windshields with a holographic grating [120,125]. The reflection holographic grating that is located between the glass plates of windshields should satisfy some requirements. First of all its high diffraction efficiency has to be combined with a quite low angular

and spectral selectivity to provide efficient reflection of the relatively broadband radiation within the angular range that is required for the observation. These properties were obtained by decreasing the thickness of the holograms and increasing the modulation depth of the refractive index. Obviously, holographic gratings should be transparent for visible light and stable against temperatures up to $140^{o}C$ and pressures up to 13 bar, qualities which are achieved by PQ-P(MMA+AA) copolymers.

The generation of the reflection grating in the photopolymeric layer was carried out by Ar-laser irradiation with intensities of the interfering beams of 30 mW each. In order to prevent coincidence between the reflections on the grating and on the rear glass surface, the grating was slightly tilted against the glass substrates with an inclination angle of $\gamma = 1.2^{0}$ [Fig. 6.1 [a]]. The geometric size of the photopolymeric sample was $5\,cm \times 5\,cm$. The recorded grating had an aperture of about $3\,cm$ with a grating period of $0.2\,\mu m$. The recorded holograms were amplified by heating at $80^{o}C$ and stabilized by ultraviolet (UV, 300-350 nm) illumination. The remaining free, not bound PQ-molecules can be transformed into a non-photosensitive product [57,117,118]. The layer containing the grating was inserted between the two glass plates of the windshield, as shown in Fig. 6.1 [a]. Finally, the whole system was heated for 2 hours at $140^{o}C$.
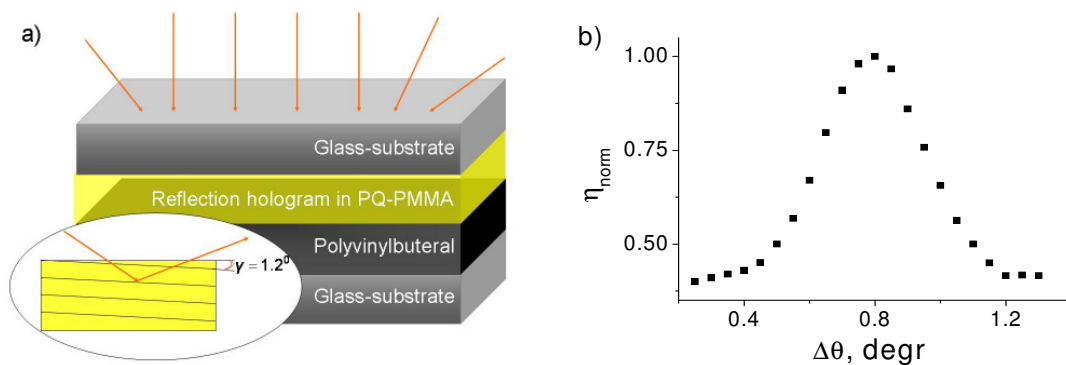

Fig. 6.1. [a] Schematic diagram of the laminated glass with the tilted reflection grating recorded in the PQ-PMMA layer [grating period is 0.2 μm, tilt angle is 1.2^{0}]; [b] normalized diffraction efficiency as a function of the angle of incidence of the light beam, providing a measure of the angular selectivity of the grating.

The values of diffraction efficiency and angular selectivity were measured by using the radiation of a solid-state laser at a wavelength of 532 nm, which possesses negligible absorption by PQ-P(MMA). Losses by Fresnel reflection and

dispersion were included. The diffraction efficiency measured relative to the incident beam amounts to 50 %. The angular selectivity was controlled by monitoring the change of the diffracted beam intensity. The angular selectivity amounts to 0.6^o [Fig. 6.1 [b]]. The shrinkage of the PMMA-photopolymeric layer is lower than the similar DuPont materials [53,55]. Thus, no wavelength shift or aberration caused by heating or pressing of the material has been observed.

The schematic HUD setup is shown in Fig. 6.2 [a]. It consists of a collimated light-emitting diode (LED, 532 nm) with a diffuser, a screen with the holographic grating, and a display with the inverted picture that is projected onto the detection screen. The reflection angle is 41° in air.
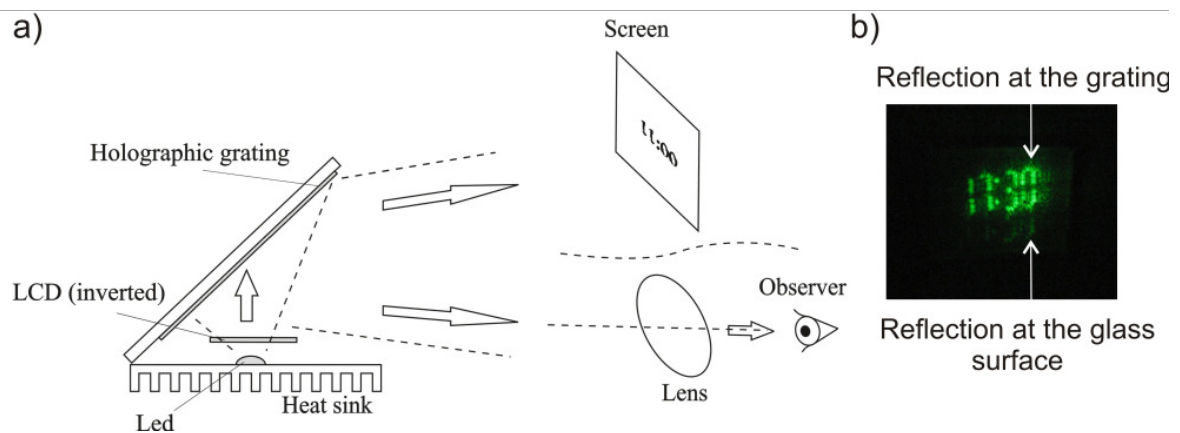

Fig. 6.2. [a] Schematic presentation of the optical path of a HUD with a light-emitting diode (LED) and [b] reflections from grating and glass substrate of the HUD-screen.

One can see on the picture [Fig. 6.2 [b]] the reflections of the signal beam (as a time image "17:30") from glass and holographic grating generated in the laminated glass. It demonstrates the good optical contrast of the newly developed HUD-screen, which in combination with an appropriate angular selectivity allows filtering out the important information independently of the background illumination.

6.2. Waveguide optics

6.2.1. Splicing of optical fibers by applying the self-trapping mechanism

The wide-ranging utilization of PQ-PMMA media for the fabrication of interference filters, displays and holographic elements and the possibility to produce straight and stable self-trapping light channels open up many possibilities of new applications in fiber-optics research. Most of the optical communication

systems are based on light transfer through optical fibers [138,155,156]. The generation of straight channels in PQ-PMMA layers could be improved by integrating an optical fiber into the polymer layer during the manufacturing process. By this technique, light can be irradiated into the sample more easily and much more accurately [Fig. 6.3 [a]]. In the case of a fiber for admitting of light, the generation of a self-trapping channel is the same as for direct light input into the polymer. The distribution of the formed straight channel in the layer can be controlled also by CCD-cameras.
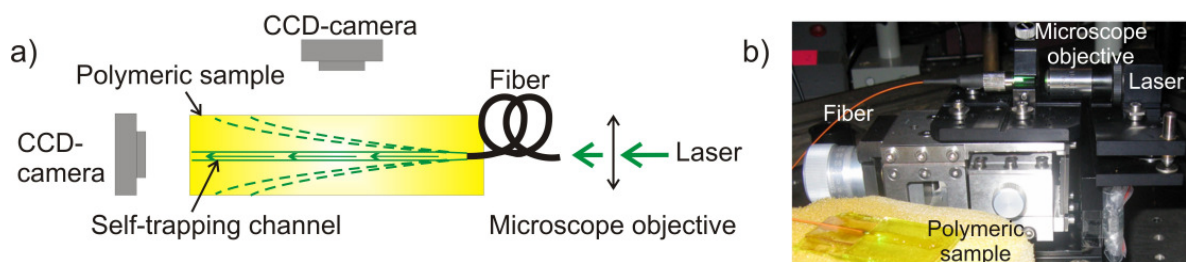

Fig. 6.3 [a] Scheme of light injection through a fiber into a PQ-PMMA layer for a self-trapping generation; [b] experimental setup for formation of a self-trapping channel using a microscope objective and an optical fiber with a core diameter of 50 µm.

Figure 6.3 [b] exhibits the experimental realization of the self-channeling in PQ-PMMA using light injection through an optical fiber. By a microscope objective and a precision rotary table it is possible to irradiate laser light into the core of the fiber with minimum radiation losses. By a careful treatment of the fiber ends the efficiency of light entrance and exit is not impaired. Self-trapping of the light beam generated by the fiber possesses the same properties as that generated by direct light injection.

The technique of light injection using optical fibers, investigated in the course of this doctoral Thesis, provides an opportunity to solve also the problem of the splicing of optical fibers. One of the common problems of data transfer using fibers is the high probability of disruption and breakage of the optical fiber during its exploitation. In such cases the ability to restore data transmission within the shortest period of time is of a great importance. A simple replacement of the cable is practically impossible in most cases. Therefore, a fast and automatic self healing of the damaged fiber is needed. Splicing a pair of waveguides usually requires complex and expensive devices, which are difficult to fabricate and are rather massive in size, since pressure, heat and/or mechanical power have to be used [157,158].

The problem of cable disruption in all kinds of networks led us to develop a splicing mechanism of waveguide fibers based on self-trapping in PQ-PMMA media. The polymer is able to represent the connecting material between the disrupted ends of an optical fiber and fixes fiber ends. The generation of a self-trapping channel inside PQ-PMMA substrate between two disrupted cables is stable over time and enables the waveguides to recover the transfer of communication signals.

To use the self-trapping mechanism for splicing of optical fibers it is necessary to align both ends of a ruptured fiber along a straight line and to connect them again [Fig. 6.4 [a]]. The ends of the optical fiber should be prepared with a flat surface perpendicular to the fiber axis. The fibers can be placed in special holders. Such support arrangements can be used after as a mould form for the liquid polymer. Pouring PQ-PMMA solution on the substrate and subsequent drying forms a solid polymer cube around the fiber.
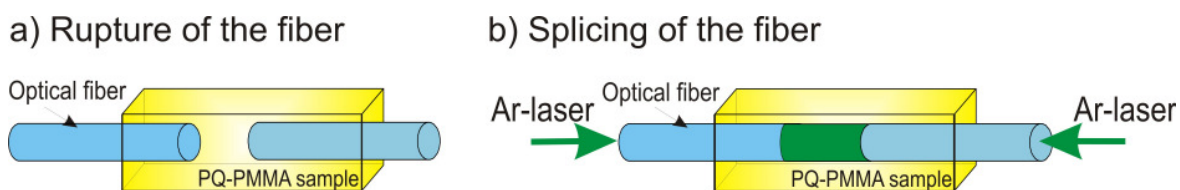

Fig. 6.4. [a] Injection of the two ends of the broken optical fiber into the polymer at the area of their disruption and [b] formation of a self-trapping channel between the two fiber tips inside the polymeric medium by laser illumination, thus repairing again the ruptured fiber.

By injection of the light from an Ar-laser into the polymer at both ends of the fiber a waveguiding channel could be generated. The two parts of the disconnected fiber, which are connected to each other in such a manner, will possess optical properties similar to a continuous fiber. This perspective application of the self-trapping mechanism for fiber splicing is shown in Fig. 6.4 [b]. It demonstrates that the damaged part of the fiber is replaced with low insertion losses by a self-formed waveguiding channel.

6.2.2. Prospects of multiple-waveguiding applications

In order to find much more applications of PQ-based, photosensitive polymeric materials our Institute together with a group from the Research Center "Vavilov State Optical Institute" (St. Petersburg, Russia) have recently developed new and

more voluminous PQ-PMMA samples with thicknesses up to millimetres [25]. The production of high-quality, thick and homogeneous polymers by pouring the liquid solution into a mould of appropriately larger volumes required the decrease of the PQ-concentration till 0.5 mol.%. Figure 6.5 [a] exhibits the sample of a polymeric medium with a 3 mm thickness together with its absorption spectrum.
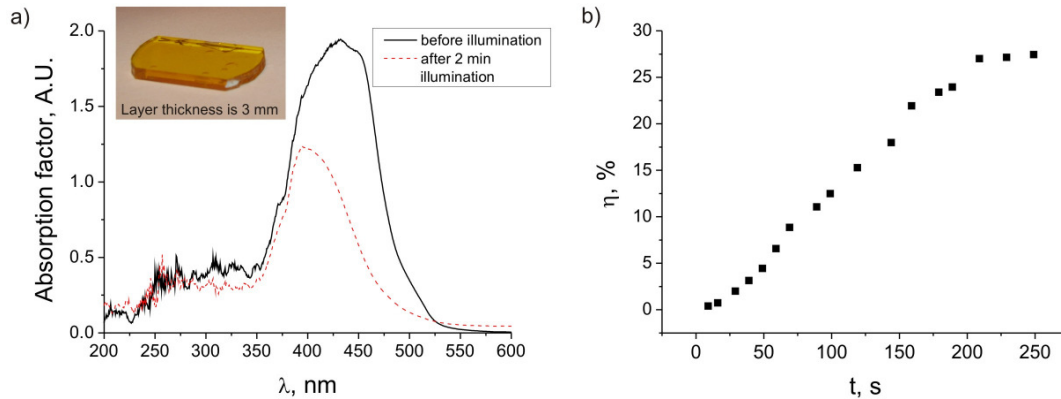

Fig. 6.5. [a] Absorption spectrum of a PQ-PMMA sample (see insert) before Ar-laser illumination and after 2 min of exposure time; [b] diffraction efficiency depending on the recording time for a transmission grating [PQ-concentration is 0.5 mol.%, input intensity is $60\,mW/cm^2$ at 514.5 nm wavelength, grating period is 0.5 μm, layer thickness is 3 mm].

The initial sample is light-sensitive up to wavelengths of ~ 530 nm [Fig. 6.5 [a]]. The reduction of the dye concentration causes a faster PQ-photoaddition to the PMMA and results as a consequence in the formation of a photoproduct, which is insensitive to the Ar-laser radiation. In thick PQ-PMMA layers smaller variations of the refractive index ($\Delta n = 0.25 \cdot 10^{-4}$) are produced during recording already after several minutes of illumination. However, the original ability to record highly efficient photoinduced structures is conserved. Diffraction efficiencies of almost 30 % are obtained by transmission gratings recorded in thick PQ-PMMA material [Fig. 6.5 [b]]. This thick polymer possesses sufficient variation of its density in order to activate the nonlinear properties of the medium and to generate the self-trapping mechanism.

The large increase of the dimensions of the polymers, maintaining at the same time the high optical properties of the recorded photoinduced structures, offers the possibility of many new applications of the self-channeling technique. These are e.g. the generation of multiple self-trapping waveguides [Fig. 6.6 [a]], of fiber optical splitters and optical switches for light control and splitting during information transfer in thick polymers, as shown in Figs. 6.6 [b] and [c].
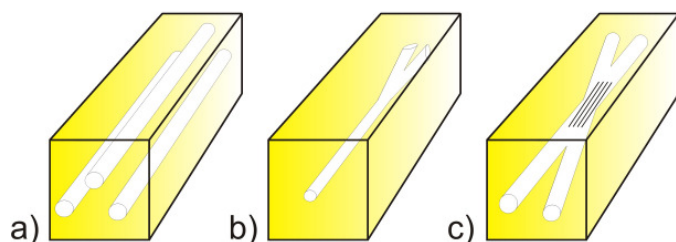
Fig. 6.6. [a] Multiple self-trapping waveguides; [b] fiber-optical splitters and [c] optical switches generated in voluminous PQ-PMMA layers.

The possibility to control the diameter of the formed channels by variation of the intensity of the incident laser radiation allows to generate waveguiding-like structures with specified cross-section parameters. Therewith, the PQ-PMMA material can possess a good optical quality suitable to transmit near-infrared light, which is widely used in optical telecommunication [43,109,110]. Besides that, by the self-trapping technique in thick PQ-PMMA layers the main elements of fiber optics, mentioned above, could rather easily be fabricated. By generating of two crossing self-trapping waveguides in thick polymeric layers at the same time diffractive elements could be produced [Fig. 6.6 [c]]. These complex photoinduced structures are the prospects to be used as switches or as optical filters for separating light waves of specified wavelengths.

6.3. Conclusion

Various applications of PQ-containing polymeric media deposited on glass substrates were demonstrated. The prototype of a head-up display based on a reflection grating recorded in a PQ-P(MMA+AA) photopolymeric layer was developed. The produced holographic grating was thermally stable up to $140^{\circ}C$. The angular selectivity amounted 0.6^{0}. The hologram is transparent and can be used for the production of laminated glasses for windshields of vehicles.

The possibility to insert optical fibers into the PQ-PMMA samples was shown. This procedure allows waveguiding-channel formation suitable for applications of fiber splicing. It was also demonstrated that polymeric media containing waveguide channels could be inserted between damaged fiber tips in order to repair ruptured optical fibers preserving their high optical qualities. The ability of preparing also voluminous PQ-PMMA samples opened new perspectives for applications of multiple self-trapping optical devices. Such multiple waveguiding structures could be perfectly used for optical switching of light beams and as optical splitters in information-transfer systems.

Chapter 7   Conclusions

In the present work comprehensive theoretical and experimental investigations of the self-trapping of a light beam in a photorefractive medium have been performed and are presented in detail. It has been shown that self-trapping of a laser beam due to the self-interaction of the propagating light wave with the nonlinear medium occurs under the condition of the well balanced concurrence of the effects of diffraction and nonlinear focusing. The nonlinear change of the refractive index, which determines the main properties of the generated waveguiding structure, was examined in a prospective polymeric medium based on polymethylmethacrylate (PMMA) with a high concentration of phenanthrenequinone (PQ) molecules. The photoinduced change and formation of structures in the PQ-PMMA material was generated by the laser light itself due to the PQ-photoattachment to the polymeric matrix and the formation of a photoproduct. The optimization of the PQ-PMMA composition was carried out with the help of recording and investigation of diffraction gratings. The holographic relaxation technique allows to establish the conditions for achieving high nonlinear modulations of the refractive index necessary to generate the self-trapping.

The results from examining the self-trapping effect of light in polymeric media, consisting of PMMA doped with PQ-molecules, can be summarized as follows:

▪ A manufacturing method for the preparation of photopolymeric layers based on the pouring of a purified PMMA solution with high concentrations of PQ-additions (up to 4 mol.%) onto a glass substrate and subsequently drying under a special operating treatment was developed. The obtained films are light-sensitive in the visible spectral range of 480–530 nm and are suitable for the generation of the stable light-induced waveguiding structures.

▪ It has been established that the light-induced change of the refractive index is due to the photoattachment of the light-sensitive PQ-molecules to the polymeric chains of the medium and the following formation of the photoproduct. The distribution of the concentration of the photoproduct is antiphased to the corresponding one of unreacted PQ-molecules in the polymeric layer. The diffusion of these free PQ-molecules leads to an increasing refractive-index

modulation by an order of magnitude up to maximum values of $\Delta n = 10^{-3}$. Diffractive structures with almost 80-90 % efficiency were generated in polymers with thicknesses of hundreds of microns using Ar-laser illumination at 514 nm wavelength.

▪ In order to increase the thermal stability of the polymeric material and to improve its adhesion properties, modifications of the monomer by adding acrylic acid (AA), methacrylamide (MAA) or methacrylic acid (MA) were performed. The thermal stability of the polymerized material has been extended to temperatures as high as $200^{\circ}C$, which significantly exceeds the glass transition temperature of the PMMA matrix. A holographic recording with a diffraction efficiency of 30 % was carried out with these materials. The non-local mechanism of the refractive-index modulation was investigated experimentally and associated with the polymerization process caused by the interacting light beam. The non-local response length of the phenanthrenequinone molecules amounts to 70 nm for PQ-P(MMA+AA).

▪ A theoretical model for the self-trapping of a (1+1)D beam based on the experimental data was developed. The conditions under which the nonlinear self-interaction of light can compensate the diffraction divergence were defined. Numerical simulations of the light-beam propagation assuming distances much longer than the Rayleigh length have confirmed the possibility of the formation of channel waveguides.

▪ The recording of self-trapping structures implemented in layers of purified PMMA with a high PQ-concentration has been performed under the action of an argon laser of 8 mW input power. A comparison of the propagation of light beams in pure PMMA and in PMMA containing sufficient amounts of PQ-molecules confirmed the decisive role, which the photoattachment process of the light-sensitive PQ-molecules to the polymeric matrix plays for the formation of the waveguide channel.

▪ It was found that the formation of the waveguide is strongly influenced by heating of the medium, which results in an additional thermal defocusing of the light beam. The theoretical modeling of the light propagation under conditions of the mutual action of the processes of PQ-photoattachment and thermal nonlinearity has confirmed the validity of the proposed approach.

- A new method for controlling the waveguide cross-sections by changing the ratio of the two competing mechanisms of the nonlinear refractive-index variation (namely the formation of the photoproducts and the heating of the medium while varying the power of the light beam) was proposed. With a diameter of the channel much larger than the diameter of the laser beam waist in the focal plane the following simple relation has been derived: the square of the ratio of the diameters of the two beams is equal to the ratio of their powers. By using this relation it is possible to generate channels with well defined and suitable cross-sections.

The obtained results have the prospect of practical application for the formation of waveguide channels and of diffractive optical elements based on the relatively cheap polymeric media. The prototype of a head-up display using a reflection grating generated in the layer of the PQ-PMMA copolymer was demonstrated. The produced holographic structure possesses good optical properties, high transparency and thermal stability suitable e.g. for their application in windshields. Besides, there is a great interest of using these holographic structures for the coupling of optical fibres as well as for the generation of optical X- and Y-splitters. The inclusion of additional diffractive elements into these waveguiding systems enables the construction of Bragg filters for the spectral separation of the laser illumination.

Chapter 8   Outlook

The obtained scientific results provide a good basis for the further research in the field of photopolymeric diffractive and waveguiding optics. From a practical point of view it seems appropriate to study the possibility of the connecting of disrupt optical fibers under conditions of the rough (imprecise) alignment of their ends. This connection could be achieved with partial overlapping of the light beams at the fiber outputs. The photoinduced change of the refractive index in the overlapping area of the beams will lead to their connection with the following formation of the waveguide channel, which will ensure a reliable information transfer. With the generation of two intersecting waveguides in PQ-PMMA polymeric media it becomes possible to realize fiber-optical splitters and optical switches. A system of parallel waveguides could realize the effect of discrete diffraction, in which a system of waveguides can implement the multiplexing of the optical signals, as well as their spectral decomposition.

Increasing scientific interest is connected with the modeling of neural networks and devices for quantum computing, when it is necessary to create a system of optical connections with complex topological structure, including even three-dimensional cases. Due to the self-interaction of the light beams in the photopolymeric medium one could observe the occurrence of the effects of light self-organization and formation of various spatial structures of the refractive index.

At the same time it should be noted that for the increasing of the refractive-index gradient over the cross-section of the waveguide during its generation it is possible to provide the high diffusion of PQ-molecules at distances much longer than the diameter of the channel. Considering the dependence of the PQ-diffusion coefficient on the temperature one can select the desired temperature conditions, at which the dye-molecules can diffuse from the significant adjacent areas of the sample into the waveguide channel. This way it can be expected to increase the photoinduced change of the refractive index of more than one order, which will allow forming waveguide structures with a small bending radius. Photocapture of the free PQ-molecules will keep a fail-safe fixation of the formed waveguide structures providing high stability against temperature and incident light.

Chapter 9   Zusammenfassung

In der vorliegenden Arbeit wurden umfangreiche theoretische und experimentelle Untersuchungen des "Self-Trapping"-Effekts eines Lichtstrahls in einem photorefraktiven Medium durchgeführt und im Detail vorgestellt. Es hat sich gezeigt, dass das "Self-Trapping" eines Laserstrahls infolge der Selbst-Wechselwirkung der sich ausbreitenden Lichtwelle mit dem nichtlinearen Medium unter der Bedingung auftritt, dass ein ausgewogenes Zusammenwirken der beiden Effekte der Divergenz und der nichtlinearen Fokussierung stattfindet. Die nichtlineare Änderung des Brechungsindex, die die wichtigsten Eigenschaften der erzeugten wellenleitenden Struktur bestimmt, wurde in einem neuartigen Polymermaterial untersucht, das aus Polymethylmethacrylat (PMMA) mit einer hohen Konzentration von Phenanthrenchinon-(PQ)-Molekülen besteht. Die photoinduzierte Änderung und die Bildung von Strukturen im PQ-PMMA-Material wurden durch das Laserlicht selbst erzeugt und zwar als Folge der lichtinduzierten Bindung der PQ-Moleküle ("PQ-Photoattachment") an die Polymermatrix unter Bildung des Photoprodukts. Die Optimierung der PQ-PMMA-Zusammensetzung basiert auf Messungen des Beugungswirkungsgrades holographischer Gitter. Diese holographische Technik ermöglicht es auch, die Bedingungen für das Erreichen einer starken nichtlinearen Modulation des Brechungsindex zu bestimmen, die die Voraussetzung für das Auftreten des "Self-Trapping"-Effekts sind.

Die Ergebnisse der Untersuchungen des "Self-Trapping"-Effekts von Licht in Polymeren, die aus PMMA dotiert mit PQ-Molekülen bestehen, können kurz wie folgt formuliert werden:

▪ Ein Verfahren zur Herstellung von photopolymeren Schichten wurde entwickelt, das aus dem Giessen einer gereinigten PMMA-Lösung mit hohen Konzentrationen von PQ-Zusätzen (bis zu 4 mol.%) auf Glassubstrate und dem anschließenden Trocknen unter besonderen Betriebsbedingungen besteht. Die erhaltenen Filme sind im sichtbaren Spektralbereich von 480 nm bis 530 nm lichtempfindlich und eignen sich zur Bildung von stabilen licht-induzierten wellenleitenden Strukturen.

▪ Es wurde gezeigt, dass die licht-induzierte Änderung des Brechungsindex eine Folge des "Photoattachment"-Prozesses der lichtempfindlichen PQ-Moleküle ist, also ihrer durch Lichteinfall bewirkten photochemischen Bindung an die Polymerketten des Mediums und der daraus resultierenden Bildung des Photoprodukts. Die Verteilung der Konzentration des Photoprodukts ist gegenphasig zur Konzentration der nicht photochemisch gebundenen PQ-Moleküle in der Polymerschicht. Die Diffusion dieser freien PQ-Moleküle führt zu einer um eine Größenordnung verstärkten Modulation des Brechungsindex bis zu Maximalwerten von $\Delta n = 10^{-3}$. Diffraktive Strukturen mit fast 80-90 % Effizienz wurden in Polymeren mit Dicken von mehreren hundert Mikrometern durch Bestrahlung mit Ar-Lasern bei 514 nm Wellenlänge erzeugt.

▪ Um die thermische Stabilität des Polymers zu erhöhen und seine Hafteigenschaften zu verbessern, wurden Änderungen des Monomers durch Zugabe von Acrylsäure (AA), Methacrylamid (MAA) oder Methacrylsäure (MA) vorgenommen. Die thermische Stabilität des polymerisierten Materials wurde bis auf hohe Temperaturen von 200°C erweitert, Temperaturen, die deutlich über der kritischen Glasübergangstemperatur der PMMA-Matrix liegen. Eine holographische Aufnahme mit einem Beugungswirkungsgrad von 30 % wurde mit diesen Materialien hergestellt. Die nicht-lokale Wirkung durch die Modulation des Brechungsindex wurde experimentell untersucht und dem Polymerisationsprozess zugeordnet, der durch die Wechselwirkung mit dem Lichtstrahl verursacht wird. Die nicht-lokale Responselänge der Phenanthrenchinon-Moleküle beträgt 70 nm für PQ-P(MMA+AA).

▪ Ein theoretisches Modell für das "Self-Trapping" eines (1+1)D-Lichtstrahls wurde auf Grundlage der experimentellen Daten entwickelt. Es wurden die Bedingungen definiert, unter denen die nichtlineare Selbst-Wechselwirkung von Licht die durch verursachte Divergenz des Strahls kompensieren kann. Berechnungen der Verteilung des Lichtstrahls durch numerische Simulation unter der Annahme, dass die Strahlwege viel länger sind als die Rayleigh-Länge, haben die Eignung zur Bildung von Wellenleiterkanälen bestätigt.

▪ Die Erzeugung von "Self-Trapping"-Strukturen in Schichten von gereinigtem PMMA mit einer hohen PQ-Konzentration wurde mit Hilfe eines Ar-Lasers von 8 mW Eingangsleistung durchgeführt. Ein Vergleich der Ausbreitung von

Lichtstrahlen in reinem PMMA und in PMMA mit ausreichenden Mengen von PQ-Molekülen, bestätigte die entscheidende Rolle, die der Prozess der photochemischen Bindung der lichtempfindlichen PQ-Moleküle an die Polymermatrix bei der Bildung eines Wellenleiterkanals spielt.

▪ Es wurde festgestellt, dass die Bildung des Wellenleiters stark durch Erwärmung des Mediums beeinflusst wird, die zu einer zusätzlichen thermischen Defokussierung des Lichtstrahls führt. Die theoretische Modellierung der Lichtausbreitung unter den Bedingungen der gegenseitigen Einwirkung der Prozesse des PQ-Photoattachment und der thermischen Nichtlinearität hat die Gültigkeit des vorgeschlagenen Ansatzes bestätigt.

▪ Eine neue Methode zur Kontrolle der Wellenleiter-Querschnitte durch Veränderung der Anteile der beiden konkurrierenden Mechanismen, die zur Variation des nichtlinearen Brechungsindex führen (nämlich die Bildung der Photoprodukte und die Erwärmung des Mediums durch Variation der Leistung des Lichtstrahls) wurde vorgeschlagen. Mit einem Kanaldurchmesser, der viel größer als der Durchmesser der Laserstrahl-Taille in der Brennebene ist, wurde die folgende einfache Beziehung abgeleitet: das Quadrat des Verhältnisses der Durchmesser der Strahlen ist gleich dem Verhältnis ihrer Strahlleistung. Mit Hilfe dieser Beziehung ist es möglich, Kanäle mit genau abgegrenzten und geeigneten Querschnitten zu erzeugen.

Die erzielten Ergebnisse bieten die Perspektive der praktischen Anwendung für die Erzeugung von Wellenleiterkanälen und von diffraktiven optischen Elementen, die aus relativ kostengünstigen Polymeren hergestellt worden sind. Der Prototyp eines "Head-Up-Displays" unter Verwendung eines Reflexionsgitters, das in der Schicht des PQ-PMMA-Copolymers generiert wurde, ist demonstriert worden. Die erzeugte holographische Struktur besitzt gute optische Eigenschaften, hohe Transparenz und thermische Stabilität, die sich z.B. für ihre Anwendung in der Windschutzscheibe eignen. Außerdem gibt es ein großes Interesse für die Verwendung dieser holographischen Strukturen zur Kopplung von optischen Fasern sowie für die Herstellung von optischen X- und Y-Verzweigern. Der Realisierung zusätzlicher diffraktiver Elemente in diesen wellenleitenden Systemen ermöglicht den Bau von Bragg-Filtern für die spektrale Trennung der Laserstrahlung.

Chapter 10　　References

[1]　M. Segev, G. Stegeman, Self-Trapping of Optical Beams: Spatial Solitons, Phys. Today. 51 (1998) 42-48.

[2]　G. Stegeman, D. Christodoulides, M. Segev, Optical spatial solitons: historical perspectives, IEEE J. Sel. Top. Quant. Electron. 6 (2000) 1419-1427.

[3]　Y.S. Kivshar, G. Agrawal, Optical Solitons: From Fibers to Photonic Crystals, San Diego, Academic Press, 2003.

[4]　D. Mihalache, D. Mazilu, Y.S. Kivshar, F. Lederer, Spatiotemporal discrete surface solitons in binary waveguide arrays, Opt. Expr. 15 (2007) 10718-10724.

[5]　U. Bortolozzo, F. Haudin, S. Residori, Diffraction properties of optical localized structures, Opt. Lett. 33 (2008) 2698-2700.

[6]　G.I. Stegeman, M. Segev, Optical Spatial Solitons and Their Interactions: Universality and Diversity, Science. 286 (1999) 1518-1523.

[7]　G.A. Askar'yan, Effects of the gradient of a strong electromagnetic beam on electrons and atoms, Sov. Phys. JETP. 15 (1962) 1088.

[8]　S.A. Akhmanov, A.P. Sukhorukov, R.V. Khokhlov, Self-focusing and diffraction of light in a nonlinear medium, Sov. Phys. Usp. 10 (1968) 609-636.

[9]　V.E. Zakharov, A.B. Shabat, Exact theory of two-dimensional self-focusing and one-dimensional self-modulation of waves in nonlinear media (Differential equation solution for plane self focusing and one dimensional self modulation of waves interacting in nonlinear media), Sov. Phys. JETP. 34 (1972) 62–69.

[10]　P. Di Trapani, D. Caironi, G. Valiulis, A. Dubietis, R. Danielius, A. Piskarskas, Observation of Temporal Solitons in Second-Harmonic Generation with Tilted Pulses, Phys. Rev. Lett. 81 (1998) 570-573.

[11]　M. Segev, B. Crosignani, A. Yariv, B. Fischer, Spatial solitons in photorefractive media, Phys. Rev. Lett. 68 (1992) 923-927.

[12]　A. Yariv, Optical waves in crystals: propagation and control of laser radiation, New York, Wiley, 1984.

[13]　D.N. Christodoulides, M.I. Carvalho, Compression, self-bending, and collapse of Gaussian beams in photorefractive crystals, Opt. Lett. 19 (1994) 1714-1716.

[14]　M. Segev, G.C. Valley, B. Crosignani, P. DiPorto, A. Yariv, Steady-State Spatial Screening Solitons in Photorefractive Materials with External Applied Field, Phys. Rev. Lett. 73 (1994) 3211-3214.

[15]　D.N. Christodoulides, M.I. Carvalho, Bright, dark, and gray spatial soliton states in photorefractive media, J. Opt. Soc. Am. B. 12 (1995) 1628-1633.

[16]　M. Segev, B. Crosignani, P.D. Porto, A. Yariv, G. Duree, G. Salamo, et al., Stability of photorefractive spatial solitons, Opt. Lett. 19 (1994) 1296-1298.

[17]　A.A. Zozulya, D.Z. Anderson, Propagation of an optical beam in a photorefractive medium in the presence of a photogalvanic nonlinearity or an externally applied electric field, Phys. Rev. A. 51 (1995) 1520-1532.

[18]　L. Eldada, L. Shacklette, Advances in polymer integrated optics, IEEE J. Sel.

Top. Quant. Electron. 6 (2000) 54-68.

[19] J. Lawrence, F. O'Neill, J. Sheridan, Photopolymer holographic recording material, Optik, Int. J. Light. Electron. Opt. 112 (2001) 449-463.

[20] B.L. Booth, Photopolymer Material for Holography, Appl. Opt. 14 (1975) 593-601.

[21] S. Calixto, Dry polymer for holographic recording, Appl. Opt. 26 (1987) 3904-3910.

[22] W.S. Colburn, K.A. Haines, Volume Hologram Formation in Photopolymer Materials, Appl. Opt. 10 (1971) 1636-1641.

[23] S.H. Lin, K.Y. Hsu, W. Chen, W.T. Whang, Phenanthrenequinone-doped poly(methyl methacrylate) photopolymer bulk for volume holographic data storage, Opt. Lett. 25 (2000) 451-453.

[24] K. Curtis, D. Psaltis, Characterization of the DuPont photopolymer for three-dimensional holographic storage, Appl. Opt. 33 (1994) 5396-5399.

[25] A.V. Veniaminov, O.V. Bandyuk, O.V. Andreeva, Materials with diffusion amplification for optical-information recording and their study by a holographic method, J. Opt. Technol. 75 (2008) 306-310.

[26] Y. Gritsay, V. Mogilnyi, A new polymeric medium for optical phase-modulated recording with diffusion enhancement, Tech. Phys. Lett. 32 (2006) 10-13.

[27] A. Veniaminov, E. Bartsch, Diffusional enhancement of holograms: phenanthrenequinone in polycarbonate, J. Opt. A: Pure Appl. Opt. 4 (2002) 387-392.

[28] A. Popov, I. Novikov, K. Lapushka, I. Zyuzin, Y. Ponosov, Y. Ashcheulov, et al., Spectrally selective holographic optical elements based on a thick polymer medium with diffusional amplification, J. Opt. A: Pure Appl. Opt. 2 (2000) 494-499.

[29] I. Cho, W. Lee, B. Rho, M. Jeong, Polymer waveguide with integrated reflector mirrors for an inter-chip link system, Opt. Commun. 281 (2008) 4906-4909.

[30] J. Zhou, W. Wong, N. Ngo, E. Pun, Y. Shen, Y. Zhao, Polymer-based waveguides with low propagation loss and polarization-dependent loss, Opt. and Las. Tech. 37 (2005) 427-431.

[31] Y. Ichihashi, P. Henzi, M. Bruendel, J. Mohr, D.G. Rabus, Polymer waveguides from alicyclic methacrylate copolymer fabricated by deep-UV exposure, Opt. Lett. 32 (2007) 379-381.

[32] H. Liang, Q. Zhang, Z. Zheng, Z. Zhang, L. Cao, A. Pan, et al., Study of Eu(DBM)3phen-doped optical polymer waveguides, J. Opt. Soc. Am. B. 22 (2005) 820-824.

[33] N.M. Ganzherli, A.S. Gurin, D.D. Kramushchenko, I.A. Maurer, D.F. Chernykh, S.N. Gulyaev, Two-dimensional holographic gratings based on silver halide photographic emulsions for the formation of raster images, J. Opt. Technol. 76 (2009) 388-391.

[34] B.J. Chang, C.D. Leonard, Dichromated gelatin for the fabrication of holographic optical elements, Appl. Opt. 18 (1979) 2407-2417.

[35] A. Villamarín, J. Atencia, M.V. Collados, M. Quintanilla, Characterization of transmission volume holographic gratings recorded in Slavich PFG04 dichromated gelatin plates, Appl. Opt. 48 (2009) 4348-4353.

[36] P.D. Berezin, I.N. Kompanets, A.G. Timushev, I.V. Tunimanova, V.A. Tsekhomskiĭ, Optimization of holographic data recording in photochromic

glasses, Sov. J. Quantum Electron. 7 (1977) 902-904.

[37] A. Pyajt, O. Andreeva, V. Bespalov, Dynamic holograms recording in fullerene-containing solid-state matrices: Porous glass slides and PMMA films, Opt. Commun. 259 (2006) 562-568.

[38] K. Beev, L. Criante, D. Lucchetta, F. Simoni, S. Sainov, Total internal reflection holographic gratings recorded in polymer-dispersed liquid crystals, Opt. Commun. 260 (2006) 192-195.

[39] G. Lashkov, A. Veniaminov, O. Ratner, Study of diffusion of compounds of anthracene structure in polymethyl methacrylate by holographic relaxometry, Polym. Sci. U.S.S.R. 28 (1986) 487-492.

[40] S.H. Lin, J.H. Lin, P.L. Chen, K.Y. Hsu, Doped poly(methyl methacrylate) photopolymers for holographicdata storage, J. Non. Opt. Phys. Mater. 15 (2000) 239-252.

[41] G.J. Steckman, I. Solomatine, G. Zhou, D. Psaltis, Characterization of phenanthrenequinone-doped poly(methyl methacrylate) for holographic memory, Opt. Lett. 23 (1998) 1310-1312.

[42] U.V. Mahilny, D.N. Marmysh, A.L. Tolstik, V. Matusevich, R. Kowarschik, Phase hologram formation in highly concentrated phenanthrenequinone–PMMA media, J. Opt. A: Pure Appl. Opt. 10 (2008) 085302.

[43] J.M. Russo, R.K. Kostuk, Temperature dependence properties of holographic gratings in phenanthrenquinone doped poly(methyl methacrylate) photopolymers, Appl. Opt. 46 (2007) 7494-7499.

[44] A.V. Veniaminov, H. Sillescu, Polymer and Dye Probe Diffusion in Poly(methyl methacrylate) below the Glass Transition Studied by Forced Rayleigh Scattering, Macromol. 32 (1999) 1828-1837.

[45] K. Takahara, H. Saito, T. Inoue, Physical aging in poly(methyl methacrylate) glass: densification via density fluctuation, Polymer. 40 (1999) 3729-3733.

[46] A. Veniaminov, E. Bartsch, A. Popov, Postexposure evolution of a photoinduced grating in a polymer material with phenanthrenequinone, Opt. Spectr. 99 (2005) 744-750.

[47] A. Veniaminov, E. Bartsch, The shape of the relaxation curve in diffusion measurements with the aid of photoinduced gratings, Opt. Spectr. 101 (2006) 290-298.

[48] N.V. Ionina, O.V. Andreeva, O.V. Banduk, A.A. Paramonov, Connection of the holographic characteristics of polymer recording samples with their hardness, Opt. J. 69 (2002) 35-37.

[49] F. Bueche, Viscosity, Self-Diffusion, and Allied Effects in Solid Polymers, J. Chem. Phys. 20 (1952) 1959-1964.

[50] T.N. Gerasimova, V.V. Shelkovnikov, G.M. Zharkova, S.A. Streltsov, E.F. Pen, Study of the characteristics of the scattering noise of holographic photopolymericmaterials, J. Opt. Technol. 69 (2002) 741.

[51] Y. Koike, N. Tanio, Y. Ohtsuka, Light scattering and heterogeneities in low-loss poly(methyl methacrylate) glasses, Macromol. 22 (1989) 1367-1373.

[52] T. Babeva, I. Naydenova, S. Martin, V. Toal, Method for characterization of diffusion properties of photopolymerisable systems, Opt. Expr. 16 (2008) 8487-8497.

[53] S. Wu, E.N. Glytsis, Characteristics of DuPont photopolymers for slanted holographic grating formations, J. Opt. Soc. Am. B. 21 (2004) 1722-1731.

[54] N. Pandey, I. Naydenova, S. Martin, V. Toal, Technique for characterization of dimensional changes in slanted holographic gratings by monitoring the

angular selectivity profile, Opt. Lett. 33 (2008) 1981-1983.

[55] V. Moreau, Y. Renotte, Y. Lion, Characterization of DuPont photopolymer: determination of kinetic parameters in a diffusion model, Appl. Opt. 41 (2002) 3427-3435.

[56] A.V. Veniaminov, V.F. Goncharov, A.P. Popov, Encancement of holograms due to diffusion destruction of antiphase periodic structures, Opt. and Spectr. 70 (1991) 864-868.

[57] V. Matusevich, R. Kowarschik, U. Mahilny, D. Marmysh, A. Stankevich, A. Tolstik, et al., Holographic volume gratings in a glass-like polymer material, Proceeding of Lasers and Electro-Optics Europe (2005) 191.

[58] D.N. Marmysh, U.V. Mahilny, E.A. Tolstik, Transformation of holographic gratings in polymeric layers containing phenanthrenequinone, Izv. Ross. Akad. Nauk, Ser. Fiz. 70 (2006) 1809-1812.

[59] S. Sowa, W. Watanabe, T. Tamaki, J. Nishii, K. Itoh, Symmetric waveguides in poly(methyl methacrylate) fabricated by femtosecond laser pulses, Opt. Expr. 14 (2006) 291-297.

[60] M. Shih, Z. Chen, M. Mitchell, M. Segev, H. Lee, R.S. Feigelson, et al., Waveguides induced by photorefractive screening solitons, J. Opt. Soc. Am. B. 14 (1997) 3091-3101.

[61] S. Lan, M.F. Shih, G. Mizell, J.A. Giordmaine, Z. Chen, C. Anastassiou, et al., Second-harmonic generation in waveguides induced by photorefractive spatial solitons, Opt. Lett. 24 (1999) 1145-1147.

[62] F.K. Abdullaev, S. Darmanyan, Optical Solitons, Berlin, Springer, 1993.

[63] P. Drazin, Solitons: An Introduction, Cambridge, Cambridge University Press, 1993.

[64] J. Zhang, K. Kasala, A. Rewari, K. Saravanamuttu, Self-Trapping of Spatially and Temporally Incoherent White Light in a Photochemical Medium, J. Am. Chem. Soc. 128 (2006) 406-407.

[65] D.V.G.L.N. Rao, J. Bickford, A. Sheri, M. Kumar, Self-focusing in polymers, J. of Polym. Sc.: Part C: Polym. Lett. 28 (1990) 247-252.

[66] X. Wang, W. She, W. Lee, Optical spatial solitons supported by photoisomerization nonlinearity in a polymer, Opt. Lett. 29 (2004) 277-279.

[67] C.B. Clausen, O. Bang, Y.S. Kivshar, Spatial Solitons and Induced Kerr Effects in Quasi-Phase-Matched Quadratic Media, Phys. Rev. Lett. 78 (1997) 4749-4752.

[68] E.M. Dianov, A.V. Luchnikov, A.N. Pilipetskii, A.N. Starodumov, Electrostriction mechanism of soliton interaction in optical fibers, Opt. Lett. 15 (1990) 314-316.

[69] A.B. Shvartsburg, L. Stenflo, P.K. Shukla, Transverse-electric polarized surface solitons, Phys. Lett. A. 268 (2000) 386-389.

[70] C. Rotschild, O. Cohen, O. Manela, M. Segev, T. Carmon, Solitons in nonlinear media with an infinite range of nonlocality: first observation of coherent elliptic solitons and of vortex-ring solitons, Phys. Rev. Lett. 95 (2005) 213904.

[71] H.S. Eisenberg, Y. Silberberg, R. Morandotti, A.R. Boyd, J.S. Aitchison, Discrete Spatial Optical Solitons in Waveguide Arrays, Phys. Rev. Lett. 81 (1998) 3383-3386.

[72] C. Huang, Q. Guo, Interaction of nonlocal incoherent spatial solitons, Opt. Commun. 277 (2007) 414-422.

[73] K. Pismennaya, O. Kashin, V. Matusevich, A. Kiessling, R. Kowarschik,

Beam self-trapping and self-bending dynamics in a strontium barium niobate crystal, J. Opt. Soc. Am. B. 25 (2008) 136-139.

[74] D. Kühlke, Optik: Grundlagen und Anwendungen, Freiburger Graphische Betriebe, 1998.

[75] A.V. Buryak, P.D. Trapani, D.V. Skryabin, S. Trillo, Optical solitons due to quadratic nonlinearities: from basic physics to futuristic applications, Phys. Rep. 370 (2002) 63-235.

[76] K. Ohta, Optical waveguide fabrication in new glasses and PMMA with temporally tailored ultrashort laser, Commercial and Biomedical Applications of Ultrafast Lasers IV , USA (2004) 172-178.

[77] A. Zoubir, C. Lopez, M. Richardson, K. Richardson, Femtosecond laser fabrication of tubular waveguides in poly(methyl methacrylate), Opt. Lett. 29 (2004) 1840-1842.

[78] S.J. Frisken, Light-induced optical waveguide uptapers, Opt. Lett. 18 (1993) 1035-1037.

[79] A.S. Kewitsch, A. Yariv, Self-focusing and self-trapping of optical beams upon photopolymerization, Opt. Lett. 21 (1996) 24-26.

[80] C.P. Jisha, V.C. Kishore, B.M. John, V.C. Kuriakose, K. Porsezian, C.S. Kartha, Self-written waveguide in methylene blue sensitized poly(vinyl alcohol)/acrylamide photopolymer material, Appl. Opt. 47 (2008) 6502-6507.

[81] M.V. Mostovoy, M.T. Figge, J. Knoester, Disorder-induced solitons in conjugated polymers, Europhys. Lett. 38 (1997) 687-692.

[82] C.R. Mendonca, L.R. Cerami, T. Shih, R.W. Tilghman, T. Baldacchini, E. Mazur, Femtosecond laser waveguide micromachining of PMMA films with azoaromatic chromophores, Opt. Expr. 16 (2008) 200-206.

[83] S. Shoji, S. Kawata, A.A. Sukhorukov, Y.S. Kivshar, Self-written waveguides in photopolymerizable resins, Opt. Lett. 27 (2002) 185-187.

[84] A.C. Sullivan, M.W. Grabowski, R.R. McLeod, Three-dimensional direct-write lithography into photopolymer, Appl. Opt. 46 (2007) 295-301.

[85] J.K. Poon, L. Zhu, G.A. DeRose, A. Yariv, Transmission and group delay of microring coupled-resonator optical waveguides, Opt. Lett. 31 (2006) 456-458.

[86] H. Hou, Y. Wei, Y. Song, Y. Zhu, Y. Fan, Two novel two-dimensional cluster polymers $\{[NMe_4]_2[MOS_3Cu_3([mu]_2-I)_3]\}$ (M=Mo,W): synthesis, crystal structure and interesting optical alternation from self-defocusing to self-focusing, Inorg. Chim. Acta. 357 (2004) 421-428.

[87] L.M. Goldenberg, Y. Gritsai, O. Sakhno, O. Kulikovska, J. Stumpe, All-optical fabrication of 2D and 3D photonic structures using a single polymer phase mask, J. Opt. 12 (2010) 015103.

[88] H. Kogelnik, Coupled wave theory for thick hologram gratings, Bell. Syst. Tech. J. 48 (1969), 2909.

[89] J. Zhang, C.H. Wang, Simultaneous measurements of the diffusion coefficients of the dye molecule and its photoproduct by the holographic relaxation technique, J. Phys. Chem. 90 (1986) 2296-2297.

[90] D.G.Jr. Miles, P.D. Lamb, W.R. Kee, C.S.Jr. Johnson, Holographic relaxation spectroscopy of a benzospiropyran in mixtures of water and dioxane, J. Phys. Chem. 87 (2010) 4815-4822.

[91] E.J. Brown, Q. Zhang, M. Dantus, Femtosecond transient-grating techniques: Population and coherence dynamics involving ground and excited states, J. Chem. Phys. 110 (1999) 5772-5788.

[92] M.G. Galushkin, K.V. Mitin, Four-wave interaction of a high-intensity signal in media with a strong nonlinearity, Quant. Elect. 25 (1995) 464-466.

[93] A.V. Veniaminov, H. Sillescu, Forced Rayleigh scattering from non-harmonic gratings applied to complex diffusion processes in glass-forming liquids, Chem. Phys. Lett. 303 (1999) 499-504.

[94] U.V. Mahilny, Photoregistering Polymeric Materials and Their Applications: Lectures, Belarusian State University Press, Minsk, 2003.

[95] J. Gillet, Photophysics and Photochemistry of Polymers, Nauka, Moscow, 1988.

[96] M. Born, E. Wolf, Principles of Optics, Oxford, Pergamon, 1968.

[97] A.V. Veniaminov, Y.N. Sedunov, A.P. Popov, O.V. Banduk, Post-exposure holograms behaviour under the influence of diffusion of macromolecules, Opt. and Spectr. 81 (1996) 676-680.

[98] O.V. Andreeva, O.V. Banduk, A.A. Paramonov, Three-dimensional holograms in a polymer medium with phenanthrenequinone, Opt. J. 67 (2000) 27-33.

[99] Y. Li, K. Yamada, T. Ishizuka, W. Watanabe, K. Itoh, Z. Zhou, Single femtosecond pulse holography using polymethyl methacrylate, Opt. Expr. 10 (2002) 1173-1178.

[100] D. Gong, Z. Zhou, H. Liu, J. Wang, H. Gao, Two-dimensional higher-diffraction-order optical beam splitter based on phenanthrenequinone-doped poly(methyl methacrylate) photopolymer, Opt. Las. Eng. 47 (2009) 662-666.

[101] H. Liu, D. Yu, Y. Jiang, X. Sun, Characteristics of holographic scattering and its application in determining kinetic parameters in PQ-PMMA photopolymer, Appl. Phys. B. Laser. Opt. 95 (2009) 513-518.

[102] H. Liu, D. Yu, X. Li, S. Luo, Y. Jiang, X. Sun, Diffusional enhancement of volume gratings as an optimized strategy for holographic memory in PQ-PMMA photopolymer, Opt. Expr. 18 (2010) 6447-6454.

[103] J. Mumbru, I. Solomatine, D. Psaltis, S.H. Lin, K.Y. Hsu, W. Chen, et al., Comparison of the recording dynamics of phenanthrenequinone-doped poly(methyl methacrylate) materials, Opt. Commun. 194 (2001) 103-108.

[104] Y. Hsiao, W. Whang, S.H. Lin, Analyses on physical mechanism of holographic recording in phenanthrenequinone-doped poly(methyl methacrylate) hybrid materials, Opt. Eng. 43 (2004) 1993-2002.

[105] K.Y. Hsu, S.H. Lin, Y. Hsiao, W.T. Whang, Experimental characterization of phenanthrenequinone-doped poly(methyl methacrylate) photopolymer for volume holographic storage, Opt. Eng. 42 (2003) 1390-1396.

[106] Y. Hsiao, W. Whang, S.H. Lin, Effect of ZnMA on Optical and Holographic Characteristics of Doped PQ/PMMA Photopolymer, Jpn. J. Appl. Phys. 44 (2005) 914-919.

[107] Y. Hsiao, W. Whang, S.H. Lin, K.Y. Hsu, Fabrication and characterization of thick zinc methacrylate/phenanthrenequinone codoped poly(methyl methacrylate) photopolymers for volume holographic recording, Jpn. J. Appl. Phys. 45 (2006) 8699-8704.

[108] S. Lin, P. Chen, Y. Hsiao, W. Whang, Fabrication and characterization of poly(methyl methacrylate) photopolymer doped with 9,10-phenanthrenequinone (PQ) based derivatives for volume holographic data storage, Opt. Commun. 281 (2008) 559-566.

[109] A. Sato, Holographic grating for dense wavelength division optical filters at 1550 nm using phenanthrenquinone-doped poly(methyl methacrylate),

Organic Holographic Materials and Applications, USA (2003) 44-52.

[110] A. Sato, M. Scepanovic, R.K. Kostuk, Holographic Edge-Illuminated Polymer Bragg Gratings for Dense Wavelength Division Optical Filters at 1550 nm, Appl. Opt. 42 (2003) 778-784.

[111] R.K. Kostuk, W. Maeda, C. Chen, I. Djordjevic, B. Vasic, Cascaded holographic polymer reflection grating filters for optical-code-division multiple-access applications, Appl. Opt. 44 (2005) 7581-7586.

[112] J.E. Castillo, J.M. Russo, R.K. Kostuk, Response of Axially Stressed Edge-Illuminated Holographic Gratings in PQ/PMMA Photopolymers, IEEE Photon. Technol. Lett. 20 (2008) 1199-1201.

[113] Y. Luo, P.J. Gelsinger-Austin, J.M. Watson, G. Barbastathis, J.K. Barton, R.K. Kostuk, Laser-induced fluorescence imaging of subsurface tissue structures with a volume holographic spatial-spectral imaging system, Opt. Lett. 33 (2008) 2098-2100.

[114] Y. Luo, P.J. Gelsinger, J.K. Barton, G. Barbastathis, R.K. Kostuk, Optimization of multiplexed holographic gratings in PQ-PMMA for spectral-spatial imaging filters, Opt. Lett. 33 (2008) 566-568.

[115] Y. Luo, J. Russo, R. Kostuk, G. Barbastathis, Silicon oxide nanoparticles doped PQ-PMMA for volume holographic imaging filters, Opt. Lett. 35 (2010) 1269-1271.

[116] M. Ortuno, E. Fernandez, S. Gallego, A. Belendez, I. Pascual, New photopolymer holographic recording material with sustainable design, Opt. Expr. 15 (2007) 12425-12435.

[117] L.P. Krul, V. Matusevich, D. Hoff, R. Kowarschik, Y.I. Matusevich, G.V. Butovskaya, et al., Modified polymethylmethacrylate as a base for thermostable optical recording media, Opt. Expr. 15 (2007) 8543-8549.

[118] V. Matusevich, A. Matusevich, R. Kowarschik, Y.I. Matusevich, L.P. Krul, Holographic volume absorption grating in glass-like polymer recording material, Opt. Expr. 16 (2008) 1552-1558.

[119] E. Tolstik, O. Kashin, A. Matusevich, V. Matusevich, R. Kowarschik, Y.I. Matusevich, et al., Non-local response in glass-like polymer storage materials based on poly (methylmethacrylate) with distributed phenanthrenequinone, Opt. Expr. 16 (2008) 11253-11258.

[120] E. Tolstik, A. Winkler, V. Matusevich, R. Kowarschik, U.V. Mahilny, D.N. Marmysh, et al., PMMA-PQ Photopolymers for Head-Up-Displays, IEEE Photon. Technol. Lett. 21 (2009) 784-786.

[121] O. Kashin, E. Tolstik, V. Matusevich, R. Kowarschik, Numerical investigation of the (1+1)D self-trapping of laser beams in polymeric films based on polymethylmethacrylate and phenanthrenequinone, J. Opt. Soc. Am. B. 26 (2009) 2152-2156.

[122] E. Tolstik, D. Hoff, V. Matusevich, R. Kowarschik, L. Yakimtsova, Y.I. Matusevich, et al., Glass-like polymer recording materials based on methylmethacrylate with methacrylamide and phenanthrenequinone, Topical Meeting Photorefractive Materials, Effects, and Devices – Control Light and Matter, Germany (2009).

[123] E. Tolstik, O. Kashin, V. Matusevich, R. Kowarschik, U.V. Mahilny, D.N. Marmysh, et al., Self-trapping of laser beams in polymeric layers, Proceeding of German Society of Applied Optics, Italy (2009) 150.

[124] D. Hoff, E. Tolstik, V. Matusevich, R. Kowarschik, Y.I. Matusevich, L.P. Krul, et al., New photosensitive polymers based on MMA+PQ, Proceeding of

German Society of Applied Optics, Italy (2009) 146.

[125] V. Matusevich, E. Tolstik, A. Winkler, R. Kowarschik, Head-Up-Displays from Plexiglas, J. of Photonik. 2 (2010) 44-45.

[126] E. Tolstik, O. Kashin, V. Matusevich, R. Kowarschik, (1+1)D self-trapping in photopolymer based on Plexiglass, Proceeding of German Society of Applied Optics, Germany (2010) 136.

[127] E. Tolstik, O. Kashin, V. Matusevich, R. Kowarschik, Influence of the temperature on the (1+1)D-self-trapping broadening in photopolymer based on Plexiglass, Proceeding of German Society of Applied Optics, Germany (2010) 136.

[128] R.J. Collier, C.B. Burckhardt, L.H. Lin, Optical Holography, New York, Academic, 1971.

[129] Ed. By N.S. Zefirov, Chemical Encyclopedia (Bol'shaya Rossiiskaya Entsiklopediya), Moskow, Soviet Encyclopedia, 1995.

[130] L. Yakimtsova, E. Egorova, E. Murashko, Y. Matusevich, A. Polikarpov, L. Krul, Thermomechanical properties and heat resistance of copolymers of methyl methacrylate with acrylic acid, Rus. J. of Appl. Chem. 81 (2008) 668-671.

[131] J.T. Sheridan, J.R. Lawrence, Nonlocal-response diffusion model of holographic recording in photopolymer, J. Opt. Soc. Am. A. 17 (2000) 1108-1114.

[132] J.T. Sheridan, M. Downey, F.T. O'Neill, Diffusion-based model of holographic grating formation in photopolymers: generalized non-local material responses, J. Opt. A: Pure Appl. Opt. 3 (2001) 477-488.

[133] M.R. Gleeson, J.V. Kelly, D. Sabol, C.E. Close, S. Liu, J.T. Sheridan, Modeling the photochemical effects present during holographic grating formation in photopolymer materials, J. Appl. Phys. 102 (2007) 023108.

[134] G. Zhao, P. Mouroulis, Diffusion Model of Hologram Formation in Dry Photopolymer Materials, J. Mod. Opt. 41 (1994) 1929-1939.

[135] S. Piazzolla, B.K. Jenkins, Holographic grating formation in photopolymers, Opt. Lett. 21 (1996) 1075-1077.

[136] S. Piazzolla, B.K. Jenkins, First-harmonic diffusion model for holographic grating formation in photopolymers, J. Opt. Soc. Am. B. 17 (2000) 1147-1157.

[137] E. Tomita, N. Kawahara, A. Nishiyama, M. Shigenaga, In situ measurement of hydrocarbon fuel concentration near a spark plug in an engine cylinder using the 3.392 μm infrared laser absorption method: application to an actual engine, Meas. Sci. Technol. 14 (2003) 1357-1363.

[138] G. Agrawal, Nonlinear Fiber Optics, Third Edition, Academic Press, 2001.

[139] T.R. Taha, M.J. Ablowitz, Analytical and numerical aspects of certain nonlinear evolution equations. II. Numerical nonlinear Schrödinger equation, J. Comput. Phys. 55 (1984) 203-230.

[140] F. Kan, F. Gan, Laser Materials, World Scientific Pub. Co. Inc., 1995.

[141] H.S. Carslaw, J.C. Jaeger, Conduction of heat in solids, Oxford Univ. Press, 2nd ed., 1959.

[142] K. Smolders, J. Baeyens, Thermal degradation of PMMA in fluidised beds, Waste Management. 24 (2004) 849-857.

[143] Z. Zhang, P. Zhao, P. Lin, F. Sun, Thermo-optic coefficients of polymers for optical waveguide applications, Polymer. 47 (2006) 4893-4896.

[144] M. Assael, S. Botsios, K. Gialou, I. Metaxa, Thermal Conductivity of

Polymethyl Methacrylate (PMMA) and Borosilicate Crown Glass BK7, Int. J. Thermophys. 26 (2005) 1595-1605.

[145] K. Hirabayashi, H. Kanbara, Y. Mori, T. Kurihara, M. Shimizu, T. Hiyama, Multilayer holographic recording using a two-color-absorption photopolymer, Appl. Opt. 46 (2007) 8402-8410.

[146] L.M. Goldenberg, Y. Gritsai, O. Kulikovska, J. Stumpe, Three-dimensional planarized diffraction structures based on surface relief gratings in azobenzene materials, Opt. Lett. 33 (2008) 1309-1311.

[147] J. Hoose, E. Popov, Two-dimensional gratings for low polarization dependent wavelength demultiplexing, Appl. Opt. 47 (2008) 4574-4578.

[148] E. Fernandez, M. Orturo, S. Gallego, A. Marquez, C. Garcia, A. Belendez, et al., Multiplexed holographic data page storage on a polyvinyl alcohol/acrylamide photopolymer memory, Appl. Opt. 47 (2008) 4448-4456.

[149] S. Gallego, M. Ortuno, C. Neipp, A. Marquez, A. Belendez, I. Pascual, et al., Physical and effective optical thickness of holographic diffraction gratings recorded in photopolymers, Opt. Expr. 13 (2005) 1939-1947.

[150] S. Orlic, S. Ulm, Hans Joachim Eichler, 3D bit-oriented optical storage in photopolymers, J. Opt. A: Pure Appl. Opt. 3 (2001) 72-81.

[151] R. Barille, S. Dabos-Seignon, J. Nunzi, S. Ahmadi-Kandjani, E. Ortyl, S. Kucharski, Nonlocal communication with photoinduced structures at the surface of a polymer film, Opt. Expr. 13 (2005) 10697-10702.

[152] W. Chao, S. Chi, Diffraction properties of windshield laminated photopolymer holograms, J. Opt. 29 (1998) 95-103.

[153] L. Eisen, M. Meyklyar, M. Golub, A.A. Friesem, I. Gurwich, V. Weiss, Planar configuration for image projection, Appl. Opt. 45 (2006) 4005-4011.

[154] G.K. Edgar, Accommodation, cognition, and virtual image displays: A review of the literature, Displays. 28 (2007) 45-59.

[155] M. Ikeda, United States Patent: 5416881 - Optical fiber and optical waveguide connecting device, U.S. Patent 5416881, 1995.

[156] K. Matsumoto, H. Takahashi, United States Patent: 7221846 - Optical communication system, U.S. Patent 7221846, 2007.

[157] R.A. Norwood, B. Brown, J. Holman, L.W. Shacklette, United States Patent: 6266472 - Polymer gripping elements for optical fiber splicing, U.S. Patent 6266472, 2001.

[158] A.F. Ware, S.K. Ware, United States Patent: 6454471 - Optical fiber splice sleeve and method for applying same, U.S. Patent 6454471, 2002.

Abbreviations and Variables

PQ   - phenanthrenequinone
PMMA   - polymethylmethacrylate
MMA   - methylmethacrylate
AIBN   - azo-bis-isobutyrolnitrile
CP   - copolymer
AA   - acrylic acid
MA   - methacrylic acid
MAA   - methacrylamide
DMF   - dimethylformamide
PVB   - polyvinylbuteral
UV   - ultraviolet
CW   - continuous wave
Ar   - argon
He-Ne   - helium–neon
FFT   - fast Fourier transform
DFT   - discrete Fourier transform
HUD   - head-up display
CCD   - charge-coupled device
$R^{\bullet}$ - macroradical
$HPQ^{\bullet}$ - semiquinone radical
HPQR   - photoproduct
LED   - light-emitting diode
d - diameter of a light beam
λ_0 - free-space wavelength
n - refractive index of the medium
n_0 - initial refractive index
Δn - photoinduced variation of the refractive index
Δn_{PQ} - change of the refractive index caused by the photoreaction of PQ
Δn_T - thermal change of the refractive index
I - light intensity
A - complex amplitude of the light wave
A_{th} - threshold amplitude of the light field
φ - phase of the wave
n_2, n_4 - expansion coefficients determined by nonlinear medium properties
x_0 - radius of the light beam (at 1/e-mean)
Ψ - angel of the total internal reflection of the beam

θ_0	- slope angle against the axis of the beam
θ_d	- angle of the diffraction divergence
P	- power of the light beam
P_{th}	- threshold power of the light beam
l_{s-f}	- self-focusing length of the optical beam
$\Delta_\perp$	- transversal Laplace operator
z	- direction of the beam propagation
k	- wave number
C_i	- concentration of the i-th component
R_i	- molar refraction of the i-th component
ΔR	- change in photorefraction of the components
ρ	- material density
W	- light exposure
t	- recording / amplification time of the hologram
t_e	- light exposure time
Y	- diffusion-rate constant of the amplification process
Λ	- spatial grating period
D	- diffusion coefficient
D_0	- initial diffusion coefficient
c_d	- diffusion constant
M	- amplification factor of the phase pattern
I_{in}	- input beam intensity
I_{out}	- transmitted beam intensity
I_{diffr}	- intensity of the diffracted beam
I_0	- incident intensity of the beam (initial intensity)
θ	- angle between direction of the wave propagation and grating
h	- thickness of the layer
η	- diffraction efficiency of the recorded structure
m	- diffraction order of the periodical structure
Q	- Klein parameter
H	- parameter characterizing contribution of the amplification process
Δn_e	- refractive-index modulation after the hologram recording
Δn_0	- refractive-index modulation at the end of the diffusion processes
ΔC_{PQ}	- changes of the PQ-concentration
N(x, z, t)	- change of the concentration of the photoproduct
C_0	- initial PQ-concentration before illumination
δ	- molar fraction of polar comonomers in the mixture of monomers
β	- molar fraction of polar comonomers in the copolymer
t_{max}	- time for achieving the maximum diffraction efficiency
F(x', t')	- copolymerization rate

$R(x,x',t,t')$ - non-local response

$\sqrt{\sigma}$ - non-local response length

ξ - constant of copolymerization

V - fringe visibility

f - spatial frequency of the grating

$\hat{n}$ - complex refractive index

$\kappa(x,z,t)$ - nonlinear coefficient of the extinction

ω - circular frequency

α - absorption coefficient of the medium

α_{mol} - molar absorption cross-section

ε - coupling rate

l_R - Rayleigh length

C_ρ - heat capacity of the unit volume (volumetric heat capacity)

$\partial n / \partial T$ - thermooptical coefficient

L - area of interaction of light and medium

a_T - thermal diffusivity coefficient

k_T - thermal conductivity

c_T - specific heat capacity

ΔT - change of the temperature in the illuminated area

b - coefficient of the heat transfer

Ehrenwörtliche Erklärung

Ich erkläre hiermit ehrenwörtlich, dass ich die vorliegende Arbeit selbständig, ohne unzulässige Hilfe Dritter und ohne Benutzung anderer als der angegebenen Hilfsmittel und Literatur angefertigt habe. Die aus anderen Quellen direkt oder indirekt übernommenen Daten und Konzepte sind unter Angabe der Quelle gekennzeichnet.

Weitere Personen waren an der inhaltlich-materiellen Erstellung der vorliegenden Arbeit nicht beteiligt. Insbesondere habe ich hierfür nicht die entgeltliche Hilfe von Vermittlungs- bzw. Beratungsdiensten (Promotionsberater oder andere Personen) in Anspruch genommen. Niemand hat von mir unmittelbar oder mittelbar geldwerte Leistungen für Arbeiten erhalten, die im Zusammenhang mit dem Inhalt der vorgelegten Dissertation stehen.

Die Arbeit wurde bisher weder im In- noch im Ausland in gleicher oder ähnlicher Form einer anderen Prüfungsbehörde vorgelegt.

Die geltende Promotionsordnung der Physikalisch-Astronomischen Fakultät ist mir bekannt.

Ich versichere ehrenwörtlich, dass ich nach bestem Wissen die reine Wahrheit gesagt und nichts verschwiegen habe.

Jena, den 04 August 2010   Elen Tolstik

Acknowledgement

Curriculum Vitae

Personal Data

Name	Elen Tolstik
Date of birth	November 25th, 1984
Place of birth	Minsk, Belarus

Education

1991 – 2000	School №191, Minsk; Graduation from physical-mathematical class.
2000 – 2002	Lyceum of Belarusian State University, Minsk; specialization: physics.
2002 – 2007	Diploma in Physics [Belarusian State University, Minsk, Faculty of Physics, Department of Laser Physics and Spectroscopy, specialty in Physics (research work)].
2007 – 2008	Master of Science [Belarusian State University, Minsk, Faculty of Physics, Department of Physical Optics].
2007 - 2010	PhD student [Friedrich-Schiller University of Jena, Germany, Institute of Applied Optics].

Practical Experience

2003 - 2007	Research assistant at the Belarusian State University of Minsk, Faculty of Physics.
Feb.- Jun. 2007	Research internship during Diploma studies at the Friedrich-Schiller-University of Jena, Germany, Institute of Applied Optics.
Aug.-Sept. 2009	Research internship during PhD studies at the National University of Ireland, College of Engineering, Mathematics and Physical Sciences, University College Dublin.

Jena, den 04 August 2010 Elen Tolstik